

DISSERTATION

EVALUATION OF NOVEL THERAPEUTICS FOR HIV PREVENTION AND
TREATMENT IN A HUMANIZED MOUSE MODEL

Submitted by

Charles Preston Tagg Neff

Graduate Degree Program in Cell and Molecular Biology

In partial fulfillment of the requirements

For the Degree of Doctor of Philosophy

Colorado State University

Fort Collins, Colorado

Fall 2011

Doctoral Committee:

Advisor: Ramesh Akkina

Tawfik Aboellail
Gerald Callahan
Chaoping Chen
Deborah Garrity

ABSTRACT

EVALUATION OF NOVEL THERAPEUTICS FOR HIV PREVENTION AND TREATMENT IN A HUMANIZED MOUSE MODEL

In the absence of an effective HIV-1 vaccine finding alternative therapeutics and preventative methods has become essential. In this regard preventative approaches such as pre-exposure chemo-prophylaxis that employ either topical applied microbicides or systemically administered anti-retroviral drugs show great promise. In these studies, we evaluated two new classes of clinically approved drugs with different modes of action namely, an integrase inhibitor raltegravir and a CCR5 inhibitor maraviroc as potential systemically and topically applied pre-exposure chemo-prophylaxis. Additionally, therapeutic strategies designed to combat HIV/AIDS using siRNAs show considerable promise. However, targeted delivery of these synthetic molecules into infected cells *in vivo* has been a formidable challenge. In addressing this need we sought to evaluate the efficacy of a chimeric construct consisting of an HIV-1 gp120 specific aptamer with viral neutralization capacity fused to a siRNA with proven efficacy against *tat/rev* viral transcripts. We also sought to evaluate the efficacy of structurally flexible, cationic PAMAM dendrimers as a siRNA delivery system.

For these novel therapeutic strategies to succeed it is important to evaluate them in both *in vitro* and *in vivo*. The rhesus macaque has been a valuable research tool for comparative HIV-1 studies. However, aspects of this model render its usefulness limited considering its expensive nature and not utilizing HIV-1 itself. In this regard the recently developed humanized mouse model that permits multi-lineage human hematopoiesis is an excellent alternative to the non human primate model. To generate humanized mice, neonatal Rag2^{-/-}γc^{-/-} or Rag1^{-/-}γc^{-/-} mice were xenografted with human CD34+ hematopoietic stem cells, resulting in a model that can permit HIV-1 infection. Upon infection by HIV-1 chronic viremia develops with a subsequent loss of CD4 T cells. These mice also successfully mimic the predominant mode of HIV-1 transmission via the sexual vaginal route which also results in chronic viremia and helper T cell loss. Thus this small animal model permits the rapid preclinical evaluation of potential candidates for pre-exposure prophylactic (PrEP) efficacy as well as novel RNA-based therapeutics.

Here we utilize these humanized mouse models to evaluate the PrEP efficacies of the drugs named above as well as the *in vivo* efficacy of siRNAs delivered by utilizing a chimeric aptamer construct or a PAMAM dendrimer. Our results showed that both of these approaches using either a chimeric aptamer or a PAMAM dendrimer resulted in suppression of viral loads *in vivo* and most importantly also resulted in protection from T-cell depletion, making these compounds attractive therapeutic candidates for the treatment of HIV-1 infection. Lastly, using the same humanized mouse model we also successfully tested a gene therapy strategy employing lentiviral vectors having RNA-based anti-HIV-1 constructs convey intracellular immunization against HIV-1 *in vivo*.

ACKNOWLEDGEMENTS

This dissertation and its completion would not have been possible without the assistance and support of many people who have contributed to the success of my studies and to my life during my more than four years as a graduate student. First and foremost, I would like to thank my Principal Supervisor Dr. Ramesh Akkina, who offered continual guidance and support throughout my studies. Dr. Akkina shared his time, knowledge, experience and wisdom. His guidance helped me to gain knowledge of research process and practice as well as to develop proficiency in writing scientific articles. I have to thank him for his patience during my education, especially in my earlier years when I was inexperienced and prone to many simple and time consuming mistakes. I am also thankful for the opportunity I have had to be successful with studies that were exciting and cutting edge and always kept my interests.

I express my gratitude to my collaborators including Dr. Jiehua Zhou and Dr. John Rossi for allowing me to work with the Apatmer and Dendrimer that they evaluated *in vitro* and supplied. I thank Dr. Zhou specifically for our multiple co-author publications that encompass this dissertation; however, I only present work done on my own accord. I would also like to thank my collaborator Dr. Brent Palmer for his expertise in FLOW/FACS analysis and for helping me define the work presented in chapter six.

Next I would like to thank the people who gave the most guidance in the methods of my studies. I thank Dr. Brad Berges who was the first to expose me to qRT-PCR which was the beginning of countless reactions and to mouse handling which was the beginning of innumerable sample collections. I thank Dr. Jes Kuruvilla who not only gave research advice but also advice on life in general. Jes has become a great friend and I will always remember his support throughout my graduate career.

To all the undergraduates and veterinary students that helped me with the numerous assays and protocols I express great gratitude. I would have not been able to accomplish a fraction of the amount I did without this help. In this I would like to particularly thank Kami Fox, Sarah Joder, Erik Golike, Sean Striech, Chelsea Sax, and Zoe Wallace. I would also like to express my gratitude to all the co-researchers of my studies for their contributions at different stages of my diverse research projects and also for the contributions in co-authoring my research papers arising from work that I carried out for this thesis. I express my gratefulness to the members of my PhD committee, Dr. Tawfik Aboellail, Dr. Gerald Callahan, Dr. Chaoping Chen, and Dr. Deborah Garrity, for their guidance, help and critical review of my work. I thank Drs. Jeff and Carol Wilusz. Without their earnest encouragement I would not have started this program and be finishing so quickly after my undergraduate degree. Lastly, I thank my parents and family for their support throughout my entire academic career.

TABLE OF CONTENTS

Abstract of Dissertation.	ii
Acknowledgements.	iv
Table of Contents.	vi

Chapter 1

Overview of Literature

1.1 Structural Organization of HIV.	2
1.2 HIV Viral Tropism.	4
1.3 HIV Viral Genome Replication.	5
1.4 Accessory Proteins.	6
1.5 HIV Viral Assembly and Budding.	7
1.6 Viral Transmission.	8
1.7 AIDS.	8
1.8 HIV latent reservoir.	10
1.9 Animal Models for HIV Research.	10
1.10 Humanized Mice.	12
1.11 HIV Vaccine.	15
1.12 Anti-retroviral Drugs.	16
1.13 Pre-exposure Prophylactics and Microbicides.	18
1.14 siRNA-based Therapeutics.	20
1.14a PAMAM Dendrimers.	23
1.14b gp120 Aptamer.	24
1.15 Gene Therapy.	27

Chapter 2

Oral pre-exposure prophylaxis by antiretrovirals raltegravir and maraviroc protects against HIV-1 vaginal transmission in a humanized mouse model

2.1 Overview	31
2.2 Materials and Methods	
2.2a Generation of humanized Rag2 ^{-/-} γc ^{-/-} mice (RAG-hu mice).	31
2.2b Oral administration of anti-HIV drugs raltegravir and	

maraviroc and HIV-1 challenge by vaginal route.	32
2.2c Measurement of viral loads.	34
2.2d Flow cytometry.	34
2.3 Results	
2.3a Oral administration of integrase inhibitor raltegravir protects humanized mice from HIV-1 infection via vaginal challenge.	35
2.3b Oral administration of CCR5 inhibitor maraviroc protects humanized mice from HIV-1 infection via vaginal challenge	36
2.3c CD4 T cell loss in non-drug treated mice versus raltegravir and maraviroc treated mice following vaginal infection.	37
2.4 Discussion.	38
2.5 Acknowledgments.	42

Chapter 3

A Topical Microbicide Gel Formulation of CCR5 Antagonist Maraviroc Prevents HIV-1 Vaginal Transmission in Humanized RAG-hu Mice

3.1 Overview.	44
3.2 Materials and Methods	
3.2a Preparation of humanized Rag2 ^{-/-} γc ^{-/-} mice (RAG-hu mice)..	45
3.2b Vaginal application of gel and HIV-1 challenge by vaginal route.	45
3.2c Measurement of viral loads.	46
3.2d Flow cytometry.	46
3.3 Results	
3.3a Vaginal application of anti-retroviral gels partially protect humanized mice against HIV-1 vaginal challenge.	47
3.3b Vaginal application of maraviroc gel protects humanized mice against HIV-1 vaginal challenge.	48
3.3c CD4 T cell loss following HIV-1 vaginal infection in placebo-gel administered mice compared to maraviroc-gel administered mice	49
3.4 Discussion.	50
3.5 Acknowledgements.	54

Chapter 4

Systemic administration of dendrimer-siRNA complexes efficiently suppresses HIV-1 infection

4.1 Overview.	56
4.2 Materials and Methods	
4.2a Materials.	57
4.2b Dendrimer synthesis and characterization.	59
4.2c Agarose gel analysis of siRNA-dendrimer complexes.	59
4.2d Stability of siRNA-dendrimer complexes against RNase A.	59
4.2e Transmission electron microscopy (TEM) analysis.	60
4.2f Cell culture.	60

4.2g	Flow cytometry analysis of CEM cells.	61
4.2h	Cellular uptake studies (Fluorescent Microscopy analysis). . .	62
4.2i	Determination of CD4 or TNPO3 gene silencing (qRT-PCR analysis)	63
4.2j	HIV-1 challenges and p24 antigen assay.	64
4.2k	Determination of <i>Tat/rev</i> gene silencing (qRT-PCR analysis). . .	64
4.2l	MTT Cytotoxicity Assay.	65
4.2m	5'-RACE PCR assay.	66
4.2n	Generation and HIV-1 infection of humanized Rag2 ^{-/-} γc ^{-/-} mice (RAG-hu mice)	66
4.2o	Treatment with dendrimer-siRNA complexes.	67
4.2p	Measurement of viral load in plasma.	68
4.2q	Flow cytometry.	68
4.2r	Determination of <i>tat/rev</i> siRNA.	68
4.2s	Determination of targeted genes expression.	69
4.2t	Interferon assays.	70
4.2u	Statistical Methods.	71
4.3	Results	
4.3a	Dendrimer-siRNAs form stable nanoscale complexes which protect the siRNAs from serum nucleases and facilitate siRNA delivery into human T-cells <i>in vitro</i>	71
4.3b	dsRNAs are released from the dendrimer complexes and mediate specific gene silencing <i>in vitro</i>	74
4.3c	The G ₅ dendrimer -delivered dsRNAs inhibit HIV-1 infection of CEM T-cells and human PBMCs.	77
4.3d	Systemic administration of the G ₅ dendrimer-dsiRNA complexes suppresses HIV-1 viral loads in viremic RAG-hu mice.	78
4.3e	The G ₅ dendrimer-dsiRNA treatment protects against HIV-1 mediated T-cell depletion.	81
4.3f	The G ₅ dendrimer-mediated dsiRNA delivery does not trigger type I interferon responses <i>in vivo</i>	84
4.4	Discussion.	86
4.5	Acknowledgements.	88

Chapter 5

An aptamer-siRNA chimera suppresses HIV-1 viral loads and protects from helper CD4(+) T cell decline in humanized mice

5.1	Overview.	90
5.2	Materials and methods	
5.2a	Reagents.	91
5.2b	Generation of aptamer-siRNA chimera RNA (Ch A-1) by <i>in vitro</i> transcription.	91
5.2c	Generation and HIV-1 infection of humanized Rag2 ^{-/-} γc ^{-/-} mice (RAG-hu mice)	92
5.2d	Measurement of viral load in plasma.	93

5.2e Flow cytometry.	93
5.2f Detection of <i>tat/rev</i> siRNA.	94
5.2g Determination of HIV-1 <i>tat/rev</i> expression.	95
5.2h 5'-RACE PCR assay to detect <i>in vivo</i> RNAi mediated target mRNA cleavage.	95
5.2i Interferon assays.	96
5.2j Statistical Methods.	97
5.3 Results	
5.3a Anti-gp120 aptamer and aptamer-siRNA chimera (Ch A-1) inhibit CCR5 and CXCR4 tropic lab and clinical isolates <i>in vitro</i>	98
5.3b Chimeric Ch A-1 aptamer-siRNA is stable in mouse serum.	99
5.3c Aptamer and Aptamer-siRNA chimera Ch A-1 suppresses HIV-1 viral loads in viremic RAG-hu mice.	100
5.3d The anti-gp120 aptamer and chimeric aptamer-siRNA provide protection against HIV-1 mediated T-cell depletion.	106
5.3e Anti-gp120 aptamer-siRNA chimera does not trigger type I interferon response <i>in vivo</i>	107
5.3f Deep sequence analyses of viral RNAs for envelope and <i>tat/rev</i> target mutations.	108
5.4 Discussion.	110
5.5 Acknowledgements.	111

Chapter 6

Inhibition of HIV-1 mediated T cell depletion in RAG-hu mice by lentiviral vector delivery of three anti-HIV genes into human HSCs

6.1 Overview.	113
6.2 Materials and methods	
6.2a Combinatorial lentiviral vector design and production.	114
6.2b Isolation and transduction of CD34 HSCs.	114
6.2c Reconstitution of Rag-hu mice with transduced CD34+ cells.	115
6.2d Measurement of viral load in plasma.	115
6.2e Flow cytometry.	116
6.2f Multi-parametric FACS analysis of transgenic hematopoietic Lineage.	116
6.2g Verification of transgene <i>tat/rev</i> siRNA expression.	117
6.3 Results	
6.3a Triple-R and HIV7-GFP vector-transduced CD34 cells can reconstitute Rag2-/- γ c-/- mice and differentiate normally.	117
6.3b Transgenic engraftment persists and has normal differentiation.	119
6.3c Triple-R vector-transduced CD34 reconstituted RAG-hu mice are resistant to HIV challenge and are completely protected against CD4 T cell depletion.	121

6.4 Discussion.	124
Chapter 7 Summary and Future Considerations	
7.1 Summary.	129
7.2 Future Considerations.	133
References.	135
Appendix (Supplemental material for chapters 4 and 5).	152

CHAPTER 1

OVERVIEW OF LITERATURE

In 1981, the first recognized case of acquired immunodeficiency syndrome (AIDS) was reported by the Centers for Disease Control and Prevention (CDC) (1). Shortly after this first AIDS case was recognized, the causative agent was discovered to be of viral origin. The virus was isolated from the lymph node of a patient with lymphadenopathy at the Pasteur Institute in Paris. The following year researchers at the U.S. National Institutes of Health and at the University of California independently found cytopathic, T-cell-tropic retroviruses from blood cells of AIDS patients (2).

Soon after individual isolates of the virus were examined by electron microscopy, it was apparent that this AIDS causing virus was morphologically similar to the lentiviruses, a group of retroviruses with the characteristic of slow disease progression and long incubation periods. In 1986 under the recommendation of the International Committee on Taxonomy of Viruses the causative was named Human Immunodeficiency Virus (HIV-1).

Following the discovery of HIV-1, screening tests were developed for diagnosis of infected individuals. Once large scale testing became available the global impact of HIV became apparent (2). According to the Joint United Nations Programme on

HIV/AIDS (UNAIDS) in January 2010 more than 35 million people worldwide are living with HIV/AIDS. With current estimates to be about 0.6 percent of the world's population living with HIV-1, this virus has grown to a global pandemic scale in need of urgent and immediate attention.

1.1 Structural Organization of HIV-1

An HIV virion is spherical in shape with a diameter of about 120nm (3). The virus consists of two copies of positive single-stranded RNAs that code for the viral genes. HIV-1 is enclosed by a capsid comprised of the viral protein p24 (4). Like all retroviruses, HIV-1 has two layers of phospholipids that form the viral envelope. The envelope (Env) protein is comprised of glycoproteins (gp), specifically, a cap, gp120, and a stem, gp41. These glycoproteins seen as “spikes” on the viral surface are used for selective binding to CD4 T cells (5).

The single stranded RNA genome of HIV has seven distinct regions. These include the long terminal repeat (LTR), trans-activation response (TAR) element, rev response element (RRE), psi element (PE), a poly(T) slippery site (SLIP), cis-acting response sequences (CRS) and the inhibitory RNA sequence (INS) (4, 5) (Figure 1.1). The LTR is responsible for the incorporation of retroviral DNA genetic sequences into host genomes and also acts as a transcription promoter. TAR is required for the trans-activation of the viral promoter as well as acting as a binding site for the transactivator of transcription (Tat) protein to activate the LTR. RRE is used as a binding site by the regulator of virion expression (Rev) protein to stabilize, export and shuttle the unspliced RNA from the nucleus to the cytoplasm. PE required for packaging of the viral genome.

SLIP is a poly(T) element that by encoding a T repeat causes a frame shift in the group specific antigen (Gag) reading frame into the polymerase (Pol) reading frame (4, 5) (Figure 1.1).

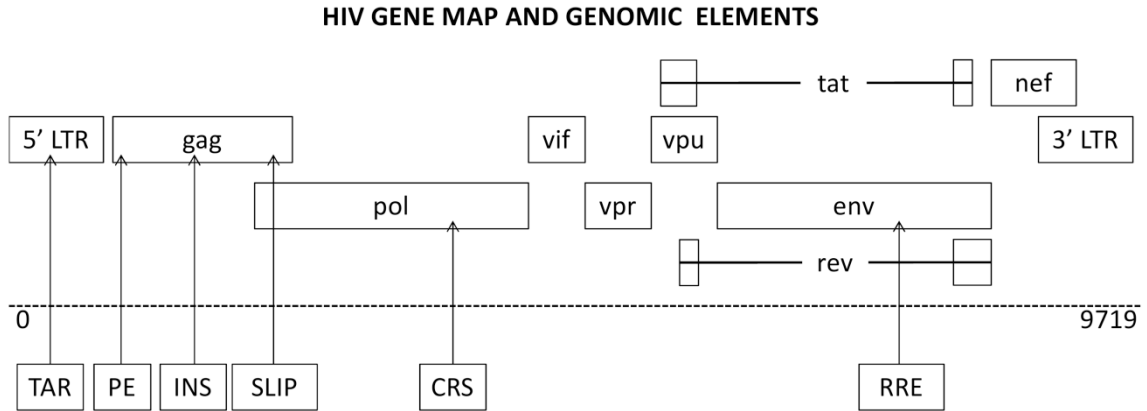


Figure 1.1 Schematic representation of the HIV genome including genes and genomic elements.

HIV-1 has nine genes including env, gag, pol, nef, rev, tat, vif, vpr, and vpu (4, 5) (Figure 1.1). As addressed above, the env gene is essential for production of gp160 protein (4-6). Gag (along with env) encode for the structural proteins of new virions. Pol codes for three essential enzymes: reverse transcriptase, integrase and HIV-1 protease. The negative factor (Nef) is involved in down regulating the CD4 receptor and the major histocompatibility complex (MHC) molecules in infected cells, thus masking them from attack by the immune system (5-8). The rev gene encodes Rev protein. Tat encodes two Tat proteins that act as transcriptional transactivators for the LTR promoter by binding to TAR (9). Viral infectivity factor (Vif) protein is used to prevent the apolipoprotein B mRNA editing enzyme, catalytic polypeptide-like protein (APOBEC) from deaminating DNA:RNA hybrids, specifically important because of its interference with Pol protein (4, 5). Viral protein R (Vpr) and viral protein U (Vpu) are other regulators of the virus and

are associated with infectivity (5). Gag, Pol, and Env are common to all retroviruses. Tat and Rev are essential for HIV replication (4, 5). The remaining genes are not essential for viral production in immortalized T-cell lines and are thus classified as accessory proteins.

1.2 HIV Viral Tropism

All strains of HIV-1 infect CD4+ cells; however, different isolates require distinct secondary coreceptors to undergo productive fusion and entry. HIV-1 entry is mediated by initial binding of virion envelope glycoprotein, gp120, with the CD4 molecule and gp41 with a chemokine coreceptor (CCR5 or CXCR4 mostly) (6). CD4 is a member of the immunoglobulin superfamily while the chemokine coreceptors are 7-transmembrane G-protein coupled receptors. HIV-1 virus that utilizes CCR5 (HIV-1 R5 or macrophage-tropic) is considered to be primary (10). There are also dual tropic variants that can recognize both CCR5 and CXCR4 (HIV-1 X4R5). Macrophages, which also express CCR5 and CXCR4, are assumed to be the first cells infected by HIV-1 and the last ones to harbor the virus after CD4 T cell depletion (6). There are also cells that do not express CD4 but are infected by HIV-1 including dendritic cells, and microglial cells which express CCR3 and/or CXCR4 (11).

Entry into the cell begins after CD4 and a chemokine receptor have been bound by the trimeric envelope complex (gp120). Upon binding with gp120, integrin is activated allowing for virological synapses, which mediates virus infection (6). With high-affinity binding of CD4 to gp120 the envelope undergoes structural changes to expose the chemokine binding domains of gp120 allowing them to bind with the

chemokine coreceptor. Gp41 is then used to penetrate the cell membrane allowing for entry of the viral capsid (6).

1.3 HIV Viral Genome Replication

After membrane fusion and upon partial disassembly of the capsid, viral enzymes and RNA are released into the cell. Microtubules are utilized for transport of the viral RNA as a complex to the nucleus (12). During transport, reverse transcriptase (RT) removes the RNA from the bound viral proteins and reverse transcribes it into DNA. After the first DNA strand is formed RT uses ribonuclease activity to degrade the viral RNA and finally acts as DNA-dependent DNA polymerase and replicates the sense DNA strand into an antisense DNA forming partial double stranded complementary DNA (cDNA) (12). This cDNA is directed by LTR binding and integrated into the host chromosome by integrase (13).

When viral mRNA is transcribed it is spliced into smaller pieces which are exported to the cytoplasm and translated into regulatory proteins Tat and Rev (4, 5). With Tat protein new virus production is encouraged and mediation of elongation of viral RNA occurs. Tat binds to the TAR RNA region that forms a stable stem-loop structure (9). Rev protein helps with viral RNA export from the nucleus, and allows unspliced RNAs to leave the nucleus. This cycle leads to a shift in viral gene expression, underlining the importance of, Rev as a facilitator for the timing of viral protein and enzyme synthesis (14). In the cytoplasm Gag and Env are translated from full length viral mRNAs. With Gag protein other full length RNAs are bound and packaged into new virus particles.

1.4 Accessory Proteins

During infection of immortalized T-cell lines by HIV-1, a number of genes are not essential for viral production. These “non-essential” genes code for what are known as accessory proteins. Of these, Nef protein held particular focus as a high potential target for HIV regulation (7). There are two forms of Nef protein translated from early transcripts that are produced by two initial codons on the 5’ end of the Nef mRNA (4-6). Each protein has several post translational modifications that cause them to vary in size from 24 to 27 kDa. Nef proteins have protein-protein (SH3) interaction domains that can mediate interactions with parts of the intracellular signaling pathways. This may provide an optimal environment for viral replication (15). The functions of Nef protein vary for different strains of virus and with different types of cells (7). It has been shown that Nef can down regulate surface expression of CD4, MHC class I molecules, as well as the immune costimulatory protein CD28 (8). This down regulation of surface expression may be a contributing factor for HIV-1 to evade typical host mediated viral removal leading to HIV-1 pathogenesis. In addition, Nef is packaged into new virions and enhances fusion of the viral envelope with the host cell membrane (7).

Later in infection full length transcripts are exported to the cytoplasm, allowing for the production of viral infectivity factor (vif), viral protein R (vpr) and viral protein U (vpu) from unspliced RNA (5). The Vif protein remains mostly in the cytoplasm and the plasma membrane of infected cells (16). It was shown in early HIV-1 studies that the mutant viruses without Vif were around a thousand times less infectious than wild type virus (16). Recent work has shown that Vif plays a role in inhibiting the antiviral action of CEM15/APOBEC3G, a cellular cytidine deaminase (16, 17). This enzyme catalyzes

the deamination of deoxycytidine (dC) to form deoxyuridine (dU) destroying the coding and replicating ability of HIV-1.

Vpr affects the rapidity of the virus to replicate in and destroy T cells (7). The functions for Vpr are induction of G2 cell cycle arrest and promotion of viral entry into the nucleus. It is unknown why G2 arrest is beneficial for virus production but is potentially associated with LTR activity. Lastly, Vpr was shown to bind nuclear pore proteins that may facilitate docking of the HIV-1 preintegration complex (7).

In HIV-1 and SIV, Vpu is required for proper maturation of progeny virions and their release (18). Without this protein, virions can contain multiple cores and budding is to intracellular vacuolar compartments rather than the plasma membrane.

1.5 HIV Viral Assembly and Budding

Assembly of new HIV-1 virions occurs at the plasma membrane of the host cell. The Env polyprotein (gp160) passes through the endoplasmic reticulum and is transported to the golgi complex where it is cleaved by protease into two HIV envelope glycoproteins gp41 and gp120 (6). These glycoproteins are transported to the plasma membrane where gp41 anchors gp120 to the membrane of the infected cell. Maturation occurs in the forming bud or in the immature virion after it buds. During this process HIV-1 proteases cleave polyproteins into individual functional HIV-1 proteins and enzymes (6). This mature virus is now able to infect another cell.

1.6 Viral Transmission

HIV is primarily acquired through unprotected sexual encounters via contacts of infected body fluids to the mucosal membranes of the other. The rate of transmission from female-to-male is 0.04% and from male-to-female is 0.08% per act, while the rate for receptive anal intercourse is 1.7% (19). These percentages can be much higher in low-income countries for many various reasons, including potential predisposing conditions such as genital ulcerations. The use of latex condoms can reduce the risk of sexual transmission of HIV by nearly 85% (20). However, the consistent use of condoms is limited by supply due to economic unavailability, belief systems and practices.

The transmission efficiency of HIV-1 varies during the course of infection and is not consistent between individuals. However, each one log increase in viral level of HIV in the blood is associated with a drastic increase in rate of transmission (21). Women have a higher susceptibility to HIV-1 infection due to hormonal changes, vaginal microbial ecology and physiology as well as a higher prevalence of sexually transmitted diseases (21).

1.7 AIDS

Once a patient is infected with HIV-1, the virus progressively depletes immune cells leading to AIDS and leaves individuals susceptible to opportunistic infections and tumors (22). The primary characterization of AIDS is depletion of CD4+ T cells to a level of 200 cells or less per mm^3 of blood, a 1000 fold difference from normal baseline levels (23). CD4 T cells are essential for establishing and maintaining the immune system. The loss of these cells occurs most abundantly during the acute phase of infection when HIV-

1 causes induced cell lysis and cytotoxic T cells target and kill infected cells. T cell population is gradually decreased as the ability of the immune system to generate and replenish cells is diminished causing viral mediated T cell loss to surpass production (23). Most CD4+ T cell loss happens during the first weeks of infection, particularly in tissues such Peyer's patches of intestinal mucosa which have high numbers of lymphocytes. Cells in intestinal mucosa additionally have a much higher expression of CCR5 coreceptor compared to the T cells of blood making them more susceptible to HIV-1 infection (22). Even with this large loss of CD4+ T cells, infected subjects usually remain subclinical for years after initial infection.

AIDS has very mild symptoms caused by the disease itself, usually limited to non-specific conditions such as fever, sweats, chills, weakness and weight lost (24). The associated indications of AIDS are therefore primarily caused by opportunistic infections from bacteria, viruses and fungi that would normally be controlled or eliminated by a competent immune system (24). These infections are common in people with AIDS and can infect almost every organ system allowing even simple infections to be life threatening. AIDS has also been associated with an increased risk of cancer development. Cancers that arise from immune cells, such as lymphomas, are specifically more common in AIDS patients (25).

Without treatment the median time of progression from HIV-1 infection to AIDS is nine years. The survival time after development of AIDS is 9.2 months (26). The rate of progression can be affected by many factors, including the body's ability to defend against HIV, age, access to health care and the presence of co-existing infections.

1.8 HIV latent reservoir

With current treatment by highly active antiretroviral therapy (HAART), many people are able to achieve suppressed HIV viral levels below the limit of detection for many years (13). However, with current drug regimens HIV is not completely eradicated, as seen when HIV viral loads rebound after withdrawal of HAART. Due to the integration of HIV into the genome of infected cells, and with its primary target being T cells which can function as long lasting memory cells, HIV-1 can remain dormant for years (13). The latent reservoir can be measured by co-culturing CD4+ T cells from infected patients with susceptible cells *in vitro* and measuring the levels of HIV-1 protein or RNA. This aspect of HIV-1 is most challenging when developing an effective treatment against infection.

1.9 Animal Models for HIV Research

The fact that HIV-1 does not infect and cause disease in any species other than in humans is problematic for the process of evaluating compounds, especially vaccines and preventative therapeutics (27). In the initial years of HIV-1 research an animal model that was suitable for efficiently predicting drug efficacy in humans was not available. Preliminary testing with nonhuman primates and their species specific lentivirus (SIV) was able to recapitulate the modes of infection, disease course and antiviral immunity that are seen in HIV-1 infections of humans (27). The nonhuman primate model has been essential in understanding the key aspects of lentiviral disease. However, many aspects of this model render its usefulness limited. First, although very similar to humans, the macaque immune system has species specific cell receptors that render HIV-1 itself

unable to cause and sustain infection (28). Utilizing SIV as a substitute for HIV-1 allows for similar retroviral experimentation but lacks the complexities and specifics of HIV-1. Additionally, various strains including drug resistant and mutant strains of HIV-1 cannot be evaluated in this model. The macaque model was utilized for the first vaccine development for HIV-1; however, after a phase III trial in humans failed, the model was unable to validate any vaccine candidate (29). Additionally, the large size of the monkey model makes it expensive, limiting its potential for evaluating a broad range of compounds. With the lack of a model to fully recapitulate infection and efficacious effects of vaccines or preventative therapeutics it was originally speculated that prophylactic approaches would solely be limited to human phase I trials (29).

The smallest available natural model for the study of lentivirus infections is the cat with feline immunodeficiency virus (FIV). FIV has a number of similarities with HIV-1 including viral structure, induced pathology and transmission (30). Like HIV-1 the primary characteristic of infection is CD4+ T cell decline. However, FIV also infects B cells and some sub populations of CD8+ T cells (31-33). As with AIDS in humans, the cause of death in FIV infected cats is opportunistic infection.

With these similarities this model has been a useful tool for parallel studies of HIV infection, particularly in immunological similarities that occur in the course of both these lentivirus infections. Additionally, due to the commonalities of HIV-1 and FIV in replication and multiple genome structures, FIV infection in the cat serves as a model for drug design (34). However, there are differences in FIV and HIV-1, including FIV lacking some of the HIV-1 accessory proteins, different viral envelopes and the repertoire

of infected cells. These differences may limit the predictability for efficacy of HIV-1 specific drugs.

For these reasons the development of a humanized model that replicates a human immune system is required for detailed pre-clinical testing. The recently developed humanized mouse has been effectively able to reproduce a human immune system that is susceptible to HIV-1 infection.

1.10 Humanized Mice

To utilize pluripotent hemopoietic stem cells (HSC) to their full potential requires a recipient capable of being repopulated for a hemopoietic system with complete multi-lineage hemopoieses. Additionally, it would be advantageous if the system could sustain such a long-term engraftment. The use of HSC *in vivo* is most appropriate for the small animal model given their small size and cheaper costs. With the use of small animal models rapid evaluation can be conducted drastically reducing the time frame for experimental observations.

The first humanized mice were produced by injection of human stem cells in irradiated mice (35-38). These studies, although successful, only displayed low engraftment levels. To enhance transplantation success, knock-outs in genes important in development of the immune system, including *Hfh11^{nu}* and *Prkdc^{scid}*, were utilized to develop immune-compromised models (38-41). Prkdc, or protein kinase DNA activated catalytic polypeptide, was identified as an essential catalytic subunit of a DNA recombinase enzyme that is disrupted by the scid allele. With *Prkdc^{scid}* the gene has a nonsense mutation (42). This scid mutation was first observed in BALB/c mice in 1983

and displayed engraftment of human peripheral blood mononuclear cells (PBMC) (43, 44). Mice homozygous for the scid mutation are unable to express rearranged antigen receptors resulting in lack of mature host T and B lymphocytes (43, 44). However, some antigen receptor rearrangements do still spontaneously occur and have been termed as “leakiness” (45).

After successful production of the scid mouse, human fetal liver or fetal bone marrow cells were injected hepatically in unirradiated pups (46). The human cells survived and maintained many of the characteristics of normal human marrow in the scid host. A number of investigators utilized this SCID-hu model for various studies, including human gene therapy protocols (47, 48), and human immunological assays (49). However, even with these advances peripheral engraftment remained low, only 0.5-5% (50). Additionally, the human cell populations failed to utilize many of the murine hemopoietic growth factors, failing to develop adequate cell proliferation and differentiation. It was also assumed that competition with host cells may be the cause for the limited engraftment levels (50).

To increase the stability of xeno-engraftment, these mice were crossed with non-obese diabetic (NOD) mice to generate the NOD-SCID model (51, 52). Further knockouts in the interleukin receptor common gamma chain and recombination activating genes has given rise to the newer generation of humanized NOD-SCID^{-/-}γc^{-/-} (hNOG) and Rag2^{-/-}γc^{-/-} (RAG-hu) mouse models (53, 54). The common gamma chain, γc, is a cytokine receptor sub-unit and is important in the formation of functional cytokine receptors on lymphocytes. The recombination activating gene (RAG) encodes enzymes that are essential for the rearrangement and recombination of the genes encoding T cell

receptors during VDJ recombination (54). These developments promote engraftment of foreign tissue, especially human hematopoietic CD34+ stem cells. RAG-hu and hNOG mice are prepared by injecting either cord blood or fetal liver derived CD34+ cells hepatically, which give rise to multilineage human hematopoiesis (53, 54) (Figure 1.2). These models have higher human engraftment levels which are sustained for more than a year (55). These mice are susceptible to HIV-1 and thus HIV can be used as the challenge virus directly (56). Furthermore, these mice are susceptible to vaginal and rectal HIV-1 transmission (57, 58). Additionally, advancement with the NOD-SCID model by transplantation of thymic and liver tissues under the kidney capsule followed by hepatic injection of autologous human CD34+ cells has led to the BLT (Blood, Liver, Thymus) mouse model (59-60). This model shows the highest levels of human engraftment including substantial T cell development; however, due to its design it requires extensive labor and manipulation resulting in limited production and higher cost.

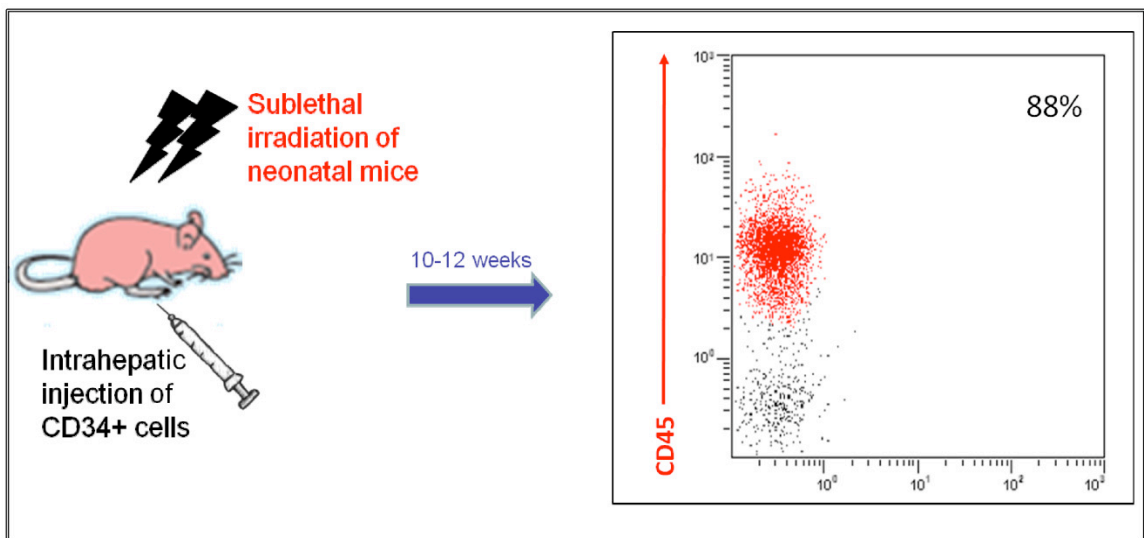


Figure 1.2 Humanized RAG-hu mice. Neonatal mice were irradiated and injected intrahepatically with FL CD34 cells. Ten to twelve weeks later, peripheral blood was collected and the cells were subjected to FACS analysis by staining for CD45 to determine human cell engraftment. Engraftment level in a representative mouse is shown.

1.11 HIV Vaccine

Almost since the time of HIV discovery the pursuit of an HIV-1 vaccine has been ongoing (61). Even with the advent of novel vector-based DNA vaccine designs, clinical trials have resulted in little protective efficacy, with the RV 144 Thailand trial providing the most positive, though modest, results to date (62, 63). HIV-1 vaccine design has been limited by the viruses' propensity for mutation, which is driven by the absence of corrective mechanisms during reverse transcription. Thus, even when a protective adaptive immune response can be developed, viral evolution is able to circumvent both antibody and cytotoxic defenses, allowing escape mutants to infect newly proliferating CD4+ T cells and further damage the already weakened immune system.

HIV vaccine development has also been limited by lack of a defined protective immunity. Research thus far indicates that the cellular mediated immune response, both innate and adaptive, are key to controlling HIV-1 replication, which is counter-intuitive when compared with the protective humoral responses elicited by other viral vaccinations. HIV-specific CTL responses combined with over-expression of specific HLA-I alleles (HLA-B*57, HLA-B*27, and HLA-C) are associated with low viral loads (64, 65). Natural killer cells can become activated via HIV-1's downregulation of HLA-A and HLA-B proteins, leading to a stronger anti-HIV CD8+ T cell response via NK-DC cross-talk (66). Other cell types, including plasmacytoid dendritic cells, T regulatory cells, and Th17 cells are likely involved, but their specific roles are still unclear, especially how they could influence vaccination (67).

One of the major obstacles to understanding exactly how an HIV-1 vaccine would function is the lack of a suitable animal model that can recapitulate a protective immune

response, or at least provide details of where a vaccine falls short. Such a model could save countless resources spent on large cohort vaccination studies and weaker animal models that fail to provide human correlative data. Currently macaques or chimpanzees are most commonly utilized, but non-human primates are unable to be infected with HIV-1, leading researchers to depend on Simian Immunodeficiency Virus (SIV) or hybrid SHIV (HIV with an SIV envelope) infections in attempts to replicate human HIV-1 infection. A mouse-model for HIV-1 infection could be a valuable resource for researchers seeking a model that more closely resembles the human immune system (59).

1.12 Anti-retroviral Drugs

The first anti-retroviral drug licensed for AIDS treatment in the United States was Zidovudine (AZT) (68). AZT is a nucleoside analog inhibitor of viral reverse transcriptase. This drug works by acting both as a competitor of normal nucleoside triphosphates and, when incorporated into viral DNA, acts as a chain terminator. AZT was successful initially but due to the rapid mutation rate of HIV long term treatment was not effective (69). The earliest protease inhibitors were made almost by chance as renin inhibitors, being developed as antihypertensive drugs, and were later adjusted for use in antiviral treatment. Derivatives and advances of these became the first generation of efficacious protease inhibitors (70). HIV-1 Protease is a virus encoded enzyme that is translated from a polycistronic RNA. Protease is required for infectivity of new virions and inhibition of this enzyme ablates viral infectivity. It was also quickly realized that efficiency of treatment could be increased, further delaying the onset of AIDS, when

three or more drugs were given as a combinatorial treatment. This treatment is known as Highly Active Antiretroviral Therapy (HAART) (71).

Treatment of HIV/AIDS by HAART has been very successful, having substantial reduction in viral loads and in patients that had remarkable recoveries (70, 71). Patients that are successfully treated with HAART sustain viral load levels below detection limits. This suppression can remain for years and can prevent the onset of AIDS. However, in all the years of HAART administration to HIV-1 infected patients none have been completely cleared of virus. This is clear when tissues are examined to show viral replication is not completely suppressed (72). Additionally, intermittent virus replication can occur allowing for the potential of drug-resistant viruses to emerge (72). Once these strains propagate, treatment efficacy becomes limited. Additionally, current HAART drugs must be taken regularly and even multiple times a day. These drugs also have significant side effects resulting in noncompliance of the patients. A major focus on drug development is timely dose efficacy and reduction or removal of side effects (72).

Many steps in the HIV-1 replication cycle offer opportunities for possible intervention. One obvious candidate is the retroviral enzyme integrase. Structural data and biochemical information about this protein have become available, and potent inhibitors of its activity have been identified, such as the clinically approved anti-retroviral drug raltegravir (73). Further, inhibitors of HIV-1 fusion that target either viral envelope protein or host cell chemokine coreceptors have been proven efficacious (74). Maraviroc, a small molecule CCR5 antagonist is one example of a clinically licensed fusion inhibitor.

Even with all the advances in drug therapy many obstacles remain. For example to accomplish a cure via drug therapy, it will be necessary to develop drugs that can enter all virus accessible sites. This includes passing the blood brain barrier and targeting hematopoietic stem cells in the bone marrow (72). For drugs to be efficacious in long term treatment the viral reservoirs in latently infected quiescent long-lived memory T cells must be addressed. Lastly, any treatment that is prolonged will develop autoimmunity untoward side effects, issues with anergy of the immune system, or activating it in an undesired way, and non-compliance from patients (73). Even with these difficulties the door to novel therapeutics for treatment and prevention of HIV-1 infection and/or AIDS development remains wide open.

1.13 Pre-exposure Prophylactics and Microbicides

The first anti-HIV microbicides were developed in an attempt to disrupt viral infection, however, these drugs lacked specificity to HIV-1 and had limited neutralizing ability to multiple strains resulting in failed protection in field trials (75). The initial failure of microbicides was also due partly to the lack of a suitable animal model that used HIV-1 directly. Without this model only clinical trials that are expensive and rely heavily on patient compliance limit not only controlled testing but also wide range screening of potentially efficacious compounds. In this regard the SCID humanized mouse model was used for evaluating the efficacy of microbicides (76). However, due to low levels of human cells in vaginal mucosa the vaginal infection rate was found to be variable making this model unreliable for microbicide testing (77). This limitation has thus been solved with the already discussed models (RAG-hu and BLT) which allow for

greater human cell engraftment resulting in higher levels of HIV-1 susceptible cells in the mucosa (57). Testing of potential HIV-1 microbicide compounds topically administered to vaginal or rectal mucosa has so far not been reported using these humanized mouse models (76). The majority of RT inhibitors such as tenofovir fill the list of potential anti-HIV microbicide candidates (78, 79). Tenofovir has already been tested in human clinical trials and showed partial protection in the field, illustrating the potential for efficient and efficacious microbicides against HIV-1 (79).

Another approach to preventative methods against HIV-1 is by systemically delivered pre-exposure chemo-prophylactic. A chemo-prophylactic can simply be the use of clinically approved effective compounds applied prior to HIV-1 exposure. An effective pre-exposure prophylactic (PrEP) that can prevent sexual transmission of HIV-1 is likely to play a major role in preventing millions of new cases (80). It will also empower women to protect themselves from HIV risk. The benefits of PrEP in the infectious disease field have been already well documented for the prevention of malaria and mother-to-child transmission in the case of HIV-1 (81-83). An effective PrEP, when available, is estimated to prevent 2.7 to 3.2 million new infections in sub-Saharan Africa and thousands of new cases in high risk individuals in the USA (84).

Currently there are numerous clinically approved effective anti-retroviral drugs that are used to treat HIV infection and some of these can be potentially exploited for developing an effective PrEP (85, 86). That PrEP can prevent sexual transmission is substantiated by the early studies in non-human primates which employed daily oral administration of RT inhibitors tenofovir (TDF) and/or emtricitabine (FTC) (87-89). This concept has reached clinical trials in which tenofovir is currently being investigated for

its prophylactic efficacy (87). It is necessary to continually evaluate new candidates since a PrEP with proven protective efficacy now may not retain its effectiveness in the future years given the propensity of HIV-1 to develop drug resistance. While the monkey model has been very useful in evaluating appropriate candidate PrEPs, there are a number of limitations for its use to screen large numbers of potential candidates (89). In this context, it was recently shown that tenofovir could prevent HIV-1 vaginal transmission using the BLT mouse model (90). Using the same model, it was also shown that systemic administration of TDF (tenofovir) and FTC (emtricitabine) prevents HIV-1 infection via vaginal and i/p challenges thus setting the stage for large scale evaluation of different anti-HIV compounds for their efficacy as PrEPs as well as topical microbicides in preventing HIV-1 infection (91).

1.14 siRNA-based Therapeutics

Small interfering RNAs (siRNAs) are 21-22 base long RNAs that guide sequence-specific degradation of target mRNAs (92). The conserved biological response of the RNAi phenomenon was originally discovered in petunia flowers after a study to introduce a pigment producing gene under the control of a strong promoter gave an unexpected result of decreased pigment (93, 94). This silencing of the introduced gene along with the homologous endogenous gene was termed “cosuppression” (93, 94). Evidence that this gene silencing resulted from dsRNA was first reported after dsRNA was injected into *Caenorhabditis elegans* and complete silencing of the homologous gene was observed (95, 96). Later, this same phenomenon was verified in the *Drosophila* model after dsRNA was injected into embryos (97).

Given the ability to direct sequence specific silencing of target mRNAs, siRNAs have the potential to function as bio-drugs for treatment of a wide range of human maladies (98-101). Naturally occurring RNAi is initiated when the cell encounters long dsRNA molecules transcribed from viral infections, degenerate cellular transcripts, or endogenously transcribed micro RNAs (miRNAs). Once these dsRNA molecules are recognized cascades of events occur that involve the RNase-III like enzyme Dicer and the multi-protein complex, RISC (RNA induced silencing complex) (102-103). Longer dsRNA molecules are cleaved by Dicer into 19-24bp dsRNA molecules which are then bound within the RISC complex (Figure 1.3). The RISC complex unwinds the short dsRNA and uses the antisense strand as a sequence specific guide. With this guide the RISC complex uses its endonuclease activity to degrade the homologous mRNA transcripts (Figure 1.3) (104, 105). In early studies using RNAi from long dsRNAs in mammalian cells resulted in the induction of interferon responses which shuts down cellular protein synthesis leading to cell death (106). This inhibited initial research with RNAi (107, 108). Later, small dsRNAs were utilized for sequence-specific inhibition of target mRNA without activating the interferon response (107). To extend the half-life of intracellular siRNAs, certain modifications have been developed including protecting siRNAs from nucleases by 2'-OH modifications (108).

Several recent studies have demonstrated the use of siRNAs in functionally down-regulating expression of HIV-1 and host mRNAs against viral and cellular targets (100, 109-111). In similarity with the use of HAART, siRNA-based therapeutics that target combinations of distinct genomic regions of HIV-1 or target HIV-1 host dependency

factors (HDFs) can be administered in a tailored fashion to minimize the possibility of viral escape mutants (113, 114).

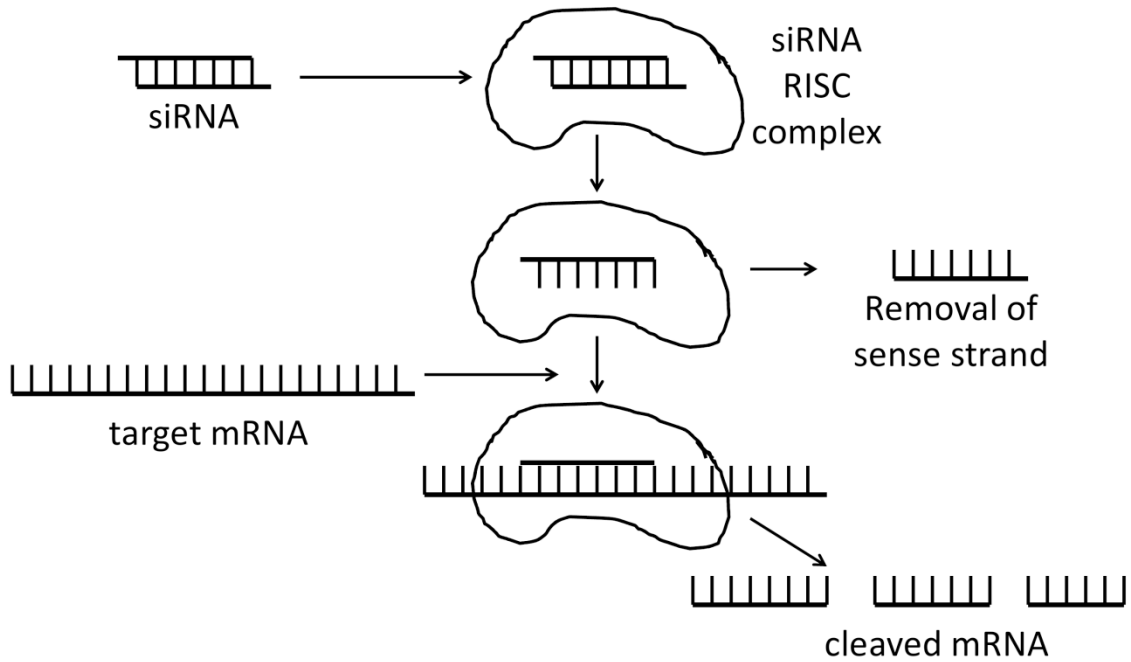


Figure 1.3 Mechanism of RNAi. Small interfering RNAs (siRNAs) are introduced to the cell exogenously or are expressed endogenously. These short dsRNA molecules are incorporated into the RISC complex where the antisense strand is used for sequence specific homologous mRNA target degradation.

Although siRNAs hold promise for treatment of HIV/AIDS, efficient, systemic delivery of siRNA *in vivo* remains a principal challenge to achieve the desired RNAi potency for successful clinical application (115, 116). Most HIV-susceptible cells (such as, CD4+ lymphocytes and monocytes) are exceedingly difficult to transfect with non-viral agents such as liposomes. Several delivery strategies such as carbon nanotubes (116) and carbosilane dendrimers (117) have been shown to deliver siRNAs into cultured human T cells and primary PBMCs. However, the complicated formulations (nanotube

functionalization and nanotube-siRNA conjugation) and high concentration of siRNA needed (> 300 nM in the case of carbosilane dendrimers) make them less favorable for *in vivo* anti-HIV applications. Other strategies, such as the use of cell-penetrating peptide-dsRNA-binding fusion proteins (118), antibody Fab fragment-protamine fusions (119) and a CD7-antibody-polyarginine conjugate (120) have been used to functionally deliver siRNAs and induce RNAi responses *in vivo* without cytotoxicity. However, protein or antibody based delivery involves rather complex and expensive production processes, poor binding capacities for siRNAs and potential immunogenicity. Therefore, there is still a pressing need for developing simple and safe non-viral siRNA delivery systems for possible clinical applications.

1.14a PAMAM Dendrimers

Poly(amidoamine) (PAMAM) dendrimers are a class of highly branched, structurally well-defined chemical polymers which bear cationic primary amine groups on their spherical surface and are able to form stable and uniform nanoscale complexes with negatively charged nucleic acids via electrostatic interactions. Once formed, the complexes can protect nucleic acids from ribonuclease degradation and promote cell uptake via endocytosis (121, 122). The dendrimers possess numerous tertiary amines in the interior, which will be protonated in the acidic endosomes and thus lead to the osmotic endosome swelling (proton sponge effect) to promote the release of nucleic acids from dendrimer/nucleic acid complexes.

A series of structurally flexible PAMAM dendrimers bearing a triethanolamine (TEA) core as effective vectors for RNA interaction (123) and siRNA delivery (124)

have been previously developed. The flexible structure imparts these dendrimers with stronger interactions with nucleic acids via a mutually induced fit process. At the same time, it promotes efficient dissociation of nucleic acids in endosomes via a proton sponge effect. Recently, these TEA-core PAMAM dendrimers have been used to deliver a heat shock protein (Hsp) siRNA into human prostate cancer (PC-3) cells, resulting in specific silencing of the Hsp gene and inhibition of cell proliferation (125). Thus, these dendrimers represent an attractive and relatively simple vehicle for siRNA delivery.

1.14b gp120 Aptamer

HIV-1 infection is initiated by the interactions between the external envelope glycoprotein gp120 of HIV and the human cell surface receptor CD4 (126-129), subsequently leading to fusion of the viral membrane with the target cell membrane (130, 131). Thus, HIV-1 entry into its target cells represents an attractive target for new anti-HIV-1 drug development (133-138). The most effective anti-HIV drugs used in the clinic consist of combinations of compounds that block the early reverse transcription step, and the late viral gag protein maturation step (139-141). Preventing the virus from binding to its primary receptor is one of the most obvious and direct ways to prevent infection. One rational antiviral approach is to create small ligands directed to the virus surface protein gp120. Successes in discovering new classes of gp120-directed inhibitors targeting initial step of HIV-1 entry have been reported in recent years (134, 141, 142). Soluble CD4 (sCD4) has demonstrated efficacy against many laboratory strains (143, 144); however disappointing results from clinical trials were attributed to poor activity of this drug against primary isolates (145, 146). Another entry inhibitor PRO-542, a CD4-IgG

recombinant fusion protein effectively neutralizes many HIV-1 strains in cell culture (147, 148) as well as clinical isolates (149, 150), but unfortunately this drug has not enjoyed widespread use in clinical treatment of HIV-1 infection.

Other inhibitors bind gp120 less specifically through electrostatic or lectin–carbohydrate interactions [sulfated polymers, cyanovirin (151)]. These properties create challenges for the practical implementation of these molecules as drugs. In 2003, Martin et al. (152) designed a 27-aa CD4 peptide mimic, CD4M33, which was shown to bind to gp120 and inhibit HIV-1 infection *in vitro*. The clinical application of this peptide has not yet taken place though. Aside from antibody or peptide mimics, nucleic acid aptamers with low to mid-range nanomole binding affinities are an attractive class of therapeutic molecules (153–156). Aptamers which block the interaction of gp120 and CD4 have been previously developed. One such aptamer was shown to specifically interact with the conserved coreceptor interacting region of R5 strain gp120 (154). Although both aptamers and antibody or engineered peptide mimics have great specificity and binding affinity, the nucleic acid-based aptamers offer more synthetic accessibility, convenience in modification, chemical versatility, stability and lack of immunogenicity (157). Therefore, aptamers can be utilized for flexible applications ranging from diagnostic to therapeutic assay formats (158,159). Aptamers that target specific cell surface proteins are employed as interesting delivery molecules to target a distinct cell type, hence reducing off-target effects or untoward side effects. The first example of aptamers used for siRNA delivery is an anti-PSMA aptamer (159) that binds tightly to the prostate-specific membrane antigen (PSMA), a prostate cancer cell-surface receptor.

McNamara et al. (160) in 2006 reported the use of this aptamer for receptor mediated siRNA delivery. In this study, they selectively delivered a 21-mer siRNA into PSMA expressing cells, resulting in silencing of target transcripts both in cell culture and *in vivo* following intra-tumoral delivery. Similarly, Chu et al. (161) used a modular streptavidin bridge to connect lamin A/C or GAPDH siRNAs to the biotinylated variants of this anti-PSMA aptamer. Consequently, this system induced silencing of the targeted genes only in cells expressing the PSMA receptor. The targeting properties of the anti-PSMA aptamer also can be exploited for localizing other therapeutic agents to tumors such as a toxin (162), doxorubicin (163) or nanoparticles (164-167). We recently described a novel dual inhibitory function anti-gp120 aptamer-siRNA chimera, in which both the aptamer and the siRNA portions have potent anti-HIV activities as described in chapter five (168). Additionally, HIV gp120 expressed on the surface of HIV infected cells was used for aptamer-mediated delivery of an anti-HIV siRNA, resulting in pronounced inhibition of HIV replication in cell culture.

For treatment of HIV using aptamer-siRNA chimeras, it is highly desirable to generate new aptamers to expand the diversity of target recognition for potential use *in vivo*. New anti-gp120 aptamers and various siRNAs targeting different genes could be combined to avert viral resistance to a single aptamer-siRNA combination. The aptamer approach thus provides a broad spectrum HIV-1 neutralizing agent and siRNA delivery vehicle. The combined aptamer-siRNA approach is an attractive, non toxic therapeutic approach for treatment of HIV infection that can be designed to circumvent viral resistance.

Among HIV-1 molecules the Tat and Rev proteins are essential for subsequent expression of HIV-1 structural genes (Gag, Pol and Env) and for the synthesis of full length viral genomic RNA (82). SiRNAs designed to destroy the *tat/rev* transcripts were found to be highly effective in viral suppression (116, 169, 170). With the advent of aptamer technology for targeted siRNA delivery it is now feasible to use the aptamer binding function for receptor mediated endocytosis of siRNAs (171-173).

1.15 Gene therapy

Without a complete cure available for complete removal of HIV-1, current therapeutics requires multiple treatments for continued viral suppression. Multiple treatments are expensive, require adherent behavior and may result in undesired side effects. In this regard anti-HIV gene therapy techniques hold considerable promise for efficacy from single treatment. Previous work has demonstrated this potential *in vitro* conveying viral resistance to primary T cells and macrophages (174-176). However, these cells do not continuously produce new cells and are subsequently eliminated from the body over time. To address this issue hematopoietic CD34+ stem cells (HSCs), originating in the fetal liver and later in the bone marrow, continuously produce the cells of hematopoietic origin that are the primary target cells of HIV. Promising data has been obtained showing that anti-rev siRNAs against HIV were functional in conferring viral resistance in differentiated T cells and macrophages derived from transduced CD34+ hematopoietic progenitor cells (177). The therapeutic transduction of anti-viral constructs should therefore focus on HSCs (178). An HIV resistant immune system harboring functional T cells, B cells and monocytes/macrophages transduced with anti-HIV

constructs can be developed and continuously replenished (178). This modified, HIV-resistant immune system may detour AIDS progression, restore immune function as well as sufficiently lower HIV-1 viremia. This single treatment therapy could effectively replace HAART, conveying significant improvement to a patient's quality of life.

The first retroviral vectors used in a gene therapy setting were derived from murine leukemia virus (178). However, these vectors preferentially integrated near transcriptional start sites (179). These vectors were also severely limited by their ability to only transduce dividing cells, due to their inability to transverse the nuclear membrane (180). This aspect of the murine leukemia vectors made the transduction of quiescent cells extremely difficult. The lentiviral vector system has proved advantageous for efficiently transducing specific genes into non-dividing cells (181). Although favorable, there are some concerns regarding safety using lentivirus vectors, including insertional mutagenesis and generation of recombinants. These concerns stem from lentiviral vectors tending to integrate in chromosomal regions that have a high concentration of transcribed genes (179). Although unlikely, it is possible that recombination of the lentiviral vectors and endogenous retroviral sequences could generate new viral strains.

To utilize the lentivirus as a safe vector numerous alterations were made including deleting the accessory proteins (Vif, Vpr, Vpu, and Nef) to decrease the likeliness of recombination and invoking an immune response, replacing the 5' LTR U3 region with the cytomegalovirus immediate early promoter to allow the vector to be Tat independent and pseudotyping with a vesicular stomatitis virus envelope (VSV-G) gives a greater range of transducible cells (182-184). Additionally, a reporter gene, enhanced green fluorescent protein (EGFP), was included to detect transduction of target cells. Lentiviral

vectors have been shown to be highly efficient in transducing hematopoietic stem cells (182).

Using this vector system three anti-HIV constructs, each with its own method of action, were combined into a single Triple-R construct, providing a combinatorial approach to overcome escape mutations (185). The Triple-R construct is comprised of a tat/rev small interfering RNA, a CCR5 ribozyme and a TAR decoy, each of which has had its mode of action previously described, both *in vitro* and *in vivo*, for efficient intracellular immunization against HIV (185). Specifically, a tat/rev siRNA degrades the viral Tat and Rev transcripts affecting tat/rev regulatory junctions. The TAR decoy competes with Tat for binding to TAR, sequestering Tat protein function and decreasing transcription normally initiated by Tat (186). The CCR5 ribozyme binds to and cleaves CCR5 RNA transcripts, preventing the surface expression of CCR5, used as a co-receptor for infection by R5-tropic HIV-1 strains. We and others have shown that a strong down-regulation of CCR5 is effective at blocking R5 strains, which are the most prevalent (187, 188).

This Triple-R construct has been previously evaluated *in vitro* showing long-term expression and anti-viral protection (175). We have also shown that Triple-R vector-transduced HSCs undergo normal lineage specific differentiation in SCID-hu mice, giving rise to phenotypically normal transgenic T cells that are resistant to HIV infection (189). However, it is unclear if a more complete *in vivo* immune system can develop from transduced CD34 stem cells and resist HIV-1 infection.

CHAPTER 2

ORAL PRE-EXPOSURE PROPHYLAXIS BY ANTIRETROVIRALS RALTEGRAVIR AND MARAVIROC PROTECTS AGAINST HIV-1 VAGINAL TRANSMISSION IN A HUMANIZED MOUSE MODEL

Neff CP, Ndolo T, Tandon A, Habu Y, Akkina R (2010) Oral pre-exposure prophylaxis by antiretrovirals raltegravir and maraviroc protects against HIV-1 vaginal transmission in a humanized mouse model. *PloS One* 5: e15257.

This chapter contains results from my experiments that were included in the publication cited above.

2.1 Overview

Sexual HIV-1 transmission by vaginal route is the most predominant mode of viral transmission, resulting in millions of new infections every year. In the absence of an effective vaccine, there is an urgent need to develop other alternative methods of pre-exposure prophylaxis (PrEP). Many novel drugs that are currently approved for clinical use also show great potential to prevent viral sexual transmission when administered systemically. A small animal model that permits rapid preclinical evaluation of potential candidates for their systemic PrEP efficacy will greatly enhance progress in this area of investigation. We have previously shown that RAG-hu humanized mouse model permits HIV-1 mucosal transmission via both vaginal and rectal routes and displays CD4 T cell loss typical to that seen in the human. Thus far systemic PrEP studies have been primarily limited to RT inhibitors exemplified by tenofovir and emtricitabine. In these proof-of-concept studies we evaluated two new classes of clinically approved drugs with different modes of action namely, an integrase inhibitor raltegravir and a CCR5 inhibitor maraviroc as potential systemically administered chemo-prophylactics. Our results showed that oral administration of either of these drugs fully protects against vaginal HIV-1 challenge in the RAG-hu mouse model. Based on these results both these drugs show great promise for further development as orally administered PrEPs.

2.2 Materials and Methods

2.2a Generation of humanized Rag2^{-/-}γc^{-/-} mice (RAG-hu mice)

Humanized BALB/c-Rag2^{-/-}γc^{-/-} (RAG-hu) mice were prepared by engraftment with human fetal liver-derived CD34+ hematopoietic progenitor cells as we previously

described (55, 56). Mice were maintained at the Colorado State University Painter Animal Center. These studies have been reviewed and specifically approved by the CSU Institutional Animal Care and Use Committee (Protocol 09-1460A). Briefly, newborn mice were conditioned by irradiating with 350 rads and then injected intrahepatically with $0.5-1 \times 10^6$ human CD34+ cells. Mice were screened for human cell engraftment at 10-12 weeks post-reconstitution. Peripheral blood was collected by tail bleed and red blood cells were lysed by using the Whole Blood Erythrocyte Lysing Kit (R&D Systems, Minneapolis, MN). The white blood cell fraction was stained with antibodies against the human pan-leukocyte marker CD45 (Caltag) and FACS analyzed to determine the levels of human cell engraftment as we previously described (55). Individual peripheral blood engraftment levels in the mice vary, as previously described, hence female mice with varying human cell reconstitution levels greater than 40% (Table 2.1) were chosen for vaginal infections (55).

2.2b Oral administration of anti-HIV drugs raltegravir and maraviroc and HIV-1 challenge by vaginal route

Female RAG-hu mice were administered with either raltegravir or maraviroc by oral gavage (6 mice each). Clinical formulations of these drugs in tablet form Maraviroc (Selzentry) 150mg, Pfizer Labs; Raltegravir (Isentress) 400mg, Merck & Co were freshly dissolved in distilled water each day prior to oral gavage. Mice received either raltegravir (3.28mg/mouse) or maraviroc (1.23mg/mouse) by oral gavage daily. Mice were challenged with HIV-1 vaginally on the 4th day of treatment and the drug treatment continued for 3 more days. For vaginal viral challenges, cell-free HIV-1 strain BaL-1

Table 2.1 Summary of human cell engraftment levels in humanized (RAG-hu) mice*

Uninfected Control			Non-Treated		
Mouse	Gender	%Engraftment	Mouse	Gender	%Engraftment
J667	Female	95.0	812	Female	91.6
J666	Female	70.0	811	Female	69.3
			810	Female	91.4
			809	Female	83.9
			J635	Female	45.4
			J634	Female	83.2
			J632	Female	75.0

Raltegravir Treated			Maraviroc Treated		
Mouse	Gender	%Engraftment	Mouse	Gender	%Engraftment
J683	Female	43.6	J672	Female	74.3
J682	Female	47.0	J671	Female	65.8
J681	Female	60.5	J670	Female	80.4
J680	Female	62.6	J642	Female	81.1
J637	Female	83.5	J641	Female	62.4
J636	Female	70.0	J640	Female	67.2

*Peripheral blood was collected from human CD34 cell reconstituted mice at 10-12 weeks post engraftment. White blood cell fraction was stained with human CD45 FITC conjugated antibody and analyzed by FACS to confirm human cell engraftment prior to drug treatments and vaginal HIV challenges.

(R5 tropic virus) contained in the original media used to produce the virus (RPMI 1640 medium supplemented with 10% fetal bovine serum) was used. Vaginal infections were performed in a volume of 25ul (200 TCID₅₀ of BaL-1 virus). Sterile P200 tips that had been previously heated over a flame to smooth any abrasive surfaces were used to deliver the virus (56). Anesthetized mice were held in an inverted position for four minutes post-inoculation to allow virus to adsorb and to prevent immediate discharge of virus. Seven control non-treated mice were also challenged similarly by the vaginal route. Mice were monitored daily for any potential gross ailments due to the drugs and blood samples drawn weekly to assess plasma viremia.

2.2c Measurement of viral loads

To detect HIV-1 in plasma of infected mice by Q-RT-PCR, RNA was extracted from 25-50ul of EDTA-treated plasma using the QIAamp Viral RNA kit (Qiagen, Valencia, CA). Q-PCR was performed using a primer set specific for the HIV-1 LTR sequence and a corresponding LTR specific probe as described previously (54,56). To detect integrated virus, cellular DNA was extracted using QIAamp DNA Qiagen kit. The cellular DNA was subjected to Q-PCR to determine the proviral loads.

2.2d Flow cytometry

Whole blood was collected and red blood cells lysed as reported previously (55, 56). Peripheral blood cells were stained for hCD3-PE and hCD4-PECy5 (Caltag) markers and analyzed using a Coulter EPICS XL-MCL FACS analyzer (Beckman Coulter, Fullerton, CA). CD4⁺ T cell levels were calculated as a ratio of the entire CD3

population (CD4⁺CD3⁺:CD4⁻CD3⁺). To establish baseline CD4⁺ T cell ratios, all mice were analyzed prior to infection.

2.3 Results

2.3a Oral administration of integrase inhibitor raltegravir protects humanized mice from HIV-1 infection via vaginal challenge

We have previously shown that RAG-hu mice are susceptible to HIV-1 infection via both vaginal and rectal routes (55). Here we used this model to determine if systemic administration of raltegravir protects against vaginal HIV-1 challenge. Mice were administered with the drug daily by oral gavage since this drug is taken orally in a clinical setting. Vaginal viral challenge was performed on the 4th day and the drug treatment continued for three more days. To determine the status of HIV infection, mouse plasma and cellular blood fractions were analyzed by Q-PCR on a weekly basis. Our results showed that all of the non-treated infected mice became virus positive by the 5th

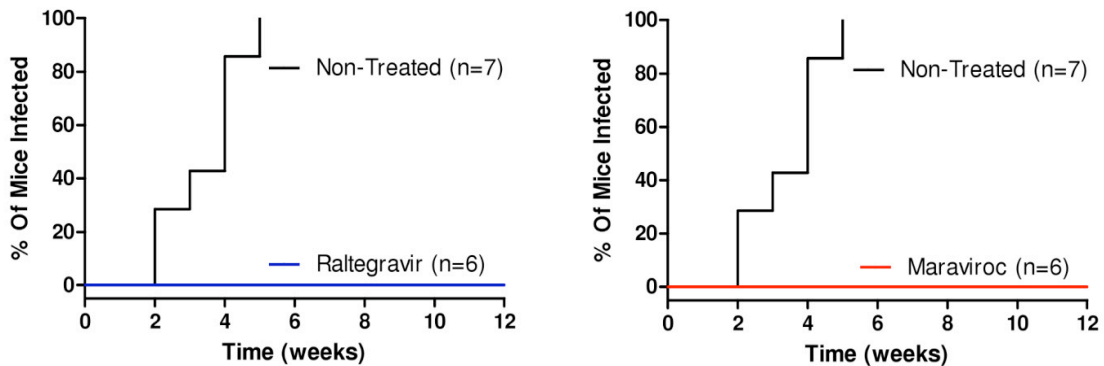


Figure 2.1 Oral administration of raltegravir or maraviroc protects humanized mice against vaginal HIV-1 challenge. RAG-hu mice were challenged by vaginal route after oral administration of raltegravir or maraviroc as described in Methods. Blood was collected weekly from infected mice and the status of HIV-1 infection was determined by Q-RT-PCR. The viral challenge experiments were performed at same time for both of the drugs and the same set of control non-treated infected mice were used for comparison. Kaplan-Meier plots of time course of appearance of viremia in drug treated versus non-treated virus challenged mice. A. Raltegravir treated B. Maraviroc treated.

week post challenge (Fig 2.1A). Persistent viremia in plasma and proviral loads in the cellular fractions was observed throughout the evaluation period with viral loads reaching 10^6 copies/ml (Fig 2.2).

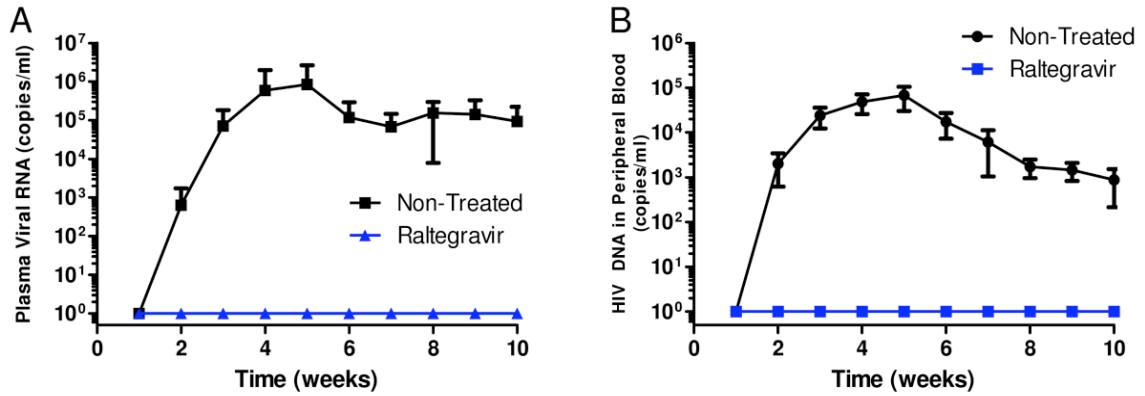


Figure 2.2 RNA and DNA viral loads in mice administered with raltegravir. RAG-hu mice were challenged by vaginal route after oral administration of raltegravir as described in Methods. Blood was collected weekly. Viral RNA was extracted from the plasma fraction and DNA was extracted from the cellular fraction. Viral RNA and DNA loads were determined by Q-RT-PCR as described in methods. A. RNA viral loads B. DNA viral loads.

In contrast, none of the raltegravir treated mice became infected at 5 weeks post-viral challenge unlike the non-treated mice (Fig 2.1A). Since it is possible that the drug treatment might have delayed the onset of infection, mice were followed for an additional 5 weeks. No evidence of infection was seen throughout the 10 week observation period as evaluated by either RNA or DNA PCR (Fig 2.2). These data collectively suggest that oral administration of raltegravir fully protects mice against HIV-1 viral challenge.

2.3b Oral administration of CCR5 inhibitor maraviroc protects humanized mice from HIV-1 infection via vaginal challenge

In addition to the viral integrase inhibitor raltegravir, we also evaluated a CCR5 antagonist maraviroc to determine its efficacy in preventing HIV-1 infection via vaginal challenge using a similar protocol, like above. This experiment was done at the same time

and the same non-treated virus infected animals were used as controls. Maraviroc was also administered orally like above in a similar time scale. Our results showed that while all the seven control untreated mice became virus positive by the fifth week, none of the six maraviroc treated mice became infected throughout the ten week observation period (Fig 2.1B). Both RNA PCR to detect plasma viremia and DNA PCR to detect integrated provirus in blood cellular fractions were negative in maraviroc treated mice in contrast to non-treated virus challenged mice (Fig 2.3). These results showed that oral administration of maraviroc fully protects humanized mice against vaginal infection.

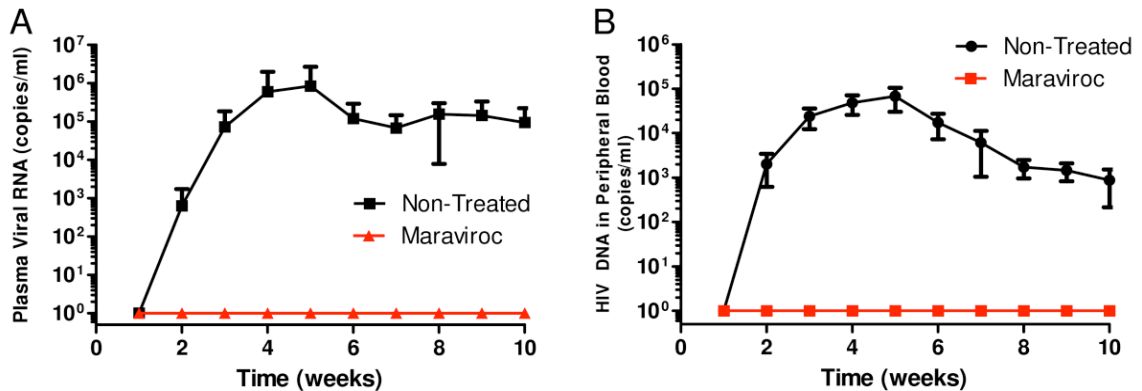


Figure 2.3 RNA and DNA viral loads in mice administered with maraviroc. RAG-hu mice were challenged by vaginal route after oral administration of raltegravir as described in Methods. Blood was collected weekly. Viral RNA was extracted from the plasma fraction and DNA was extracted from the cellular fraction. Viral RNA and DNA loads were determined by Q-RT-PCR as described in methods. A. RNA viral loads B. DNA viral loads.

2.3c CD4 T cell loss in non-drug treated mice versus raltegravir and maraviroc treated mice following vaginal infection.

The above criteria of viral detection showed that both raltegravir and maraviroc treated mice were fully protected from vaginal HIV-1 challenge. Since CD4 T cell loss is a main characteristic of HIV-1 infection in humanized mice akin to that seen in the human, we further evaluated the virus challenged mice for any evidence of such loss (55, 56). Accordingly, peripheral blood was collected weekly and subjected to FACS analysis.

Baseline CD4 T cell levels for each of the experimental mice was determined prior to viral challenge and these values were compared to the levels post-viral challenge. While there was a clear pattern of CD4 T cell decline in un-treated mice, their levels were stable in both groups of mice receiving raltegravir or maraviroc further confirming the absence of HIV-1 infection in these mice (Fig 2.4).

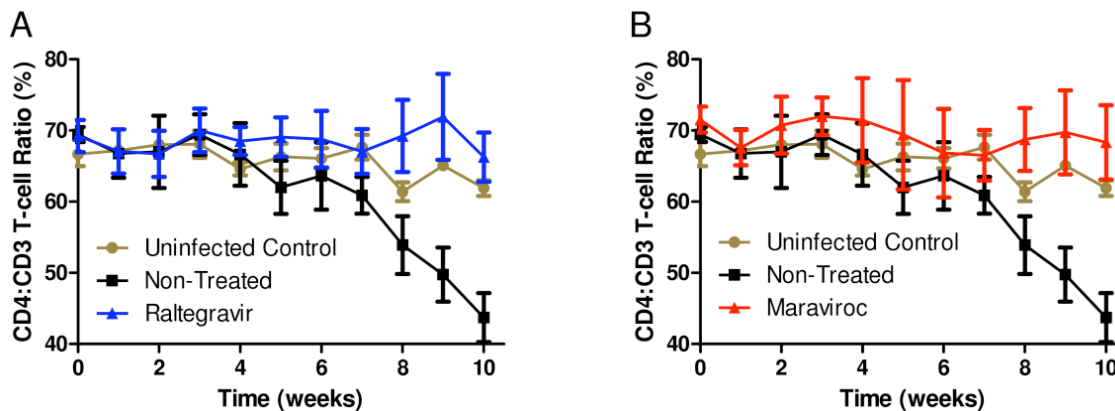


Figure 2.4 CD4 T cell decline in non-treated vaginally challenged mice in contrast to mice protected with raltegravir and maraviroc treatment. Levels of CD4 T cells were monitored on a weekly by FACS basis to determine their decline in treated versus non-treated mice. Baseline values for each of the mice were established prior to infection as described in Methods. A. Raltegravir treated, B. Maraviroc treated

2.4 Discussion

Here we have shown that oral administration of two clinically approved drugs namely, raltegravir or maraviroc fully protect humanized mice against HIV-1 infection from vaginal viral challenge suggesting their potential utility as PrEPs. These two compounds have different modes of action (190). Maraviroc is a low molecular weight CCR5 antagonist which inhibits the binding of the natural ligands of CCR5, namely chemokine ligand 3 (CCL3 also known as MIP-1a), CCL4 (MIP1-b) and CCL5 (RANTES) (191). It is a functional CCR5 antagonist devoid of agonist activity and shown to have a long lasting physical and functional occupancy of CCR5 leading to

sustained antiviral activity (192). It has been shown to have potent effect against all R5 tropic viruses representing various viral clades in addition to being effective against a wide range of drug resistant viruses (193). Topical vaginal application of maraviroc as a microbicide was recently shown to protect rhesus monkeys against SHIV virus challenge (194). Raltegravir is an integrase strand transfer inhibitor that interferes with the viral DNA integration which is an essential step in viral replication. It is active against multidrug-resistant and both CCR5-tropic and CXCR4-tropic HIV-1 strains (195, 196). To our knowledge this is the first report evaluating these two drugs as potential systemic PrEPs against HIV-1 vaginal transmission.

To simulate the clinical situation in mice, we administered each of the drugs orally as the prescription suggested for human use thus permitting intestinal absorption and reaching systemic effective concentrations. With regards to oral dosing in these proof-of-concept studies, we treated the animals for three days with the drug to achieve systemic drug equilibrium *in vivo* prior to vaginal challenge and continued the drug treatment for an additional four days. In these treated animals we preferred mice with higher engraftment in the chance that this aspect would result in a higher probability of infection. This is similar to the studies of Denton et al in BLT mice that employed FTC/TDF (Truvada) for PrEP testing (91). Whereas the drug combination FTC/TDF (Truvada) was injected *i/p* to the mice to demonstrate PrEP efficacy in the above studies, we used oral administration as clinically suggested for the above drugs. While all the control non-treated, vaginally HIV-1 challenged mice became infected within five weeks, none of the raltegravir or maraviroc treated mice (6 mice each) showed any evidence of infection. Furthermore, DNA extracted from splenic tissue samples after euthanizing the

mice at sixteen weeks post-challenge also did not show any evidence of infection by PCR analysis (data not shown). Thus protection conferred by either of these two drugs is highly significant (p value 0.0006, Fisher's exact test). We further evaluated the mice for evidence of helper CD4 T cell loss which is a characteristic hallmark of HIV-1 infection. As expected, a declining trend for CD4 T cell counts was observed in control non-treated mice in contrast to either of the treatment groups receiving raltegravir or maraviroc (Fig 2.4). These data collectively showed that treated mice resisted vaginal viral challenge thus indicating full protection in contrast to non-treated mice. To further, no animals were seen to have gross adverse side effects when monitored daily.

Whereas topical microbicides received the major attention other than vaccines to preventing HIV infection thus far with many clinical trials currently ongoing in the field, experimental studies on systemic PrEPs for HIV have been limited to very few compounds with a main focus on RT inhibitors (80, 197, 198). These included tenofovir, emtricitabine and efavirenz which showed efficacy in non-human primates against i/v, vaginal or rectal challenges with either SIV and/or different versions of SIV/HIV chimeric viruses (90, 197). In addition to showing efficacy in the monkey models, the RT inhibitors tenofovir and emtricitabine also showed efficacy in the BLT mouse model against HIV challenge (91). Based on the effectiveness of tenofovir as a PrEP in the experimental studies it is currently in clinical trials to evaluate its efficacy in the human (199). With regard to fusion inhibitors, oral administration of CMPD167, a small molecule CCR5 inhibitor, protected macaques against vaginal SHIV viral challenge (200). As can be seen, there is a paucity of number of compounds tested for systemic PrEP.

Our present results have provided the proof-of-concept data for further investigating the potential of raltegravir and maraviroc as PrEPs thus identifying additional novel class of molecules with different modes of action (80, 191). Based on their proven broad spectrum of activity against divergent HIV strains in the clinic, both these drugs make excellent candidates for PrEP. In this proof-of-concept study only one dose given sequentially for 7 days was tested and found to be efficacious in the prevention of HIV-1 infection. Future studies should evaluate variations in the dose, timings of drug administration prior to vaginal challenge and duration of efficacy without further dosing after viral challenge to determine the memory effect. Additionally, although not tested in these studies, drugs with a similar mechanism may be examined in the future for their likely similar protection. It is also necessary that field and drug resistant viruses be tested in this humanized mouse model. Furthermore, use of more than one drug in any PrEP will be more effective in field conditions. This can also be tested in this mouse model using a combination of raltegravir and maraviroc to derive pre-clinical data. Such evaluations will fine tune the PrEP regimens to be more practically applicable for clinical testing.

In addition to the systemic PrEP, another highly promising method of prevention of HIV-1 sexual transmission is the topical use of effective microbicides as mentioned above. Therefore, testing of raltegravir and maraviroc as topical microbicides in the RAG-hu mouse model of sexual HIV-1 transmission is likely to provide critical pre-clinical data in this context as well.

2.5 Acknowledgments

We thank Leila Remling and Jes Kuruvilla for assistance in RAG-hu mouse production, Thomas Campbell for providing us with the antiretroviral drugs Raltegravir and Maraviroc, and the NIH AIDS Research and Reference Reagents Program for HIV-1 related reagents used in this work.

CHAPTER 3

A TOPICAL MICROBICIDE GEL FORMULATION OF CCR5 ANTAGONIST MARAVIROC PREVENTS HIV-1 VAGINAL TRANSMISSION IN HUMANIZED RAG-HU MICE

Neff CP, Kurisu T, Ndolo T, Fox K, Akkina R. (2011) A Topical Microbicide Gel Formulation of CCR5 Antagonist Maraviroc Prevents HIV-1 Vaginal Transmission in Humanized RAG-hu Mice. PLoS One.;6(6):e20209.

This chapter contains results from my experiments that were included in the publication cited above as well as preliminary work not published.

3.1 Overview

For prevention of HIV infection many currently licensed anti-HIV drugs and new ones in the pipeline show potential as topically applied microbicides. While macaque models have been the gold standard for *in vivo* microbicide testing, they are expensive and sufficient numbers are not available. Therefore, a small animal model that facilitates rapid evaluation of potential candidates for their preliminary efficacy is urgently needed in the microbicide field. We previously demonstrated that RAG-hu humanized mouse model permits HIV-1 mucosal transmission via both vaginal and rectal routes and that oral pre-exposure chemo-prophylactic strategy could be tested in this system. Here in these proof-of-concept studies, we extended this system for topical microbicide testing using HIV-1 as the challenge virus. Maraviroc, a clinically approved CCR5 inhibitor drug for HIV treatment, was formulated as a microbicide gel at 5 mM concentration in 2.2% hydroxyl ethyl cellulose. Female RAG-hu mice were challenged vaginally with HIV-1 an hour after intravaginal application of the maraviroc gel. Our results showed that maraviroc gel treated mice were fully protected against vaginal HIV-1 challenge in contrast to placebo gel treated mice which all became infected. These findings highlight the utility of the humanized mouse models for microbicide testing and, together with the recent data from macaque studies, suggest that maraviroc is a promising candidate for future microbicide clinical trials in the field.

3.2 Materials and Methods

3.2a Preparation of humanized Rag2^{-/-}γc^{-/-} mice (RAG-hu mice)

Humanized BALB/c-Rag2^{-/-}γc^{-/-} (RAG-hu) mice were generated by transplanting with human fetal liver-derived CD34⁺ hematopoietic progenitor cells as we previously described (55, 56). Briefly, newborn mice were conditioned by irradiating at 350 rads and then injected intrahepatically with 0.5-1x10⁶ human CD34⁺ cells. Mice were screened for human cell engraftment at 10-12 weeks post-reconstitution. Peripheral blood was collected by tail bleed and red blood cells were lysed by using the Whole Blood Erythrocyte Lysing Kit (R&D Systems, Minneapolis, MN). The white blood cell fraction was stained with antibodies against the human pan-leukocyte marker CD45 (Caltag) and FACS analyzed to determine the levels of human cell engraftment as we previously described (56). Female mice with over 60% engraftment were chosen for vaginal infections as detailed below.

3.2b Vaginal application of gel and HIV-1 challenge by vaginal route

Female RAG-hu mice were topically administered with either a placebo gel or an anti-retroviral gel formulation an hour before viral challenge. Clinical formulations were ground and freshly dissolved in phosphate-buffered saline, sterile-filtered and adjusted to a final known concentration. A 3.4% gel preparation of hydroxyl-ethyl cellulose (HEC) was added to the dissolved drug to achieve a final concentration of 0.4mM, 1mM, or 5mM in 2.2% HEC gel. A 25 μ l volume of the gel formulation was carefully applied in to

the vaginal vault of mice. Control mice received 2.2% HEC placebo gel. An hour post-gel application, mice were challenged vaginally with HIV-1 BaL (3000 TCID) in a 25 μ l volume. The gel and viral inoculums were applied by using the bulbous end of a gavage needle to assure no abrasions and tearing. Anesthetized mice were held in an inverted position for four minutes post-inoculation to allow virus to adsorb and to prevent immediate discharge of virus as described previously (56, 201). Animals were observed daily and blood samples collected on a weekly basis to assess plasma viremia and CD4 T cell counts.

3.2c Measurement of viral loads

Viral infection and viral loads were assessed by Q-RT-PCR. RNA was extracted from 25-50ul of EDTA-treated plasma using the QIAamp Viral RNA kit (Qiagen, Valencia, CA). Q-PCR was performed by using a primer set specific for the HIV-1 LTR sequence and a corresponding LTR specific probe as described previously (201). To detect integrated form of the virus, cellular DNA was extracted from the cellular fraction using the QIAamp DNA Blood kit (Qiagen, Valencia, CA) and subjected to Q-RT-PCR by the iQ SYBR Green Supermix (Bio-Rad, Hercules, CA) to determine proviral loads.

3.2d Flow cytometry

Mice were monitored to measure the levels of CD4 T cells in the peripheral blood. Whole blood was collected and red blood cells lysed as reported previously (55, 56). Peripheral blood cells were stained for hCD3-PE and hCD4-PECy5 (Caltag)

markers and analyzed using a Coulter EPICS XL-MCL FACS analyzer (Beckman Coulter, Fullerton, CA). CD4⁺ T cell levels were calculated as a ratio of the entire CD3 population (CD4⁺CD3⁺:CD4⁻CD3⁺). All mice were analyzed prior to infection to establish baseline CD4⁺ T cell ratios.

3.3 Results

3.3a Vaginal application of anti-retroviral gels partially protect humanized mice against HIV-1 vaginal challenge

In our preliminary studies we evaluated topically applied microbicide gels to prevent HIV-1 sexual transmission. To assess efficacy, the various compounds were administered vaginally one hour prior to vaginal viral challenge to mimic a coital dependant context, including gels formulated with tenofovir, raltegravir, maraviroc and a cocktail of the three drugs. Mouse plasma and blood cellular fractions were analyzed by Q-PCR weekly to ascertain HIV-1 infection status. These results showed limited protection at a 0.4mM active drug concentration (Fig3.1A). With these studies the previously evaluated

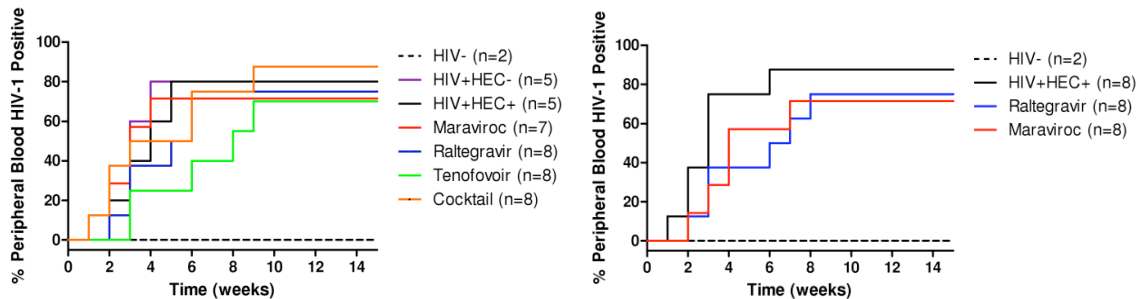


Figure 3.1 Vaginal application of .4mmol and 1mmol anti-retroviral gel formulations partially protect humanized mice against vaginal HIV-1 challenge. RAG-hu mice were challenged by vaginal route one hour after vaginal administration of treatment as described in Methods at a concentration of A) .4mmol and B) 1mmol. Blood was collected weekly from infected mice and the status of HIV-1 infection was determined by Q-RT-PCR. Kaplan-Meier plots of time course of appearance of viremia in drug treated versus non-treated virus challenged mice.

tenofovir was used as a effective control. In this regard when the microbicide gel was formulated with 0.4mM active drug tenofovir had the best protection but was only able to protect 25% of the mice (Fig3.1A).

To derive better protection the active drug concentration was increased to 1mM. The 1mM provided slightly higher partial protection as seen in three antiretroviral drug treated groups (Fig 3.1B). These data, although only deriving partial protection, are promising in proof of principal further supported by the delayed infection rates seen in all treated groups (Fig 3.1B).

3.3b Vaginal application of maraviroc gel protects humanized mice against HIV-1 vaginal challenge

Upon further optimization for a topical applied microbicide, including utilizing a bulbous gavage needle for non abrasive application, maraviroc was chosen as it is an extra-cellular effective molecule (Fig 3.1A and B). To assess efficacy, maraviroc was administered one hour prior to vaginal viral challenge to mimic a coital dependant context. Mouse plasma and blood cellular fractions were analyzed by Q-PCR weekly to ascertain HIV-1 infection status. Our results showed that the placebo-gel administered and HIV-1 challenged mice started becoming virus positive by the third week with all of them infected by the 5th week post challenge (Fig 3.2). Persistent viremia in plasma and proviral loads in the cellular fractions were observed throughout the evaluation period with viral loads reaching up to 10^6 RNA copies/ml (Fig 3.3A) and proviral DNA copies

at 10^5 DNA copies/ml (Fig. 3.3B). In contrast, none of the maraviroc treated mice became infected (Fig 3.3A). No evidence of infection was seen throughout the 16 week observation period as evaluated by either RNA or DNA PCR (Fig 3.3A and B). These data taken together suggest that vaginal administration of maraviroc fully protects mice against HIV-1 viral challenge.

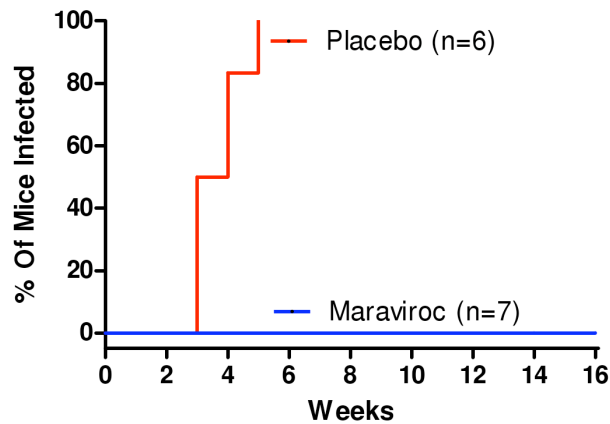


Figure 3.2 Vaginal application of maraviroc gel protects humanized mice against vaginal HIV-1 challenge. RAG-hu mice were challenged by vaginal route one hour after vaginal administration of maraviroc as described in Methods. Blood was collected weekly from infected mice and the status of HIV-1 infection was determined by Q-RT-PCR. Kaplan-Meier plots of time course of appearance of viremia in drug treated versus non-treated virus challenged mice.

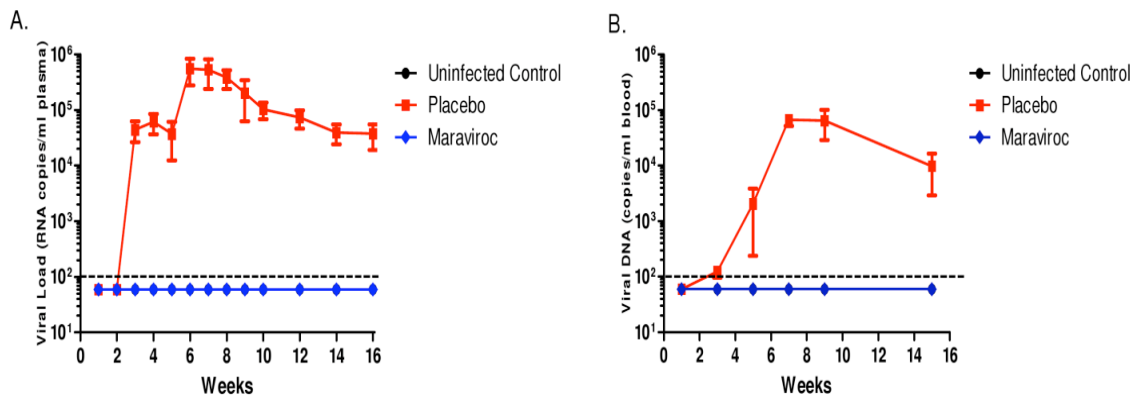


Figure 3.3 RNA and DNA viral loads in mice administered with maraviroc. RAG-hu mice were challenged by vaginal route after an hour after vaginal application of maraviroc as described in Methods. Blood was collected weekly. Viral RNA was extracted from the plasma fraction and DNA was extracted from the cellular fraction. Viral RNA and DNA loads were determined by Q-RT-PCR as described in methods. A. RNA viral loads B. DNA viral loads.

3.3c CD4 T cell loss following HIV-1 vaginal infection in placebo-gel administered mice compared to maraviroc-gel administered mice

A typical finding in HIV-1 infected humanized mice is a gradual CD4 T cell loss as seen in the human. Although the PCR data demonstrated no viral infection in maraviroc treated mice, we further evaluated the virus challenged mice for any evidence of CD4 T cell loss to confirm lack of any HIV associated pathology (55, 56). Peripheral blood was collected bi-weekly and subjected to FACS analysis. To establish a baseline, CD4 T cell levels were measured prior to viral challenge for each of the experimental mice and later compared to the levels determined post-viral challenge. While there was a clear pattern of CD4 T cell decline in placebo-gel treated and viral challenged mice, their levels were stable in mice receiving maraviroc gel (Fig. 3.4) further validating the prevention of HIV-1 transmission in these mice.

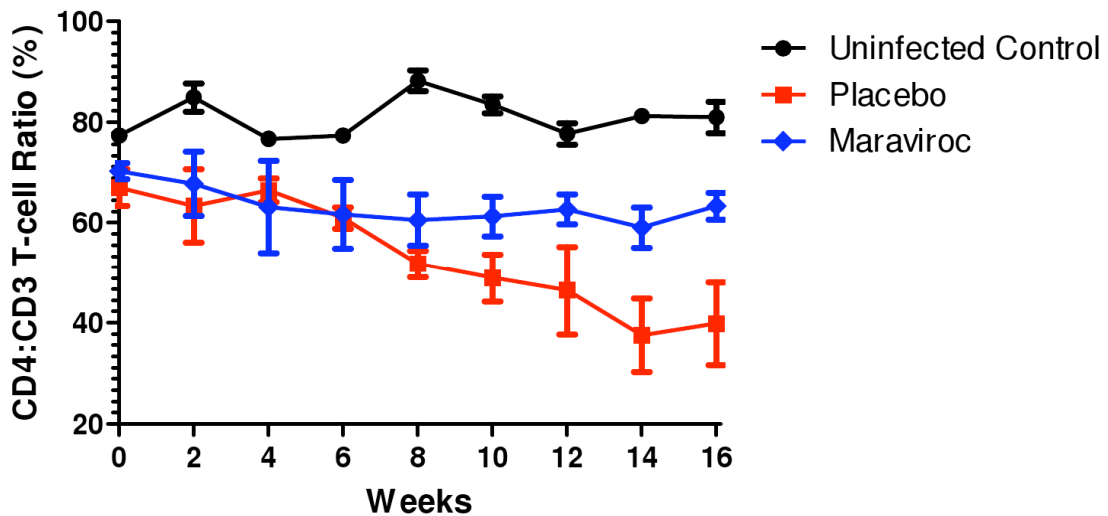


Figure 3.4. CD4 T cell decline in non-treated vaginally challenged mice in contrast to mice protected with maraviroc gel. Levels of CD4 T cells were monitored on a weekly basis by FACS basis to determine their decline in treated versus non-treated mice. Baseline values for each of the mice were established prior to infection as described in Methods.

3.4 Discussion

With dearth of a protective vaccine in the immediate future, deployment of an effective vaginally applied anti-HIV microbicide would greatly aid in stemming the HIV epidemic (202). To reach this goal, new viral specific anti-HIV compounds need to be tested as microbicides using a suitable *in vivo* system.

In these proof-of-concept studies, we have shown that topical microbicide gel formulations partially protect humanized mice from HIV-1 challenge via vaginal route which is the predominant mode of viral transmission. While these studies initially did not fully protect against HIV vaginal infection their findings aided in optimization of gel formulations and topical application. With these developments we successfully formulated a complete protection against HIV vaginal transmission using the CCR-5 antagonist maraviroc.

While a recent study had shown the efficacy of maraviroc in preventing vaginal infection in rhesus macaques by a hybrid virus, namely CCR-5 using SHIV-162P3 (203), our results demonstrated the efficacy of the drug against HIV-1 in a human target cell context in humanized mice. In addition to supporting the results of the macaque studies, our findings extended them to the primary culprit HIV-1 itself against which the drug is originally designed and intended thus providing more direct evidence.

Due to its capacity as a CCR5 antagonist, the small molecular drug maraviroc inhibits the binding of native physiological ligands of CCR5, namely CCL3 (also known as MIP-1a), CCL4 (MIP1-b) and CCL5 (RANTES) (192). It is shown to have sustained antiviral activity due its long lasting physical and functional occupancy of CCR5 receptor. It has potent effect against all R5 tropic viruses representing various viral

clades, and is also shown to be effective against a wide array of drug resistant viruses (193). A major advantage with drugs such as maraviroc compared to RT inhibitors is that the first step in infection, viral entry, is inhibited thus providing an up-front protection.

To simulate the use of the microbicide in coital context, gel formulations were applied vaginally one hour before HIV-1 R5 viral challenge. In contrast to the macaque studies, it was not necessary to subject the humanized mice to Depo-Provera (progesterone) hormonal treatment to induce vaginal thinning for achieving efficient vaginal infection. The 5mM maraviroc concentration we used is close to the dose (6mM) found to be most protective in monkey studies using a similar 2.2% HEC carrier gel formulation (194). While all the placebo-gel treated, vaginally HIV-1 challenged mice (n=6) became infected within five weeks, none of the maraviroc treated mice (n=7) showed any evidence of infection by either RT-PCR or DNA-PCR throughout the sixteen week observation period. Thus protection conferred by maraviroc gel against HIV-1 vaginal challenge is highly significant (p value 0.0006, Fisher's exact test). In addition to viral detection, we also looked for any evidence of helper CD4 T cell loss which is a typical feature of HIV-1 infection. A trend of declining CD4 T cell counts was noticed as expected in placebo-gel treated mice in contrast to those receiving maraviroc (Fig 3.4). These data taken together showed that maraviroc fully protected mice from vaginal HIV-1 challenge.

The above promising data together with those using SHIV viral challenges in macaques strongly suggest maraviroc as an attractive candidate for further development as a topically administered anti-HIV microbicide. Since it is not yet widely used in other parts of the world where HIV prevalence is high, it will have a good resistance barrier.

However it should be noted that maraviroc will not protect against X4 tropic and/or dual tropic viruses. With regard to the drugs that are in clinical trials or nearing that stage, the HIV microbicides arena is currently focused on only a few HIV-1 specific compounds such as RT inhibitors tenofovir and emtricitabine (197). While the partial protection afforded by tenofovir gel is encouraging, it is by no means adequate to be deployed as a sole candidate to protect the large at-risk population (199). Therefore, it is necessary that many new compounds be tested to identify candidates with a good chance for success. Furthermore, it is generally understood that a single drug would not be adequate to achieve broad efficacy and therefore a combination of drugs need to be tested. Such testing in a primate model will be cost-prohibitive (203, 204). In this regard, humanized mice are likely to fill the gap for deriving preliminary data and in laying the ground work for subsequent macaque studies. Since HIV-1 itself can be used as a challenge virus, various drug resistant mutants that exist in the field can also be evaluated against different combinations of potential promising compounds.

While both RAG-hu mice and BLT mice models have been successfully used to demonstrate the efficacy of systemically administered anti-HIV drugs for pre-exposure prophylaxis (65, 205), our present results have extended the utility of RAG-hu mouse model for microbicide testing as well. In the future, both these models are likely to play an important role in the development of new PrEP strategies that encompass systemic and topical use of anti-HIV drugs (206). In this context, the RAG-hu mouse model offers some practical advantages over BLT mice. First, its preparation is not technically intensive as no surgical procedure is required to implant thymic and liver tissues under the kidney capsule as is necessary to generate BLT mice. Second, RAG-hu mice have a

longer life span compared to BLT mice (NOD/SCID mice used to prepare BLT mice experience a high incidence of lymphomas), thus permitting long-term studies. For example, effect of microbicides on the mucosal membranes during long-term application can be evaluated. Third, for any large scale testing, an adequate cohort of humanized mice is needed. In this regard, greater numbers of RAG-hu mice can be generated per human tissue donor compared to BLT mice.

In summary, we have shown that various clinically approved compounds derive some protection and that the CCR5 inhibitor maraviroc formulated as a topical gel can completely prevent HIV-1 vaginal transmission. These data also helped validate the utility of humanized mice for testing topical microbicides. Now it is possible to conduct large scale *in vivo* preliminary screenings of a large number of potential microbicide candidates in a cost effective manner.

3.5 Acknowledgements

We thank Leila Remling and Jes Kuruvilla for assistance in RAG-hu mouse production, Thomas Campbell for providing us with the antiretroviral drug Maraviroc and NIH AIDS Research and Reference Reagents Program for HIV-1 related reagents used in this work.

CHAPTER 4

SYSTEMIC ADMINISTRATION OF COMBINATORIAL dsRNAs VIA NANOPARTICLES EFFICIENTLY SUPPRESSES HIV-1 INFECTION IN HUMANIZED MICE

Jiehua Zhou^{*}, C. Preston Neff^{*}, Xiaoxuan Liu, Jane Zhang, Haitang Li, David D. Smith, Piotr Swiderski, Tawfik Aboellail, Yuanyu Huang, Quan Du, Zicai Liang, Ling Peng, Ramesh Akkina and John Rossi (2011) Systemic administration of combinatorial dendrimer-siRNA via nanoparticles efficiently suppresses HIV-1 infection. *Molecular Therapy* doi:10.1038/mt.2011.207

(*authors contributed equally)

This chapter contains results from my experiments that were included in the publication cited above.

4.1 Overview

The potent ability of small interfering (si)RNAs to direct inhibition of the expression of complementary RNA transcripts is being exploited as a possible therapeutic approach for the treatment of a variety of diseases. Although current anti-retroviral drug therapies for treatment of HIV/AIDS show considerable promise, there are still associated problems of toxicity, viral resistance and cost for a daily, lifelong medication. In this regard, systemic administration of siRNAs targeting host and viral transcripts is an attractive alternative, but delivery of the siRNAs remains a key obstacle to successful therapeutic applications and clinical development.

To address this problem we evaluated the *in vivo* efficacy of structurally flexible, cationic PAMAM dendrimers (Figure 4.1) as a siRNA delivery system in a Rag2^{-/-}γc^{-/-} (RAG-hu) humanized mouse model for HIV-1 infection. HIV-infected humanized Rag2^{-/-}γc^{-/-} mice (RAG-hu) were injected intravenously with dendrimer-siRNA complexes consisting of a cocktail of siRNAs targeting both viral and cellular transcripts. We report in this study that the dendrimer-siRNA treatment suppressed HIV-1 infection by several orders of magnitude and protected against viral induced CD4 T-cell depletion. We also demonstrate that follow up injections of the dendrimer-siRNAs following viral rebound resulted in complete inhibition of HIV-1 titers. Collectively, these data demonstrate that dendrimer-mediated delivery system has the capacity for combining anti-viral and anti-host siRNAs to avert viral escape mutants and suppress viral loads *in vivo*. The dendrimer delivery approach therefore represents a promising method for systemic, delivery of combinations of siRNAs for treatment of HIV-1 infection.

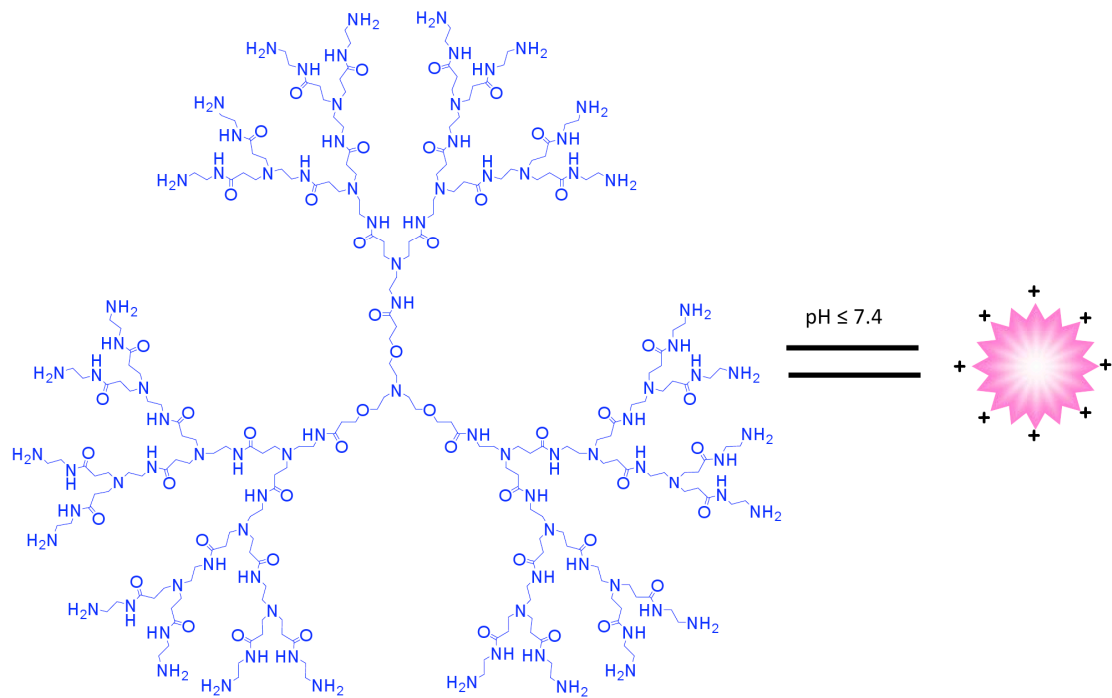


Figure 4.1: Structure of a flexible poly(amidoamine) (PAMAM) dendrimer with a triethanolamine core. At $\text{pH} \leq 7.4$, the terminal amino groups (NH₂) possess positive charges *via* protonation. For clarity, the generation 3 (G₃) dendrimer is shown as an example.

4.2 Materials and Methods

4.2a Materials

Unless otherwise noted, all chemicals were purchased from Sigma-Aldrich, all restriction enzymes were obtained from New England BioLabs (NEB) and all cell culture products were purchased from GIBCO (Gibco BRL/Life Technologies, a division of Invitrogen.). Reverse transcriptase III, Random primers and oligo(dT)₂₀ primers (Invitrogen, CA); Lipofectamine 2000 (Invitrogen, CA); Trans IT-TKO (Mirus, Madison, WI); (Invitrogen); DNase I (Ambion); HEK 293 and CCRF-CEM (ATCC); the HIV-1

NL4.3 and HIV-1 IIIB viruses were obtained from the AIDS Research and Reference Reagent Program.

siRNAs: siRNA and Cy3-labeled single strand RNA were purchased from Integrated DNA Technologies (IDT).

Site I (*tat/rev*) 27 mer: Sense: 5'- GCG GAG ACA GCG ACG AAG AGC UCA UCA - 3'; Antisense: 5'- UGA UGA GCU CUU CGU CGC UGU CUC CGC dTdT-3';

Mutated Site I (*tat/rev*) 27 mer: Sense: 5'-GCG CUA ACA GCG UGU AAG AGC GAC UCA -3'; Antisense: 5'- UGA GUC GCU CUU ACA CGC UGU UAG CGC UU -3'.
(The mutated sequences were underlined.)

Anti-CD4 21 mer: Sense: 5' - GAU CAA GAG ACU CCU CAG U dGdA - 3';
Antisense: 5'- ACU GAG GAG UCU CUU GAU C dTdG -3'

Anti-CD4 27 mer: Sense: 5'- GAU CAA GAG ACU CCU CAG UGA GAA G -3';
Antisense: 5'- CUU CUC ACU GAG GAG UCU CUU GAU CUG -3' (2'-OMe modified U was underlined.)

Anti-TNPO3 21 mer: Sense: 5' - CGA CAU UGC AGC UCG UGU AUU -3'; Antisense: 5'- UAC ACG AGC UGC AAU GUC GUU -3'.

Anti-TNPO3 27 mer: Sense: 5'- CGA CAU UGC AGC UCG UGU ACC AG dGdC -3';
Antisense: 5'- GCC UGG UAC ACG AGC UGC AAU GUC GUU -3'.

4.2b Dendrimer synthesis and characterization

The PAMAM dendrimers were synthesized as previously described and characterized by IR, NMR, MS and HPLC (121, 122)

In vitro assay:

4.2c Agarose gel analysis of siRNA-dendrimer complexes

The dendrimers were serially diluted to an appropriate concentration in 50 mM Tris-HCl buffer (pH 7.4), with all solutions stored at -20°C. The 27 mer *Tat/rev* siRNA was diluted with H₂O. Both solutions were mixed at various N/P (= [total end amines in cationic dendrimer] / [phosphates in siRNA]) ratios and incubated at 37°C for 30 min in Tris-HCl buffer. The final concentration of siRNA was adjusted to 25 ng/ L (100 ng per well). After incubation the binding complexes were loaded on a 1.2% agarose gel for electrophoresis. The siRNA bands were stained by ethidium bromide and then detected by a Herolab EASY CCD camera (Type 429K) (Herolab, Wiesloch, Germany).

4.2d Stability of siRNA-dendrimer complexes against RNase A

An aliquot of 27 mer *Tat/rev* siRNA (1 g) and the indicated amounts of dendrimers were kept at 37°C for 30 min. The complexes were then incubated in the presence of 0.01 g/ L RNase A for different times as indicated in the gel at 37°C. Aliquots (4 L) of the corresponding solution were withdrawn, added to 1.5 L 1% SDS

solution on ice, and the subjected to electrophoresis in 1.2% agarose gel in standard TBE buffer. The siRNA bands were stained by ethidium bromide and then detected by a Herolab EASY CCD camera (Type 429K) (Herolab, Wiesloch, Germany).

4.2e Transmission electron microscopy (TEM) analysis

Studied were performed with a JEM-2000FX transmission electron microscopy. A solution (10 μ L) of 27 mer *Tat/rev* siRNA (5 ng/ μ L) was mixed with a solution (10 μ L) of G₅ dendrimer in Opti-MEM transfection medium. After equilibration (30 min), this mixture (4 μ L) was dropped on a standard carbon-coated copper TEM grid and allowed to evaporate (1 h at 30°C, ambient pressure). In the case of siRNA-dendrimer solutions, the samples were premixed and allowed to equilibrate for 30 min before placing on the grid. The grid was then stained with uranyl acetate (2% in 50% alcoholic solution) for 3 min. Imaging was performed after air-drying for 20 min.

4.2f Cell culture

HEK 293 cells and CCRF-CEM cells were purchased from ATCC and cultured in DMEM and RPMI 1640 supplemented with 10% FBS. CHO-WT and CHO-EE cells were obtained through the AIDS Research and Reference Reagent Program and were grown in GMEM-S medium. Cells were cultured in a humidified 5% CO₂ incubator at 37°C.

PBMCs. Peripheral blood mononuclear samples were obtained from healthy donors from the City of Hope National Medical Center. PBMCs were isolated from whole blood by centrifugation through a Ficoll-Hypaque solution (Histopaque-1077, Sigma). CD8 cells (T-cytotoxic/suppressor cells) were depleted from the PBMCs by CD8 Dynabeads (Invitrogen, CA) according to the manufacturer's instructions. CD8⁺ T cell-depleted PBMCs were washed twice in PBS and resuspended in culture media (RPMI 1640 with 10% FBS, 1×PenStrep and 100 U/mL interleukin-2). Cells were cultured in a humidified 5% CO₂ incubator at 37°C.

4.2g Flow cytometry analysis of CEM cells

2×10⁵ CEM cells per well were seeded in 24-well tissue culture plate in 300 μ L fresh complete medium containing 10% FBS. Before transfection, complexes of Cy3-labeled siRNA/dendrimer reagents were prepared. The desired amount of siRNA and dendrimer reagent was diluted in 50 μ L of serum-free medium (Opti-MED), respectively. The dendrimer solution was mixed gently and incubated for 10 min at room temperature. After the 10-minute incubation, the diluted siRNA and the dendrimer reagent was mixed gently and incubated for 30 minutes at room temperature. The 100 μ L of siRNA/dendrimer complexes was added to each well containing CEM cells and medium. Mix gently by rocking the plate back and forth. Incubate the cells at 37°C in a CO₂ incubator for 24 hours, and then the cells were washed three times with 1 mL PBS buffer. Cell pellets were resuspended in prewarmed PBS and analyzed by flow cytometry. In this

case, a commercial reagent TransIT-TKO (Mirus, Madison) was used as control according to the manufacturer's instructions.

4.2h Cellular uptake studies (Fluorescent Microscopy analysis)

2×10^5 CEM cells per well were seeded in 24-well tissue culture plate in 300 μ L fresh complete medium containing 10% FBS. CEM cells were transfected with 50 nM Cy3-labeled *Tat/Rev* Site I siRNA (27 mer) using dendrimer G₄ and G₅ as above described. After 24 hours of post-transfection, the images were collected using a Nikon Eclipse TE2000-S fluorescent microscopy system at 40 magnifications.

Northern Blot analysis of CEM cells and PBMCs. Cells were transfected with 50 nM *Tat/Rev* Site I siRNA (27 mer) using dendrimer G₄ and G₅ as above described. After 48 hours of post-transfection, the total RNAs were harvested for analysis with STAT-60 (TEL-TEST "B", Friendswood, TX) according to the manufacturer's instructions. Five micrograms of total RNAs were electrophoresed in a 15% polyacrylamide-8 M urea gel and then transferred to a Hybond N+ membrane (Amersham pharmacia Biotech, USA). Prehybridization and hybridization were carried out using PerfectHyb Plus Hybridization buffer (Sigma, USA) at 37°C with 3 pmol of a 27-mer DNA oligonucleotide probe end-labeled with T4 polynucleotide kinase and γ -³²P-ATP. Filters were washed three times at 37°C for 15 min, prior to autoradiography. We also probed for human U6 snRNA as an internal RNA loading standard. In this case, the same siRNA was electroporated into CEM cells as system control following the manufacturer's instructions (Amaxa, MD).

4.2i Determination of CD4 or TNPO3 gene silencing (qRT-PCR analysis)

For CD4 expression, cells were transfected with 50 nM of 21-mer or 27-mer anti-CD4 siRNA or anti-TNPO3 siRNA using dendrimers as above described. After 48 hours of post-transfection, the total RNAs were isolated with STAT-60 (TEL-TEST “B”, Friendswood, TX). Expression of the target genes was analyzed by quantitative Real time-PCR using 2× iQ SyberGreen Mastermix (BIO-RAD) and specific primer sets at a final concentration of 400 nM. Primers were as follows: CD4 forward primer: 5' – GCT GGA ATC CAA CAT CAA GG -3'; CD4 reverse primer: 5'- CTT CTG AAA CCG GTG AGG AC -3'; TNPO3 Forward primer: 5' – CCT GGA AGG GAT GTG TGC -3'; TNPO3 Reverse primer: 5'- AAA AAG GCA AAG AAG TCA CAT CA -3'; GAPDH forward primer: 5'- CAT TGA CCT CAA CTA CAT G-3'; GAPDH reverse primer: 5'- TCT CCA TGG TGG TGA AGA C-3'.

RNA-Stat60 was used to extract total RNA according to the manufacturer's instruction (Tel-Test). Residual DNA was digested using the DNA-free kit per the manufacturer's instructions (Ambion). cDNA was produced using 2 µg of total RNA Moloney murine leukemia virus reverse transcriptase and random primers in a 15 µL reaction according to the manufacturer's instructions (Invitrogen). GAPDH expression was used for normalization of the qPCR data.

4.2j HIV-1 challenges and p24 antigen assay

The CEM cells or PBMCs were infected with HIV IIIB for 5 days (MOI: 0.001). Prior to transfection, the infected cells were gently washed with PBS three times to remove free virus. 1.0×10^5 infected cells and 1.0×10^5 uninfected cells were mixed and transfected with 50 nM 27-mer *tat/rev* siRNA using dendrimers in 24-well plates as previously described. The culture supernatants were collected at the 3rd day. The p24 antigen analyses were performed using a Coulter HIV-1 p24 Antigen Assay (Beckman Coulter) according to the manufacturer's instructions.

4.2k Determination of *Tat/rev* gene silencing (qRT-PCR analysis)

For *tat/rev* gene, cells were infected with HIV-1 IIIB for 5 days (MOI: 0.001). Prior to assays, the infected cells were gently washed 3 times to eliminate free virus. 1.0×10^5 infected cells and 1.0×10^5 uninfected cells (total 2×10^5 per well) were mixed and transfected with 50 nM *Tat-rev* siRNA using dendrimers in 24-well plates as above described. After 72 hours of post-transfection, total RNAs were isolated and expression of the *tat/rev* coding RNAs was analyzed by qRT-PCR as previously described. Primers were as follows: *tat/rev* forward primer: 5'- GGC GTT ACT CGA CAG AGG AG -3'; *tat/rev* reverse primer: 5'- TGC TTT GAT AGA GAA GCT TGA TG -3'; GAPDH expression was used for normalization of the qPCR data.

Interferon assay (qRT-PCR analysis). CEM cells were directly treated with siRNA/dendrimer complex or IFN-alpha (100 U/mL). After 48 h, total RNAs were

isolated with STAT-60 (TEL-TEST “B”, Friendswood, TX). Expression of human mRNAs encoding p56(CDKL2) and OAS1 were analyzed by quantitative RT-PCR using 2X iQ SyberGreen Mastermix (BIO-RAD) as described above and specific primer sets for these genes at final concentrations of 400 nM. Primers were as follows: P56 (CDKL2) forward, 5'-GCC TCC TTG GGT TCG TCT ATA A - 3'; P56 (CDKL2) reverse, 5'-CTC AGG GCC CGC TCA TAG TA - 3'; OAS 1 forward, 5' -GGA GGT TGC AGT GCC AAC GAA G - 3'; OAS 1 reverse, 5'-TGG AAG GGA GGC AGG GCA TAA C - 3'. GAPDH expression was used for normalization of the qPCR data.

4.21 MTT Cytotoxicity Assay

The cell viability of siRNAs plus dendrimers on CEM or PBMCs was determined by 3-(4, 5-dimethylthiazol-2-yl)-2, 5-diphenyltetrazolium bromide (MTT) assay (Sigma-Aldrich, USA). Cells were seeded in each well of 96-well microtiter plates and then treated with dendrimer-siRNA complexes. After 48 hour of post-transfection with dendrimer-siRNA, cells pellets were collect by centrifuge and replaced fresh medium. 10 L MTT solution (5 mg/mL in PBS) was added in each well and then incubated with cells for 2 h in the 37°C. After removal of supernatant carefully, the cells were frozen for at least 1 h at -80°C. Each well was added 100 L of DMSO to dissolve the crystals properly, the absorbance was measured at the wallack plate reader using Kamings protocol for 595 nm. And the viability was expressed as the ratio of absorbance obtained from transfected cells to non-transfected cells (n=6).

4.2m 5'-RACE PCR assay

Total RNA (5 µg) from HEK 293 cells transfected with 50 nM experimental RNAs (TNPO3 25/27-mer siRNA or scrambled siRNA) in presence of G₅ dendrimer was isolated using Trizol as manufacturer's protocol. Residual DNA was digested using the DNA-free kit per the manufacturer's instructions (Ambion). Subsequently, total RNA was ligated to a GeneRacer adaptor (Invitrogen, Carlsbad, CA) without prior treatment. Ligated RNA was reverse transcribed using a gene specific primer 1 (GSP-Rev 1: 5'-TCC CGT AAA GAG GCA TGA GAG TCT GT -3'). To detect cleavage products, PCR was performed using primers complementary to the RNA adaptor (5'-cDNA primer) and gene-specific primer 2 (GSP-Rev 2: 5'- CCG GAT CTG TAA CAA CTG GTC TGA GA -3'). Amplification products were resolved by agarose gel electrophoresis and visualized by ethidium bromide staining. The specific PCR products were recovered using a QIAquick Gel purification Kit and then were cloned into TOPO TA cloning vector pCR 2.1-TOPO vector (Invitrogen). Individual clones were identified by DNA sequencing.

In vivo assay:

4.2n Generation and HIV-1 infection of humanized Rag2^{-/-}γc^{-/-} mice (RAG-hu mice)

Humanized BALB/c-Rag2^{-/-}γc^{-/-} mice were prepared as previously described using human fetal liver-derived CD34⁺ cells. Briefly, neonatal mice were conditioned by irradiating at 350 rads and then injected intra-hepatically with 0.5 ~ 1×10⁶ human CD34⁺ cells. Approximately 12 weeks post-reconstitution, mice were screened for human cell

engraftment. Blood was collected by tail bleeds, and red blood cells were lysed using the Whole Blood Erythrocyte Lysing Kit (R&D Systems). The white blood cell fraction was stained with antibodies against the human pan-leukocyte marker CD45 (Caltag) and FACS analyzed as described. To infect human cell reconstituted RAG-hu mice, HIV-1 NL4-3 (1.2×10^5 i.u.) in a 100 μ L volume was injected intraperitoneally at least 12 weeks after cell engraftment. Viral loads were examined weekly and viremia was established in all the mice by 4 weeks.

4.2o Treatment with dendrimer-siRNA complexes

G₅ dendrimers were diluted to an appropriate concentration in PBS buffer (pH 7.4) and the experimental siRNAs were diluted with H₂O, with all solutions stored at -20°C. Both solutions were mixed at N/P (= [total end amines in cationic dendrimer] / [phosphates in siRNA]) ratio 5 and incubated at 37°C for 30 min in PBS buffer. Treatment was done by intravenous (IV) injection on the last day of week 4 with 0.25 nmol experimental RNAs (4.6 μ g cocktailed siRNAs including equal amount of three siRNAs: *tat/rev* siRNA, TNPO3 siRNA and CD4 siRNA, or preparations of G₅ dendrimer-siRNAs conjugates with equal amount of three siRNA portions) in a 40 μ L volume, followed by another the next day. Later, the injections were continued on a weekly basis for 4 weeks. In the second *in vivo* treatment experiment, 0.25 nmol conjugates in a 40 μ L volume were administered at 12.5 and 13.5 weeks post last-infection like above.

4.2p Measurement of viral load in plasma

To quantify cell-free HIV-1 by qRT-PCR, RNA was extracted from 25 to 50 μ L of EDTA-treated plasma using the QIAamp Viral RNA kit (QIAGEN). cDNAs were produced with Superscript III reverse transcriptase (Invitrogen) using a primer set specific for the HIV-1 LTR sequence, and qPCR was performed with the same primer set and a LTR specific probe using Supermix UDG (Invitrogen) as described.

4.2q Flow cytometry

Whole blood was collected and red blood cells were lysed as reported previously. Peripheral blood cells were stained for hCD3-PE and hCD4-PECy5 (Caltag) markers and analyzed using a Coulter EPICS XL-MCL FACS analyzer (Beckman Coulter). CD4+ T-cell levels were calculated as a ratio of the entire CD3 population ($CD4+CD3+ : CD4-CD3+$). To establish baseline CD4+ T-cell ratios, all mice were analyzed prior to infection.

4.2r Determination of *tat/rev* siRNA

At one, three and nine weeks post-injection, blood samples were collected and small RNAs were isolated with MirVana miRNA isolation Kit (Applied Biosystems) according to the manufacturer's instruction. The siRNA quantification was performed using TaqMan MicroRNA Assay according to manufacturer's recommended protocol

(Applied Biosystems). 10 nanograms of small RNA, 0.2 M stem-loop RT primer, RT buffer, 0.25 mM dNTPs, 3.33 units/mL MultiScribe reverse transcriptase (RT) and 0.25 units/mL RNase inhibitor were used in 15 L RT reactions for 30 min at 16°C, 30 min at 42°C, and 5 min at 85°C, using the TaqMan MicroRNA reverse transcription Kit (Applied Biosystems). For real-time PCR, 1.33 L of cDNA, 0.2 mM TaqMan Probe, 1.5 mM forward primer, 0.7 mM reverse primer, and TaqMan Universal PCR Master Mix were added in 20 L reactions for 10 min at 95°C and 40 cycles of 15 sec at 95°C and 1 min at 60°C. All real-time PCR experiments were done using an iCycler iQ system (Bio-Rad). Primers were as follows: Site I Looped RT primer: 5'- GTC GTA TCC AGT GCA GGG TCC GAG GTA TTC GCA CTG GAT ACG ACA CAG CG -3'; Site I Forward Primer: 5'- GCT GAT GAG CTC TTC GTC G - 3'; Site I Reverse Primer: 5'- GTG CAG GGT CCG AGG T - 3'; Site I probe primer: 5'- 6- FAM- TCG CAC TGG ATA CGA CAC AGC GAC GA -BHQ1 -3'. In this case, a synthetic 27 mer duplex RNA was used as positive control.

4.2s Determination of targeted genes expression.

Human PBMCs were obtained from treated mice at one and three weeks post-injection and total RNAs were isolated with STAT-60 (TEL-TEST "B") according to the manufacturer's instructions. Residual DNA was digested using the DNA-free kit per the manufacturer's instructions (Ambion). cDNA was made using 2 g of total RNA. Reverse transcription was carried out using Moloney murine leukemia virus reverse

transcriptase and random primers in a 15 μ L reaction according to the manufacturer's instructions (Invitrogen). Expression of the *tat/rev* coding RNAs was analyzed by quantitative RT-PCR using 2 \times iQ SyberGreen Mastermix (BIO-RAD) and specific primer sets at a final concentration of 400 nM. *Gapdh* expression was used for normalization of the qPCR data. Primers were as follows: IIB or NL4-3 *tat/rev* forward primer: 5'- GGC GTT ACT CGA CAG AGG AG -3'; IIB or NL4-3 *tat/rev* reverse primer: 5'- TGC TTT GAT AGA GAA GCT TGA TG -3'; CD4 forward primer: 5' – GCT GGA ATC CAA CAT CAA GG -3'; CD4 reverse primer: 5'- CTT CTG AAA CCG GTG AGG AC -3'; TNPO3 Forward primer: 5' - CCT GGA AGG GAT GTG TGC -3'; TNPO3 Reverse primer: 5'- AAA AAG GCA AAG AAG TCA CAT CA -3'; *gapdh* forward primer 1: 5'- CAT TGA CCT CAA CTA CAT G-3'; *gapdh* reverse primer 2: 5'- TCT CCA TGG TGG TGA AGA C-3'.

4.2t Interferon assays

Total RNA was isolated from PBMCs of treated mice using STAT-60. Expression of mRNAs encoding p56(CDKL2) and OAS1 were analyzed by quantitative RT-PCR using 2 \times iQ SyberGreen Mastermix (BIO-RAD) as described above and specific primer sets for these genes at final concentrations of 400 nM. Primers were as follows: P56 (CDKL2) forward, 5'- TCA AGT ATG GCA AGG CTG TG -3'; P56 (CDKL2) reverse, 5'- GAG GCT CTG CTT CTG CAT CT -3'; OAS1 forward, 5' - ACC GTC TTG GAA CTG GTC AC -3'; OAS1 reverse, 5'- ATG TTC CTT GTT GGG TCA GC -3'; *gapdh* expression was used for normalization of the qPCR data. To measure any induced IFN- α

directly, Human IFN- α 1 ELISA Ready-SET-Go! (eBioscience) was used. Mice were injected with G₅ dendrimer mutant *tat/rev* dsRNA complex, dsRNA alone, G₅ dendrimer alone, G₅ dendrimer-siRNA *tat/rev*, or G₅ dendrimer-cocktail. At 2 and 24 hours post treatment 25-50 μ L of EDTA-treated plasma was collected from 3 mice per treatment group and from 3 positive control mice intravenously injected with 5 μ g of poly (I:C) (Sigma) in a 50 μ L volume. Plasma was evaluated as per instructions supplied in the kit.

4.2u Statistical Methods

The mouse viral loads and CD4:CD3 T-cell ratios were plotted by using a lowess smoother across values. Viral loads were first log-transformed prior to smoothing and then anti-transformed for plotting. Missing values were imputed with a last observation carried forward scheme. The calculations were conducted as previously described (207).

4.3 Results

4.3a Dendrimer-siRNAs form stable nanoscale complexes which protect the siRNAs from serum nucleases and facilitate siRNA delivery into human T-cells *in vitro*

The polycationic vectors must form stable, nanometer-scale complexes with negatively charged siRNAs to ensure protection from serum ribonucleases and provide efficient delivery to cells and tissues *via* endocytosis. The TEA-core PAMAM dendrimer

of generation 5 (G_5) formed stable complexes with the 27-mer Dicer substrate *tat/rev* siRNA (dsiRNA), resulting in complete gel retardation of the dsiRNA at an N/P (total terminal amines in the cationic dendrimer / phosphates in the siRNA) ratio ≥ 2 . We next used transmission electron microscopy (TEM) to analyze the size and morphology of the dendrimer G_5 -dsiRNA complexes at a N/P ratio of 5. The TEM results show well-condensed spherical particles with diameters of ~ 100 nm a size which favors efficient endocytosis-mediated cell uptake. The stable G_5 -siRNA nanoparticles at an N/P ratio of 5 protected the dsiRNA from RNase degradation, even after 90 min exposure to RNase. In contrast, the uncomplexed, naked dsiRNA was rapidly degraded within 10 minutes of RNase incubation.

Flow cytometry and fluorescent microscopy were carried out to analyze the cellular uptake of the G_5 -dsiRNA complexes. Cy3-labeled dsiRNAs were complexed with the G_5 dendrimer and the complex was added to HEK293 cells (an adherent cell line) or human T-lymphoblast CCRF-CEM cells (a suspension cell line). For comparison purposes, the same cell lines were transfected with the Cy3-labeled dsiRNAs using commercial lipid based transfection agents. Flow cytometry analyses conducted 24 hours after transfection with HEK293 cells indicated that the G_5 dendrimer mediated cellular uptake of Cy3-dsiRNA approached 60% at the tested concentration of 10 nM, whereas only $\sim 15\%$ uptake was obtained with the commercial lipid based carrier. The cellular uptake of the dendrimer-Cy3-dsiRNA complexes was dose dependent. Similarly, fluorescence microscopic imaging revealed efficient delivery of the Cy3-dsiRNA to the suspension CEM T-cells cells, with an efficiency comparable to a commercial lipid based reagent. No uptake was observed when uncomplexed Cy3-dsiRNAs were tested.

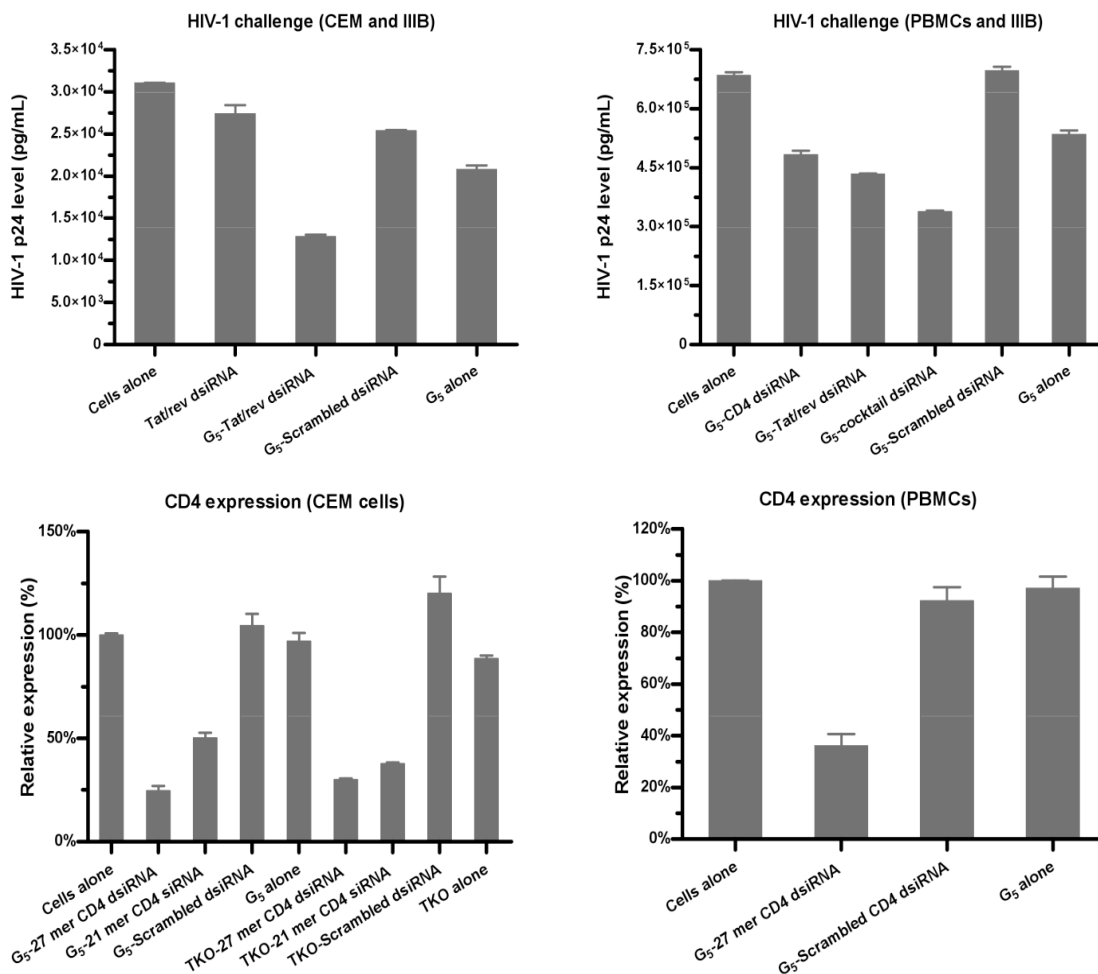


Figure 4.2: Dendrimer-dsRNA nanoparticles mediate specific gene silencing in vitro. Inhibition of CD4 expression by dendrimer G₅-mediated delivery of 21-mer or 27-mer anti-CD4 siRNAs (at an N/P ratio of 5) was assayed using qRT-PCR two days post-treatment in culture (a) CEM T-cells and (b) human PBMCs. Dendrimer-siRNA complexes inhibit HIV-1 infection in (c) CEM T-cells and (d) human PBMCs previously infected with HIV-1. HIV-1 infected cells were incubated at 37°C with the G₅-27-mer anti-tat/rev dsRNA complexes or G₅-cocktail siRNAs (combination of 27-mer anti-tat/rev dsRNA and anti-CD4 dsRNA) complexes. The culture supernatants were collected at 3 day following addition of the complexes for HIV p24 antigen analyses. Data represent the average of triplicate measurements of p24 and the average of three replicates.

As a further confirmation of the cellular uptake of the G₅ dendrimer-siRNA complex, we carried out live-cell confocal microscopy using HeLa cells and a G₅ dendrimer diRNA complex. These analyses demonstrated that the G₅ dendrimer complexed with the Alexa488 labeled dsRNA was effectively internalized (Figure S4.1A). No green fluorescence was observed when the cells were incubated with

uncomplexed dsRNA (data not shown). To further evaluate the mechanism of dendrimer-mediated siRNA delivery, we tested different endocytic inhibitors (Figure S4.1). No significant effects on uptake were observed when Genistein (a caveolae-mediated endocytosis inhibitor) or Chlorpromazine (a Clathrin-mediated endocytosis inhibitor) were used. However, an increasing concentration of cytochalasin D (a macropinocytosis inhibitor) reduced the cellular uptake of the dendrimer-siRNA complex, suggestive of a cell uptake mechanism involving macropinocytosis (Figure S4.1).

4.3b dsRNAs are released from the dendrimer complexes and mediate specific gene silencing *in vitro*

TNPO3 and CD4 are HIV-1 host dependency factors that are potential therapeutic targets (212, 213). CD4 is the primary receptor for HIV-1, and transient knocking down of this receptor blocks HIV-1 infection (208, 209). TNPO3 is a cellular factor that is involved in facilitating the cytoplasmic to nuclear trafficking of the HIV-1 pre-integration complex and was shown by a siRNA screen to block HIV-1 infection at the afferent stage (209). We therefore asked whether the G₅ dendrimer delivered dsRNAs targeting transcripts encoding these proteins effectively mediated gene silencing in human T-lymphoblast CEM cells. The siRNA mediated knockdowns of the target transcripts were evaluated *via* quantitative real-time PCR (qRT-PCR). The G₅ dendrimer delivered anti-CD4 dsRNA complex resulted in a 75% decrease in CD4 mRNA levels 48 hours post-transfection (Figure 4.2C). The dendrimer G₅ delivered

dsiRNA gave somewhat better target knockdown than the corresponding conventional 19+2 mer siRNA. In similarity to the CD4 knockdown results, the G₅ dendrimer delivered dsiRNA targeting TNPO3 resulted in somewhat better target knockdown than the 19+2 siRNA (Figure S4.2). These data confirm previous reports of enhanced efficacy when dsiRNAs are used (210).

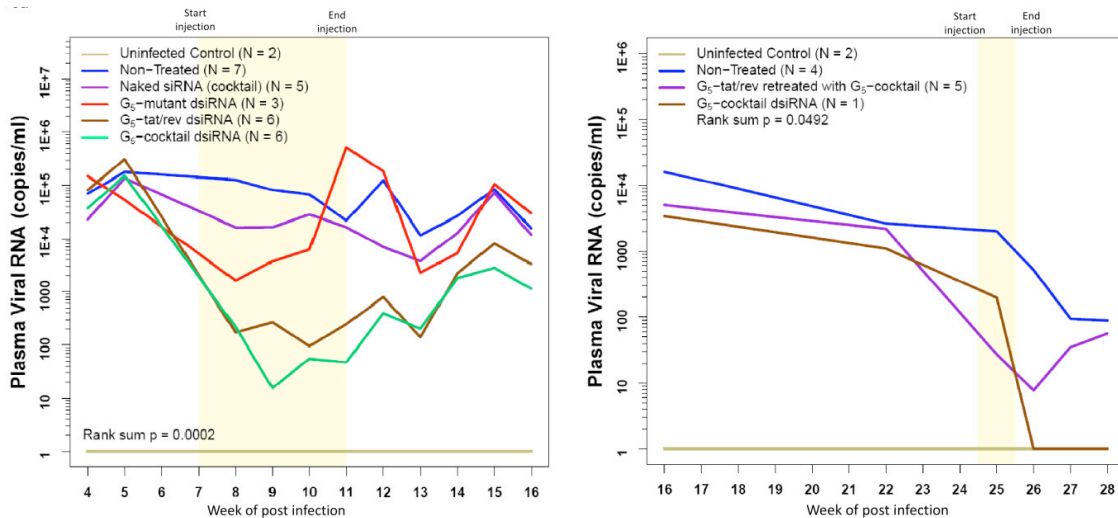


Figure 4.3: Dendrimer-dsiRNA complexes suppress viral loads in HIV-1 infected RAG-hu mice. HIV-1 viral loads at different weeks post infection and treatment are indicated. The treatment period is indicated by the yellow framed in region. Viral loads at each indicated week pre- and post-treatment. Weeks post-injection and the time point of treatment start and end are indicated. **(a)** The first-treatment included five weekly injections: The viral loads of uninfected mice (n = 2), non-treated mice (n = 7), naked cocktail dsiRNA treated mice (n = 5), G₅-mutant-tat/rev dsiRNA complex treated mice (n = 3), G₅-tat/rev dsiRNA complexes treated mice (n = 6) and G₅-cocktail siRNA complex treated mice (n = 6) are indicated. **(b)** The re-treatment including twice weekly injections with G₅-cocktail siRNA complexes: The viral loads of uninfected mice (n = 2), non-treated mice (n = 4), G₅-tat/rev dsiRNA complex treated mice (n = 5) and G₅-cocktail dsiRNA complex treated mice (n = 1) are indicated. P values for both experiments were determined as described in Materials and Methods. The viral RNA was detected through qRT-PCR as described in Methods. If there was no detectable viral RNA we established this as a value of 1 (10⁰) to allow for the use of logarithmic values on the Y-axis.

Since the dsiRNAs are cleavage substrates Dicer, we asked whether the dendrimer G₅ delivered dsiRNAs were processed into 21-23 base siRNAs in CEM cells. Northern blotting analyses (Figure S4.3) demonstrated both unprocessed 27 mer dsiRNAs as well as processed 21-22 mer siRNAs in the transfected cells.

We next evaluated target knockdown directed by dsRNAs delivered with the G₅ dendrimer into primary human peripheral blood mononuclear cells (PBMCs). Primary PBMC-CD8 depleted CD4⁺ cells were incubated with the G₅ dendrimer anti-CD4 dsRNA complex for 48 hours, and the CD4 mRNA levels were subsequently monitored by qRT-PCR (Figure 4.2D). The G₅ dendrimer delivered dsRNA resulted in ~ 60% knockdown of the levels of the CD4 mRNA at the tested concentration of 50 nM. In contrast, no inhibition was observed with G₅ dendrimer alone or G₅ dendrimer delivered scrambled dsRNA.

To validate that the G₅ dendrimer delivered dsRNAs were functioning through the RNAi mechanism, we carried out a modified 5'-RACE (Rapid amplification of cDNA end) on total RNAs isolated from control and G₅ dendrimer delivered anti-TNPO3 dsRNA in CEM cells. For these analyses we used the Ago2 cleavage specificity which takes place between bases 10 and 11 relative to the 5' end of the guide strand siRNA (211, 212). RACE PCR product sequence analyses should reveal a linker addition on the siRNA complementary target at the base 10 nucleotides downstream from the 5' end of the antisense siRNA strand. We obtained PCR bands of the predicted length for a Dicer processed siRNA directed cleavage product following nested PCR reactions (Figure S4.4). No appropriately sized products were generated from total RNAs prepared from cells treated with a G₅ dendrimer scrambled dsRNA treated cells. The PCR amplified, gel-purified bands of the predicted lengths were cloned and the individual clones characterized by DNA sequencing. The results obtained showed that the cleavage reaction took place at the predicted position for the Dicer processed dsRNA between positions 10 and 11 from the 5' end of the predicted dicer processed siRNA antisense

strand. Based upon the position of the cleavage site these results also reconfirm Dicer processing of the dsRNA to 21-23 base siRNAs (as shown in Figure S4.4).

We next investigated whether the G₅ dendrimer delivered siRNAs triggered type I interferon responses. The levels of two different type I interferon stimulated mRNAs were quantified by quantitative RT-PCR (Figure S4.5 A, B). From these data we concluded that the G₅ dendrimer delivered dsRNA complex did not activate the type I interferon pathways (Figure S4.5 C, D).

4.3c The G₅ dendrimer -delivered dsRNAs inhibit HIV-1 infection of CEM T-cells and human PBMCs

Having established that the G₅ dendrimer delivered anti-HIV dsRNAs effectively downregulated the cellular CD4 and TNPO3 targets, we next assessed the anti-HIV-1 activity of the dendrimer G₅-delivered dsRNAs (172, 173); In these assays the G₅ dendrimer dsRNA complexes were incubated with cells that had been previously infected with HIV-1 IIIB followed by assays for the HIV-1 encoded p24 peptide as previously reported (172, 173). The results presented in Figure 4.2 A and B show the HIV-1 p24 antigen levels following treatment with the G₅ dendrimer-siRNA complexes. The HIV-1 p24 production in CEM cells and PBMC-derived CD4⁺ cells was reduced approximately three fold 72-hours post-transfection. Since these experiments were carried out in cells which were previously infected with HIV-1 the dsRNAs cannot completely eliminate p24 production. When two dsRNAs targeting CD4 and the HIV-1

encoded *tat/rev* transcripts were combined, the G₅ dendrimer-combinatorial siRNA complex provided strong inhibition of HIV-1 replication and spread in PBMC-CD4+ cells.

To validate the RNAi efficacy in these experiments, we evaluated the down-regulation of HIV-1 *tat/rev* gene expression following treatment of CEM cells with the G₅ dendrimer anti-*tat/rev* dsRNA complex. The expression levels of *tat/rev* encoding RNAs were determined by quantitative RT-PCR analysis three days post-treatment of cells with the complex. Substantial down regulation of the *tat/rev* mRNA was observed, a direct consequence of the G₅ dendrimer-anti-*tat/rev* siRNA delivery. In contrast, treatment of infected cells with the empty dendrimer or siRNA alone had no effect on HIV *tat/rev* levels (Figure 4.2A and B).

4.3d Systemic administration of the G₅ dendrimer-dsRNA complexes suppresses HIV-1 viral loads in viremic RAG-hu mice

Given the promising results of the G₅ dendrimer mediated dsRNA delivery in CD⁺ T cells, we next sought to determine if the dendrimer-siRNA complexes could functionally deliver dsRNAs *in vivo* and provide protection and/or inhibition of HIV-1 infection in humanized mice. RAG-hu mice were first infected with HIV-1 NL4-3 by intraperitoneal (IP) injection until they became viremic, usually 3 weeks post infection. The viral loads in these animals averaged 10⁵ viral RNA particles per mL. These viremic mice were subsequently given weekly intravenous (IV) injections of dendrimer G₅-

dsiRNA complexes as described in the methods section. As control groups, animals were administered a G₅ dendrimer mutant *tat/rev* dsiRNA complex, dsiRNA alone or G₅ dendrimer alone.

Plasma RNA viral levels were monitored by qPCR on a weekly basis. There were six animals in each treatment group. The siRNA treatment groups consisted of dendrimer complexed with 0.25 nmols of the anti-*tat/rev* dsiRNA or 0.25 nmols of a combination of the anti-*tat/rev*, anti-CD4 and anti-TNPO3 dsiRNAs (Figure 4.3A). We observed a general pattern of decreased viral loads in the majority of the G₅ dendrimer treated mice when the functional dsiRNAs were applied (weeks 8-12 as shown). The suppression of viral loads was on average three logs relative to the controls and these reductions reached statistical significance with a rank sum $P = 0.0002$ (Figure 4.3A). Even three weeks following the termination of the treatment, viral loads were still suppressed in the majority of treated animals (weeks 13-15), indicating a prolonged antiviral effect in these animals. Importantly, there was no viral suppression in the animals treated with the G₅ dendrimer delivered mutant *tat/rev* dsiRNA complex (Figure 4.3) or the G₅ dendrimer alone (Figure S4.6).

Comparison of the inhibitory activity afforded by a single anti-HIV *tat/rev* dsiRNA *versus* a combination of three dsiRNAs targeting HIV-1 *tat/rev* and the HIV dependency factors (HDFs) CD4 and TNPO3 showed that the combinatorial complex provided more effective inhibition of HIV-1 than the single anti-*tat/rev* dsiRNA when viral loads were analyzed from the second through the fifth weeks of treatment.

Although viral levels remained lower in animals treated with the functional G₅ dendrimer-dsiRNAs three weeks following the termination of treatment, these levels continued to slowly rise. We asked if re-treatment with the G₅ dendrimer-dsiRNA complexes could restore suppression of viral levels. At three months following the last administration of the initial treatment, G₅ dendrimer cocktail of dsiRNAs was re-administered to verify efficacy of re-treatment. The re-treatments were conducted at weeks 24.5 and 25.5 post infection as shown (Figure 4.3B). These re-treatments resulted in a statistically significant (P=0.0492) re-inhibition of HIV-1 levels (Figure 4.3B). Complete suppression persisted for 3 weeks beyond the re-treatment period in the G₅ dendrimer-cocktail dsiRNA treated mice.

In efforts to further evaluate the effectiveness of the dendrimer mediated dsiRNA delivery, we assessed the intracellular levels of the delivered dsiRNAs. Taqman qPCR assays were carried out to quantify the *tat/rev* dsiRNA levels in cells collected from peripheral blood collected at various times during and after treatment. The results presented in Figure 4.4A reveal that the *tat/rev* dsiRNA was quantifiable in all of the G₅ dendrimer dsiRNA treated mice at two weeks into the treatment period (week 9) and even at two weeks following the last injection (week 13), the dsiRNAs were still detectable in cells prepared from all the dendrimer-dsiRNA treated mice (Figure 4.4B). No dsiRNAs were detected in the cellular fractions from mice treated with naked dsiRNAs.

We next evaluated the sequence specific gene silencing in the HIV-1 infected Rag-Hu mice. The relative levels of reduction of the three targeted genes (HIV *tat/rev*, CD4 and TNPO3) in PBMCs of treated mice were evaluated by quantitative real-time

PCR. The G₅ dendrimer-dsiRNA treated mice had reduced levels of the corresponding targeted mRNA levels relative to the controls following the first and second treatments with the G₅ dendrimer -dsiRNA complexes (weeks 8 and 9) (Figure 4.4C and D).

4.3e The G₅ dendrimer-dsiRNA treatment protects against HIV-1 mediated T-cell depletion.

HIV-1 infection characteristically results in a progressive loss of helper CD4⁺ T cells. During the course of infection, CD4⁺ T cell levels fall transiently during the acute stage of infection followed by a return to a set point for several months/years with an eventual depletion leading to AIDS (186, 187). The levels of CD4⁺ T-cells show similar declines in the HIV-1 infected humanized mice (56). Considering the siRNA mediated suppression of HIV-1 viral replication in the G₅ dendrimer -dsiRNA treated animals; we sought to determine whether the reduced viral loads impacted on the T-cell levels of the treated animals. To determine this, we monitored the levels of CD4⁺ T-cells in peripheral blood collected at different times post-treatment (Figure 4.5). In uninfected mice, the levels of CD4⁺ T cells remained stable (within a 10% variation range) throughout the course of the experiments. For those animals treated with the *tat/rev* or combination dsiRNAs, the protection against T-cell depletion reached statistical significance ($P = 0.0562$) (Figure 4.5). In contrast, in the animals that were HIV-1 infected but not receiving treatment, the viral infection resulted in a rapid decline in CD4⁺ T cells beginning at week 4 post infection, falling to below 40% of the starting levels at 20 weeks post infection.

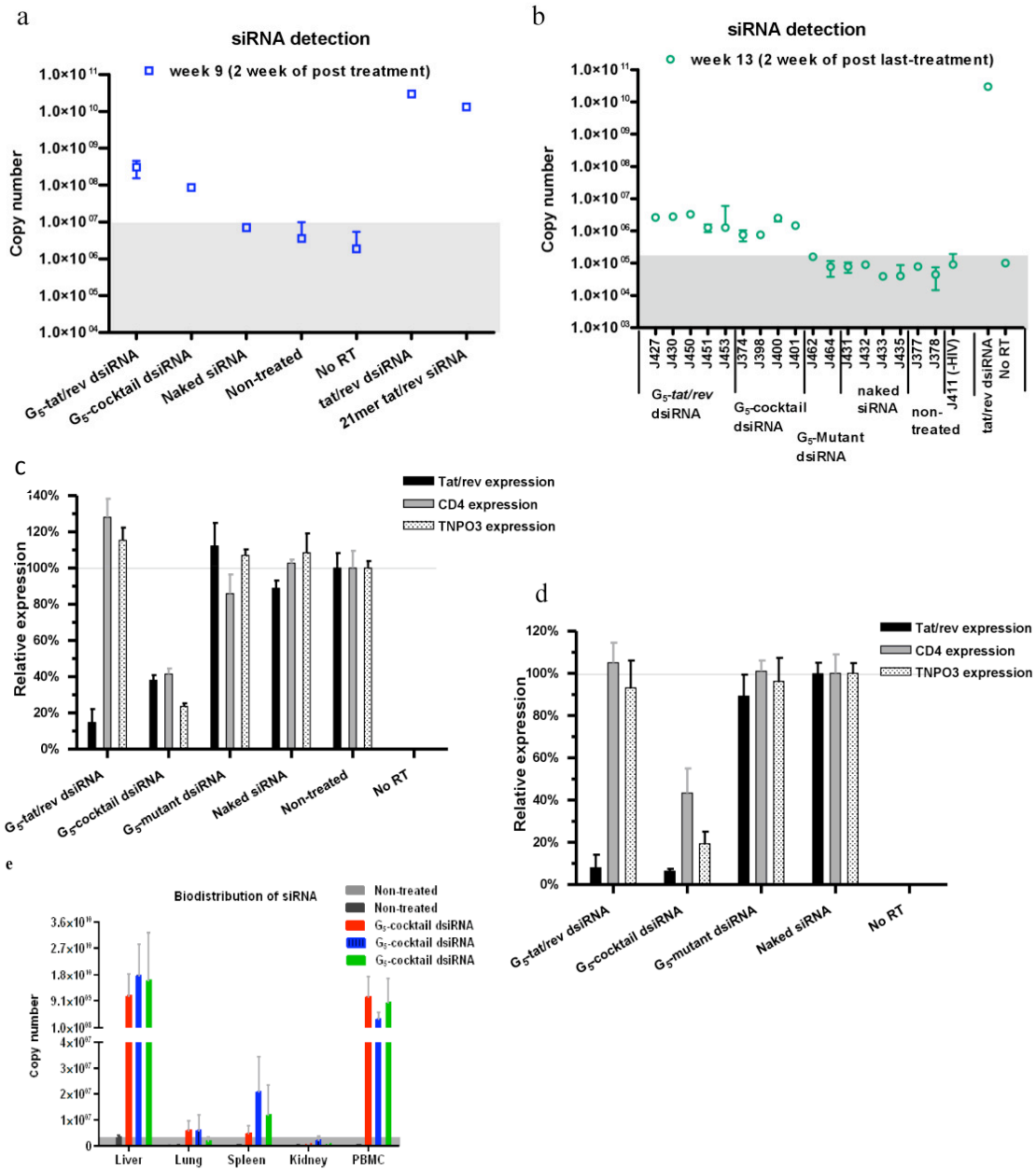


Figure 4.4: The detection and function of siRNAs in blood cells of HIV-1 infected RAG-hu mice and *in vivo* biodistribution. (a, b) Detection of the *tat/rev* siRNA sequences at weeks 9 and 13 post-infection using naked siRNAs versus G_5 -dsiRNA complex treated animals from Figure 3a. The background copy number of siRNA is $<10^7$ (gray). Error bars indicate SD (n = 4). (c, d) Expression levels of targeted *tat/rev*, CD4 and TNPO3 gene transcripts at weeks 8 and 9 post infection are shown relative to HIV-1 infected, non-treated animal samples (c) and naked siRNA treated animal samples (d), respectively. (e) *In vivo* biodistribution analyses. The delivery of the anti-*tat/rev* siRNA was monitored using Taqman qRT-PCR on RNAs isolated from various tissues and PBMCs following systemic administration of the G_5 dendrimer-dsiRNA nanoparticles in RAG-hu mice. The background copy number of siRNA is $<5 \times 10^6$ (gray). Error bars indicate SD (n = 3).

There was no protection in the mice treated with the G₅ dendrimer -mutant *tat/rev* dsRNA complex (Figure 4.5) or the empty G₅ dendrimer (Figure S4.5). In animals treated with the G₅ dendrimer-cocktail of dsRNAs the levels of CD4+ T cells remained stable well beyond the last treatment.

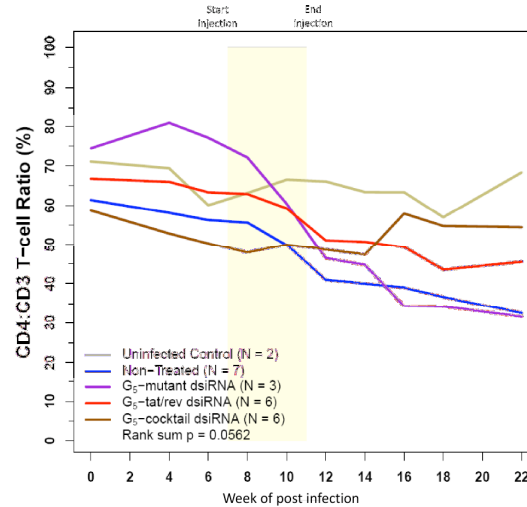


Figure 4.5: Dendrimer-dsRNA complexes protect RAG-hu mice from CD4+ T-cell loss. CD4+ T-cell levels were assessed by FACS at each indicated week pre- and post-siRNA treatment. Start and end of treatments are indicated by the yellow framed in region. Mice from the first treatment depicted in Figure 3a. Uninfected mice (n = 2), non-treated mice (n = 7), G₅-mutant-*tat/rev* dsRNA complex treated mice (n = 3), G₅-*tat/rev* dsRNA complex treated mice (n = 6) and G₅-cocktail dsRNA complex treated mice (n = 6) are indicated. *P* values for the experiment are indicated and were determined as described in Materials and Methods. BL (base line): each individual mouse was bled two times prior to HIV-1 infection and the CD4:CD3 levels were averaged within treatment groups to establish a baseline CD4:CD3 level.

4.3f The G₅ dendrimer-mediated dsRNA delivery does not trigger type I interferon responses *in vivo*

It has been previously reported that synthetic siRNAs delivered by liposomes or other polymers can trigger innate immune responses, such as Toll-like receptor (TLR) mediated induction of type I interferon (IFN), tumor necrosis factor-alpha (TNF- α) and interleukin-6 (IL-6) (211). We therefore assessed whether or not treatment of the animals with the G₅ dendrimer-dsRNAs resulted in induction of type I IFN-regulated

gene expression. To assay for this we used quantitative RT-PCR expression assays on PBMC derived RNAs isolated from the G₅ dendrimer-dsiRNA treated animals as well as controls. IFN- α treated PBMCs was used as a positive control to confirm up-regulation of p56 and OAS1 gene expression. No significant differences in IFN responsive gene expression were discernable in samples from either the treated or control animals at different times post-treatment (Figure 4.6A and B). Using an ELISA assay we also directly monitored IFN- α levels in treated mice at 2 hours and 24 hours post-injection of the experimental RNAs and found no significant elevation of IFN- α (Figure 4.6C).

Since microRNA levels can be perturbed *via* competition with the exogenously introduced siRNAs, we therefore monitored PBMC encoded microRNA miR21 expression levels by Taqman assays on RNAs prepared from cells isolated from animals receiving the dendrimer delivered dsiRNAs versus samples from the control animals. Figure S4.6 depicts the results, which show no perturbation of miR-21 levels in the animals receiving the dsiRNAs.

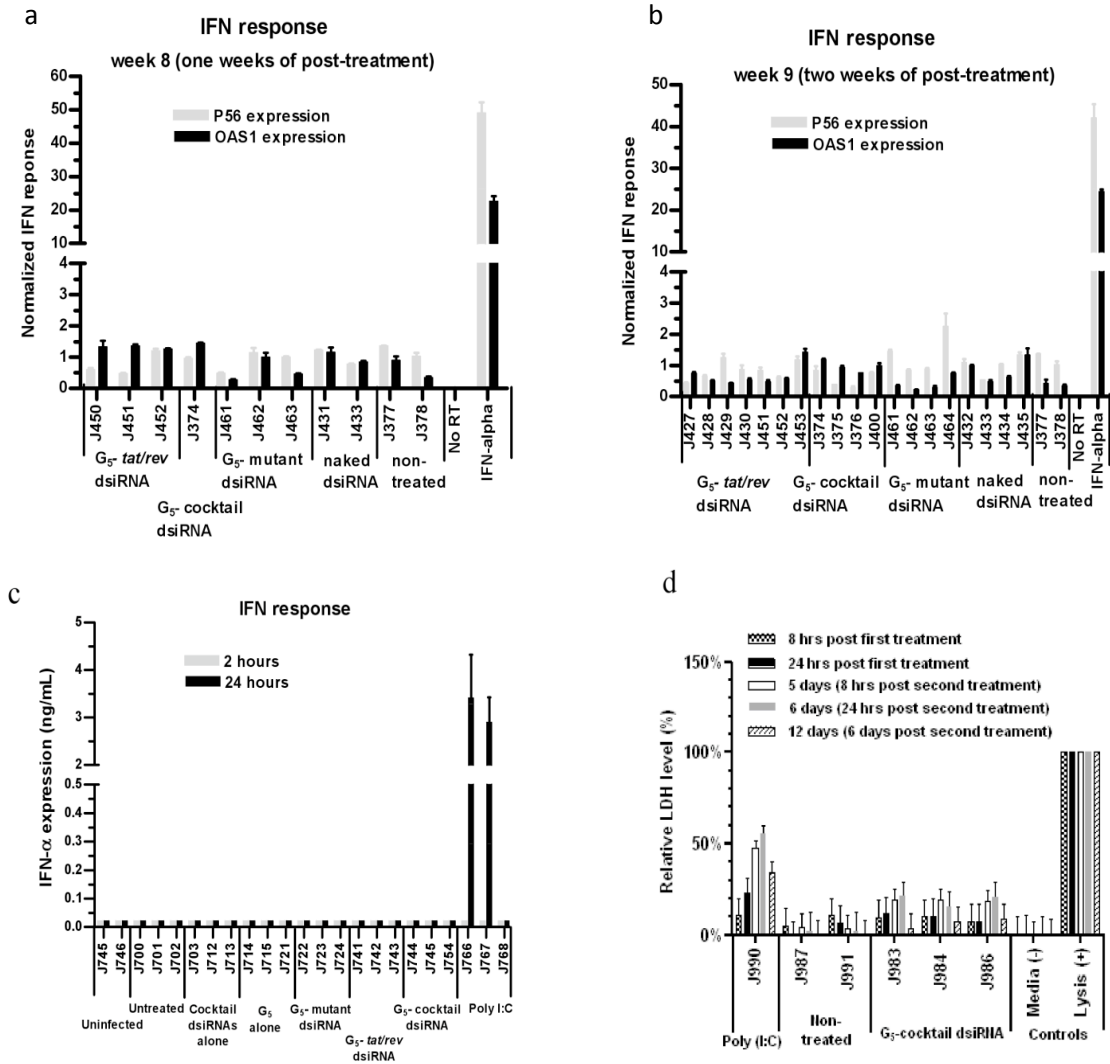


Figure 4.6: *In vivo* administration of dendrimer-dsRNA complexes do not induce interferon or toxicities. (a, b) The expression of type I interferon response genes (P56 and OAS1) at week 8 (a) and 9 (b) post infection after treatment with siRNAs and G_5 -dsRNA complexes. IFN- treated, HIV-1 infected human PBMCs were used as a positive control. Gene expression was normalized to the *gapdh* mRNA. Error bars indicate SD (n = 4). (c) The expression levels of IFN- α at 2 hours or 24 hours post G_5 -dsRNA nanoparticle injections as measured by an ELISA are shown. Poly (I:C) treated infected Rag-hu mice were used as a positive control. Error bars indicate SD (n = 3). (d) The levels of LDH (lactate dehydrogenase) post G_5 -dsRNA nanoparticles injections are shown. Cellular lysate treated human PBMCs were used as a positive control. The data are cumulative from three mice per experimental group.

Recent studies have demonstrated that applications of siRNAs targeting viral or cellular transcripts provide inhibition of HIV-1 replication *in vitro* and *in vivo*. Cell-type-specific delivery of siRNAs to primary T cells in humanized mice has been accomplished *via* the use of a CD7 specific antibody. Although the use of antibody mediated targeted delivery is appealing there are potential cost and production issues for preparing the siRNA complexed antibodies as well as potential problems of immunogenicity. On the other hand, synthetic vehicles such as dendrimers can be synthesized with controlled and defined structures, are amenable to chemical modification, stable in biological fluids and are not immunogenic. Importantly, an ideal siRNA delivery system for treatment of HIV-1 infection should have the capacity for combining siRNAs to different targets, both viral and cellular, to avert viral escape mutants.

We have tested a PAMAM generation 5 dendrimer-dsiRNA delivery system for the treatment of HIV-1 infection both in cell culture and in a humanized mouse model. In the mouse model the animals are first infected with HIV-1 until they become viremic, and are subsequently treated with the dendrimers-dsiRNAs to model how a treatment might be structured for human applications. Dendrimers are a class of structurally highly branched and well-defined synthetic polymers. The dendrimer used in this study is a fifth generation dendrimer (G₅) that contains 96 terminal amine groups on the surface and a TEA core with a flexible structure. They are able to form stable and uniformly sized complexes with nucleic acids *via* electrostatic interactions, and the flexible structure further enhances the interaction with nucleic acids through mutually induced fit. By simply mixing the G₅ dendrimer with siRNAs, stable nanometer-scale (ca 100 nM diameter) particles were formed. Following internalization in cells *via* macropinocytosis,

the G₅ dendrimer-dsiRNA complexes release the dsiRNAs, which are subsequently processed by Dicer into 21-23 base siRNAs that trigger sequence specific gene silencing of the targeted mRNAs.

In this study we provided data demonstrating that a cocktail of three dsiRNAs targeting HIV-1 *tat/rev* and two cellular targets, CD4 and TNPO3 resulted in down-regulation of all three targeted transcripts *in vivo*. The inhibition of these targets resulted in a reduction of the viral RNA load and protection of CD4+ T cells from HIV-1 mediated depletion. Furthermore the results of this study demonstrate that a combination of dsiRNAs can be functionally delivered to T-lymphocytes *in vivo* in the absence of any apparent or measured toxicity. Importantly, we also show 3 months after we stopped the first treatments-allowing viral loads to become elevated again, animals were re-treated with the dendimer- cocktail dsiRNA, resulting once again in strong inhibition of HIV-1. This suppression persisted for an additional 3 weeks beyond the re-treatment period. Collectively, our results demonstrate the capacity of the G₅ dendrimer delivered dsiRNAs to achieve marked viral suppression *in vivo*, resulting in protection of CD4 T cells from HIV-1 mediated depletion. Given the importance and challenge of siRNA delivery, it is of significance that these results provide the first demonstration of nano-particle mediated delivery of siRNAs to hematopoietic cells *in vivo*, and provide the impetus for further clinical development of this strategy. The data presented also support the use combinatorial multi-targeting dsiRNAs for treating HIV-1 infection as a standalone therapy or adjuvant to the HAART therapy.

4.5 Acknowledgements

We thank NIH AIDS Research and Reference Reagents Program for HIV-1 related reagents used in this work.

CHAPTER 5

AN APTAMER-siRNA CHIMERA SUPPRESSES HIV-1 VIRAL LOADS AND PROTECTS FROM HELPER CD4(+) T CELL DECLINE IN HUMANIZED MICE

Neff CP, Zhou J, Remling L, Kuruvilla J, Zhang J, Li H, Smith DD, Swiderski P, Rossi JJ, Akkina R. (2011) An aptamer-siRNA chimera suppresses HIV-1 viral loads and protects from helper CD4(+) T cell decline in humanized mice. *Sci Transl Med.*;3(66):66ra6.

This chapter contains results from my experiments that were included in the publication cited above.

5.1 Overview

Therapeutic strategies designed to treat HIV infection with combinations of antiviral drugs have proven to be the best approach for slowing the progression to AIDS. Despite this progress, there are problems with viral drug resistance and toxicity, necessitating new approaches to combating HIV-1 infection. We have therefore developed a different combination approach for the treatment of HIV infection in which an RNA aptamer, with high binding affinity to the HIV-1 envelope (gp120) protein and virus neutralization properties, is attached to and delivers a small interfering RNA (siRNA) that triggers sequence-specific degradation of HIV RNAs. We have tested the antiviral activities of these chimeric RNAs in a humanized $Rag2^{-/-}\gamma c^{-/-}$ (RAG-hu) mouse model with multilineage human hematopoiesis. In this animal model, HIV-1 replication and CD4(+) T cell depletion mimic the situation seen in human HIV-infected patients. Our results show that treatment with either the anti-gp120 aptamer or the aptamer-siRNA chimera suppressed HIV-1 replication by several orders of magnitude and prevented the viral-induced helper CD4(+) T cell decline. In comparison to the aptamer alone, the aptamer-siRNA combination provided more extensive inhibition, resulting in a significantly longer antiviral effect that extended several weeks beyond the last injected dose. The aptamer thus acts as a broad-spectrum HIV-neutralizing agent and an siRNA delivery vehicle. The combined aptamer-siRNA agent provides an attractive, nontoxic therapeutic approach for treatment of HIV infection.

5.2 Materials and methods

5.2a Reagents

Unless otherwise noted, all chemicals were purchased from Sigma-Aldrich, all restriction enzymes were obtained from New England BioLabs (NEB) and all cell culture products were purchased from GIBCO (Gibco BRL/Life Technologies, a division of Invitrogen.). Sources for the other reagents were: DuraScribe T7 transcription Kit (EPICENTRE Biotechnologies); Silencer siRNA Labeling Kit (Ambion); Hoechst 33342 (nuclear dye for live cells) (Molecular Probes, Invitrogen); Random primers (Invitrogen); SuperScript III RT kit (Invitrogen); Bio-Spin 30 Columns (Bio-Rad); CHO-Env Transfectants (CHO-WT and CHO-EE), the HIV-1 NL4-3 and HIV-1 BaL viruses, and clinical isolates (X4-strain: HIV-1 92UG021; R5-strain: HIV-1 RU570 and HIV-1 98CN009) were obtained from the AIDS Research and Reference Reagent Program.

5.2b Generation of aptamer-siRNA chimera RNA (Ch A-1) by *in vitro* transcription

The design, synthesis and *in vitro* efficacies of the aptamer A-1 and aptamer-siRNA conjugates have been described in detail previously (156). SiRNA Dicer substrate sense, antisense strand RNAs and DNA oligonucleotides were purchased from Integrated DNA Technologies (IDT).

Tat/rev Site I 27 mer siRNA:

Sense strand: 5' - GCG GAG ACA GCG ACG AAG AGC UCA UCA -3'

Antisense strand: 5' - UGA UGA GCU CUU CGU CGC UGU CUC CGC dTdT-3'

Aptamer A-1: 5'- GGG AGG ACG AUG CGG AAU UGA GGG ACC ACG CGC UGC UUG UUG UGA UAA GCA GUU UGU CGU GAU GGC AGA CGA CUC GCC CGA -3'

Chimera A-1-sense strand: 5'- GGG AGG ACG AUG CGG AAU UGA GGG ACC ACG CGC UGC UUG UUG UGA UAA GCA GUU UGU CGU GAU GGC AGA CGA CUC GCC CGA *UU* GCG GAG ACA GCG ACG AAG AGC UCA UCA -3'

Chimera A-5-sense strand: 5'- GGG AGG ACG AUG CGG GAA ACU AGU UUG AAU AAU GGU GUA GAG GAG GGU CAA UAG UUU CGU UGG UGC AGA CGA CUC GCC CGA *UU* GCG GAG ACA GCG ACG AAG AGC UCA UCA -3'

Antisense strand: 5'- UGA UGA GCU CUU CGU CGC UGU CUC CGC dTdT-3'

The sense strands of the chimeras are underlined. The italic *UU* is the linker between the aptamer and siRNA portions. The assembly of these chimeric constructs was described previously (156) and a schematic is presented in Fig 5.1.

5.2c Generation and HIV-1 infection of humanized Rag2^{-/-}γc^{-/-} mice (RAG-hu mice)

Humanized BALB/c-Rag2^{-/-}γc^{-/-} mice were prepared as previously described (56) using human fetal liver-derived CD34⁺ cells. Briefly, neonatal mice were conditioned by irradiating at 350 rads and then injected intra-hepatically with 0.5 ~ 1×10⁶ human CD34⁺ cells. Approximately 12 weeks post-reconstitution, mice were screened for human cell engraftment. Blood was collected by tail bleeds, and red blood cells were lysed using the Whole Blood Erythrocyte Lysing Kit (R&D Systems). The white blood cell fraction was stained with antibodies against the human pan-leukocyte marker CD45 (Caltag) and FACS analyzed as described (56). To infect human cell reconstituted RAG-hu mice,

HIV-1 NL4-3 (1.2×10^5 i.u.) in a 100 μ L volume was injected intraperitoneally at least 12 weeks after cell engraftment. Viral loads were examined weekly and viremia was established in all the mice by 3 weeks. Treatment was done by intravenous (IV) injection on the last day of week 4 with 0.25 nmol experimental RNAs (4.6 μ g *tat/rev* siRNA, or 11.3 μ g Ch A-1) in a 40 μ L volume, followed by another the next day. Later, the injections were continued on a weekly basis for 4 weeks. In the second *in vivo* treatment experiment, 0.25 nmol each of Mutant Chimera Ch A-5, Aptamer alone A-1 or Aptamer-siRNA chimera Ch A-1 in a 40 μ L volume were administered at 5 weeks post infection like above and continued only for 3 weekly injections.

5.2d Measurement of viral load in plasma

To quantify cell-free HIV-1 by qRT-PCR, RNA was extracted from 25 to 50 μ L of EDTA-treated plasma using the QIAamp Viral RNA kit (QIAGEN). cDNAs were produced with Superscript III reverse transcriptase (Invitrogen) using a primer set specific for the HIV-1 LTR sequence, and qPCR was performed with the same primer set and a LTR specific probe using Supermix UDG (Invitrogen) as previously described (56).

5.2e Flow cytometry

Whole blood was collected and red blood cells were lysed as reported previously (44-55). Peripheral blood cells were stained by hCD3-PE and hCD4-PECy5 (Caltag) antibodies and analyzed using a Coulter EPICS XL-MCL FACS analyzer (Beckman Coulter). CD4⁺ T-cell levels were calculated as a ratio of the entire CD3 population

(CD4+CD3+:CD4–CD3+). To establish baseline CD4+ T-cell ratios, all mice were analyzed prior to infection.

5.2f Detection of *tat/rev* siRNA

At five, seven and twelve weeks post-infection (one, three and nine weeks post-injection), blood samples were collected and small RNAs were isolated with MirVana miRNA isolation Kit (Applied Biosystems) according to the manufacturer's instruction. The siRNA quantification was performed using TaqMan MicroRNA Assay according to manufacturer's recommended protocol (Applied Biosystems). 10 nanograms of small RNA, 0.2 M stem-loop RT primer, RT buffer, 0.25 mM dNTPs, 3.33 units/mL MultiScribe reverse transcriptase (RT) and 0.25 units/mL RNase inhibitor were used in 15 L RT reactions for 30 min at 16°C, 30 min at 42°C, and 5 min at 85°C, using the TaqMan MicroRNA reverse transcription Kit (Applied Biosystems). For real-time PCR, 1.33 L of cDNA, 0.2 mM TaqMan Probe, 1.5 mM forward primer, 0.7 mM reverse primer, and TaqMan Universal PCR Master Mix were added in 20 L reactions for 10 min at 95°C and 40 cycles of 15 sec at 95°C and 1 min at 60°C. All real-time PCR experiments were done using an iCycler iQ system (Bio-Rad). Primers were as follows: Site I Looped RT primer: 5'- GTC GTA TCC AGT GCA GGG TCC GAG GTA TTC GCA CTG GAT ACG ACA CAG CG -3'; Site I Forward Primer: 5'- GCT GAT GAG CTC TTC GTC G - 3'; Site I Reverse Primer: 5'- GTG CAG GGT CCG AGG T - 3'; Site I probe primer: 5'- 6- FAM- TCG CAC TGG ATA CGA CAC AGC GAC GA – BHQ1 -3'. In this case, a synthetic 27 mer duplex RNA was used as positive control.

5.2g Determination of HIV-1 *tat/rev* expression.

Human PBMCs were obtained from treated mice at five and seven weeks post-infection (one and three weeks post-injection) and total RNAs were isolated with STAT-60 (TEL-TEST “B”) according to the manufacturer’s instructions. Residual DNA was digested using the DNA-free kit per the manufacturer’s instructions (Ambion). cDNA was made using 2 µg of total RNA. Reverse transcription was carried out using Moloney murine leukemia virus reverse transcriptase and random primers in a 15 µL reaction according to the manufacturer’s instructions (Invitrogen). Expression of the *tat/rev* coding RNAs was analyzed by quantitative RT-PCR using 2× iQ SyberGreen Mastermix (BIO-RAD) and specific primer sets at a final concentration of 400 nM. *Gapdh* expression was used for normalization of the qPCR data. Primers were as follows: IIB *tat/rev* forward primer: 5'- GGC GTT ACT CGA CAG AGG AG -3'; IIB *tat/rev* reverse primer: 5'- TGC TTT GAT AGA GAA GCT TGA TG -3'; BaL *tat/rev* forward primer: 5'- GAA GCA TCC AGG AAG TCA GC -3'; BaL *tat/rev* Reverse primer: 5'- TGC TTT GAT AGA GAA ACT TGA TGA -3'; *gapdh* forward primer 1: 5'- CAT TGA CCT CAA CTA CAT G-3'; *gapdh* reverse primer 2: 5'- TCT CCA TGG TGG TGA AGA C-3'.

5.2h 5'-RACE PCR assay to detect in vivo RNAi mediated target mRNA cleavage

Total RNA was isolated from PBMCs of treated mice using STAT-60 as described above. Residual DNA was digested using the DNA-free kit per the manufacturer’s instructions (Ambion). Subsequently, total RNAs (5 µg) were ligated to a GeneRacer adaptor (Invitrogen) without prior treatment. Ligated RNA was reverse

transcribed using a gene specific primer 1 (GSP-Rev 1: 5'- CCA CTT GCC ACC CAT CTT ATA GCA -3') and SuperScript III reverse transcriptase according to the manufacturer's instructions (Invitrogen). To detect cleavage products, PCR and nested PCRs were performed using primers complementary to the RNA adaptor (5'-cDNA primer: 5'- GGA CAC TGA CAT GGA CTG AAG GAG TA -3') and gene-specific primers (GSP-Rev 2: 5'- CCC AGA AGT TCC ACA ATC CTC GTT -3'; GSP-Rev 3: 5'- TGG TAG CTG AAG AGG CAC AGG CTC -3'; GSP-Rev 4: 5'- CGC AGA TCG TCC CAG ATA AGT GCT AA -3'). Amplification products were resolved by agarose gel electrophoresis and visualized by ethidium bromide staining. The specific PCR products were recovered using a QIAquick Gel purification Kit and then were cloned into TOPO TA cloning vector pCR 2.1-TOPO vector (Invitrogen). Individual clones were identified by DNA sequencing.

5.2i Interferon assays

Total RNA was isolated from PBMCs of treated mice using STAT-60. Expression of mRNAs encoding p56(CDKL2) and OAS1 were analyzed by quantitative RT-PCR using 2× iQ SyberGreen Mastermix (BIO-RAD) as described above and specific primer sets for these genes at final concentrations of 400 nM. Primers were as follows: P56 (CDKL2) forward, 5'- TCA AGT ATG GCA AGG CTG TG -3'; P56 (CDKL2) reverse, 5'- GAG GCT CTG CTT CTG CAT CT -3'; OAS1 forward, 5' - ACC GTC TTG GAA CTG GTC AC -3'; OAS1 reverse, 5'- ATG TTC CTT GTT GGG TCA GC -3'; *gapdh* expression was used for normalization of the qPCR data. In addition, 25-50 μ L of EDTA-treated plasma was collected 2 and 24 hours post treatment. As a positive control for INF-

α induction, mice were injected with 5 μ g of poly (I:C) (Sigma) intravenously in a 50 μ L volume. IFN- α levels were evaluated by Human IFN- α 1 ELISA Ready-SET-Go! (eBioscience).

5.2j Statistical Methods

The mouse viral loads and CD4:CD3 T-cell ratios were plotted by using a lowess smoother across values. Viral loads were first log-transformed prior to smoothing and then anti-transformed for plotting. Missing values were imputed with a last observation carried forward scheme.

To measure the differences between mouse treatment groups, we considered a primary endpoint evaluating longitudinal behavior over time. Our method was to calculate a cumulative area under the curve (AUC) for each mouse, and then compare aggregate mean AUCs between mouse groups. For any sequential time points, (x_i, x_j) , and their corresponding endpoints, (y_i, y_j) , the area under the curve was calculated by using the area of a trapezoid: $0.5 \times (x_j - x_i) \times (y_i + y_j)$. The cumulative AUC of a single observation for the duration of the experiment was the cumulative sum of trapezoids.

The Kruskal-Wallis rank sum ANOVA analog was used for the groupwise cumulative AUC comparisons. We compared pairwise group mean AUCs using t-tests and exact permutation tests under the Hothorn and Hornik *exactRankTests* package for the R language (212-214). Details for deriving the permutation p-values in general are discussed in Streitberg and Röhmel (212).

5.3 Results

5.3a Anti-gp120 aptamer and aptamer-siRNA chimera (Ch A-1) inhibit CCR5 and CXCR4 tropic lab and clinical isolates *in vitro*

We previously described the *in vitro* selection of gp 120 aptamers that bind the HIV-1 Bal 1 envelope with low nanomolar dissociation constants. The lead aptamer, designated as A-1 was fused to an siRNA targeting the HIV-1 *tat/rev* encoding RNAs, and the chimeric construct Ch A-1 (Figure 5.1) delivered the siRNA to HIV-1 infected cells resulting in targeted RNAi mediated knockdown of *tat/rev* expression. In these

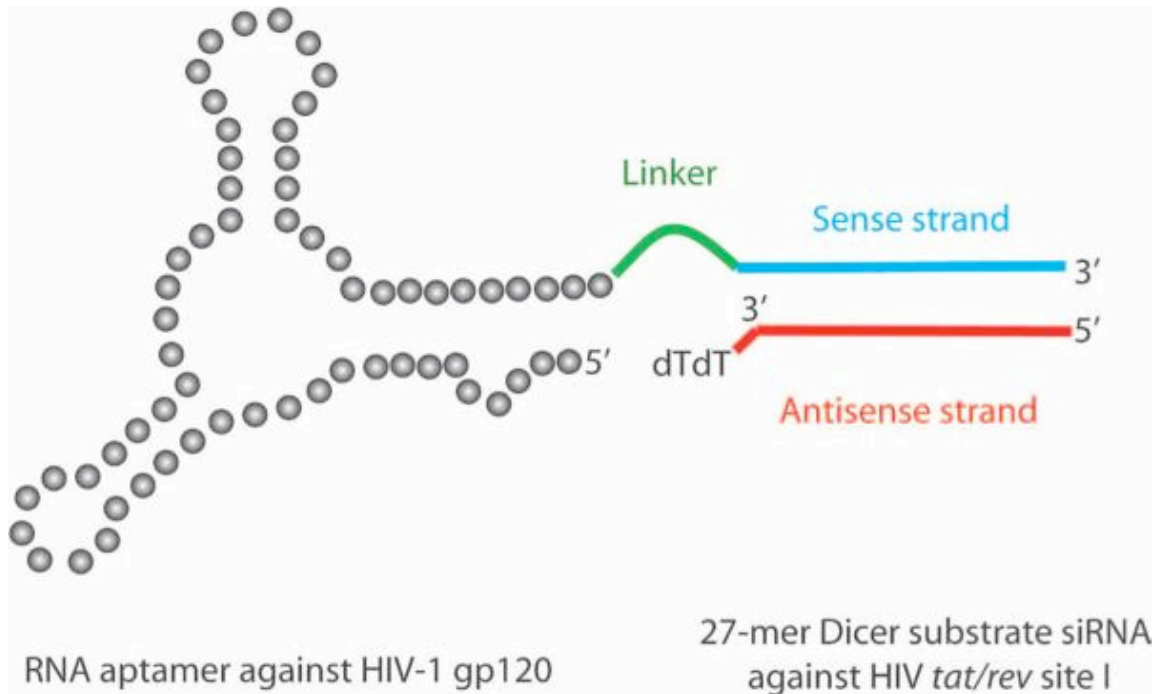


Fig. 5.1 Schematic of anti-HIV-1 gp120 aptamer-siRNA chimera (Ch A-1). The aptamer and sense strand segment of the siRNAs contain nuclease-resistant 2'-fluoro uridine triphosphate and 2'-fluoro cytidine triphosphate. The aptamer portion of the chimera binds to gp120 protein, whereas the 27-mer Dicer substrate siRNA duplex is targeted to the HIV-1 *tat/rev* common exon. A linker (UU) between the aptamer and siRNA is indicated in green.

studies the chimera Ch A-1 provided enhanced inhibition over the A-1 aptamer alone.

Both the A-1 aptamer and Ch A-1 chimera were shown to be capable of inhibiting the replication of both CXCR4 tropic (NL4-3 and IIB) and CCR5 tropic (Bal1) strains of

HIV-1 in cultured T-lymphocytes (CEM cells) and in peripheral blood mononuclear cells (PBMCs) (174).

To better determine the range of envelope types the aptamer and aptamer chimera could recognize, we examined their *in vitro* inhibitory activities using several CXCR4 tropic and CCR5 tropic laboratory and clinical isolates (Figure S5.1 A-F). HIV-1 viral challenge assays were carried out *in vitro* using human PBMCs and CEM T-cells. Cells were infected with the HIV-1 isolates followed by addition of the A-1 or Ch A-1 constructs to the culture media three days post infection and viral replication was monitored by p24 ELISA assays. The results of these viral replication assays show that the aptamer A-1 and Ch A-1 chimera are capable of inhibiting a variety of clinical and lab isolates of HIV-1 to varying degrees (Figure S5.1A-H). Relative to treatment with the aptamer alone the Ch A-1 chimera proved better at inhibiting the two laboratory strains of HIV-1 (Figure S5.1E and F) as well as *tat/rev* expression (Figure S5.1G and H).

5.3b Chimeric Ch A-1 aptamer-siRNA is stable in mouse serum

In order to effectively use the chimeric aptamer *in vivo*, we established that the 2' Fluoro backbone modified aptamer-siRNA chimera is resistant to rapid degradation by serum nucleases. The 2' Fluoro-modified Ch A-1 was incubated in 50% or 5% mouse serum for different lengths of time followed by denaturing polyacrylamide gel electrophoretic analyses and imaging of the transcripts. The serum incubations revealed that the 2'-Fluoro modified Ch A-1 was partially degraded during 24 hours of incubation in 50% serum but was stable out to 72 hours in 5% mouse serum (Figure S5.2). Thus the RNAs should persist for several hours in mouse serum following *in vivo* injections.

5.3c Aptamer and Aptamer-siRNA chimera Ch A-1 suppresses HIV-1 viral loads in viremic RAG-hu mice

In order to evaluate the potential efficacy of the Ch A-1 chimeric aptamer *in vivo*, we chose to test its anti-viral efficacy in the humanized $Rag2^{-/-} \gamma c^{-/-}$ (RAG-hu) mouse model of HIV-1 infection (54, 56). RAG-hu mice infected with HIV-1 NL4-3 became viremic by 3 weeks post infection with viral loads averaging 10^5 per mL, indicating an established infection. We first compared the anti-HIV-1 activity of the chimeric Ch A-1 RNA versus using the *tat/rev* siRNA as an RNA injection control. Six animals were given five weekly injections of 0.25 nmols Ch A-1 or *tat/rev* siRNA alone. Plasma viral loads were monitored at various times to determine the treatment efficacies (Figure 5.2A and Table S5.1A). A general pattern of decreased viral loads was seen in the majority of chimera Ch A-1 treated mice compared to the HIV-1 infected, untreated and siRNA treated controls, and this reached statistical significance with a rank sum $P = 0.0029$ (Figure 5.2A, Table S5.3A). The viral loads were suppressed to below detectable levels in all the chimera treated mice within a week post treatment (week 5 as shown) and this marked viral suppression persisted throughout the treatment period in the majority of mice. Four out of six mice had undetectable viral loads even up to three weeks post-treatment, indicating the sustained efficacy of the Ch A-1 chimera (Table S5.1A). However, while there was a marked suppression during first three weeks, there was viral rebound in two of the Ch A-1 treated mice, suggestive of the emergence of Ch A-1

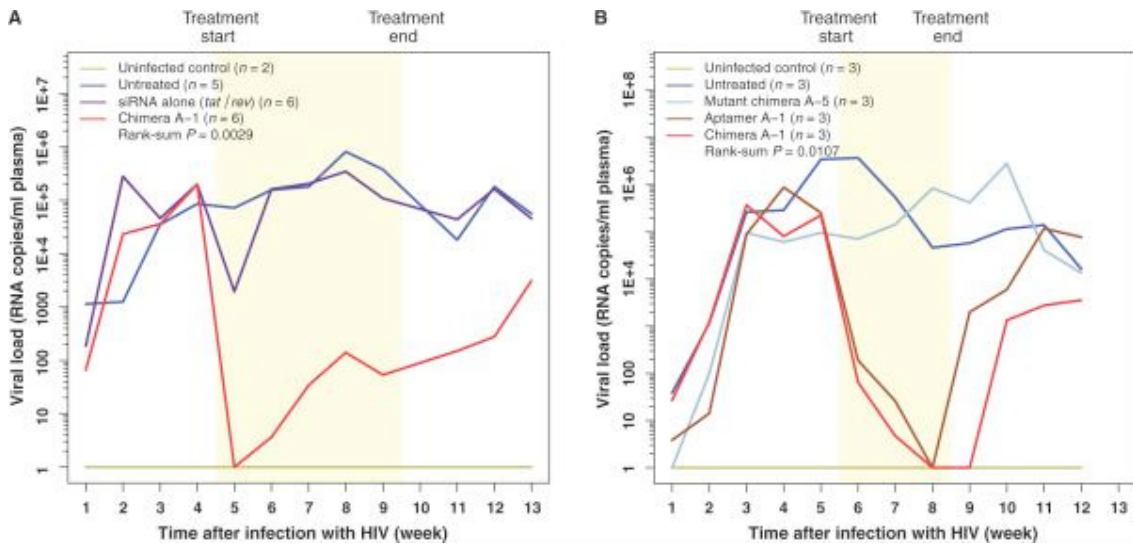


Fig. 5.2 Aptamer A-1 and chimera Ch A-1, but not a mutant chimera, suppress viral loads in HIV-1-infected RAG-hu mice. Mice were infected with HIV-1 at week 0, and 5 weeks later, weekly treatments were started. The treatment period is indicated by the yellow region. **(A)** Viral loads in uninfected mice ($n = 2$), untreated mice ($n = 5$), *tat/rev* siRNA only-treated mice ($n = 6$), and ChA-1-treated mice ($n = 6$). **(B)** In a separate experiment, viral loads in uninfected mice ($n = 3$), untreated mice ($n = 3$), A-1 aptamer-treated mice ($n = 3$), Ch A-1 chimera-treated mice ($n = 3$), and mutantA-5 chimera-treated mice ($n = 3$). The viral RNA was detected through qRT-PCR as described in Materials and Methods. Thus, if there was no detectable viral RNA, we established this as a value of 1 (10^0) to allow for the use of logarithmic values on the y axis. P values for the effects of A-1 and Ch A-1 are indicated and were calculated as described in Materials and Methods. The data for individual mice are presented in fig. S6.3 and table S6.1.

resistance. Importantly, even though these animals had high viral loads, their levels of T-cells did not decline (Table S5.2A). The “naked” anti-*tat/rev* siRNA treatment did not provide viral suppression beyond one week.

To determine the relative anti-HIV contribution of the siRNA component of the Ch A-1 aptamer-siRNA chimera, additional groups of 3 viremic animals treated with 0.25 nmols of the A-1 aptamer, the chimeric Ch A-1 molecule and a mutant aptamer-*tat/rev* siRNA chimera Ch A-5, as described in the Materials and Methods. The A-5 aptamer portion of Ch A-5 has previously been shown to have poor affinity for gp120. Plasma viral loads were monitored to ascertain the efficacy of each treatment (Figure 5.2B). Viral loads were strongly suppressed in A-1 and Ch A-1 treated mice compared to the non-treated group, reaching statistical significance ($P = 0.0107$). As expected, there was no

notable viral suppression in the mice treated with the control, mutant aptamer-siRNA chimera Ch A-5 (Figure 5.2B and Table S5.1B). The viral levels remained suppressed in all of the A-1 and Ch A-1 treated mice throughout the 3 week treatment period (weeks 6, 7 and 8). In the aptamer treated animals, there was viral suppression during the 3 week treatment period followed by moderate suppression continuing for an additional 2 weeks. In contrast all of the Ch A-1 treated animals had undetectable viral loads at week 9, which is one week after the last injection (Figure 5.2B and Table S5.1B). The lower viral loads in the Ch A-1 treated animals persisted through week 12. In contrast, viral loads returned to pretreatment levels by week 11 in the animals treated with the A-1 aptamer alone. The enhanced duration of HIV-1 suppression afforded by the inclusion of the siRNA in Ch A-1 is statistically significant ($p=0.04$).

To validate that the Ch A-1 delivered the anti-*tat/rev* siRNA to infected T-lymphocytes, PBMCs were collected at one and three weeks during, and three weeks after the last treatment of the first set of animals (Figure 5.2A). Small RNAs were extracted and analyzed for the presence of the *tat/rev* siRNA by real-time Taqman qRT-PCR assays (Figure 5.3A). The results of these analyses showed that the *tat/rev* siRNA was detectable in PBMCs from all of the Ch A-1 treated mice at weeks five and seven, and in three of the animals at week 12, which is three weeks after the last injection. In contrast, no siRNAs were detected in the PBMCs of mice treated solely with *tat/rev* siRNA. We also assayed for the down-regulation of *tat/rev* gene expression in PBMCs of infected and treated mice using qRT-PCR. Our results showed a 75-90% reduction in the levels of *tat/rev* transcripts in chimera treated mice at both 1 and 3 weeks during the treatment period (Figure 5.3B).

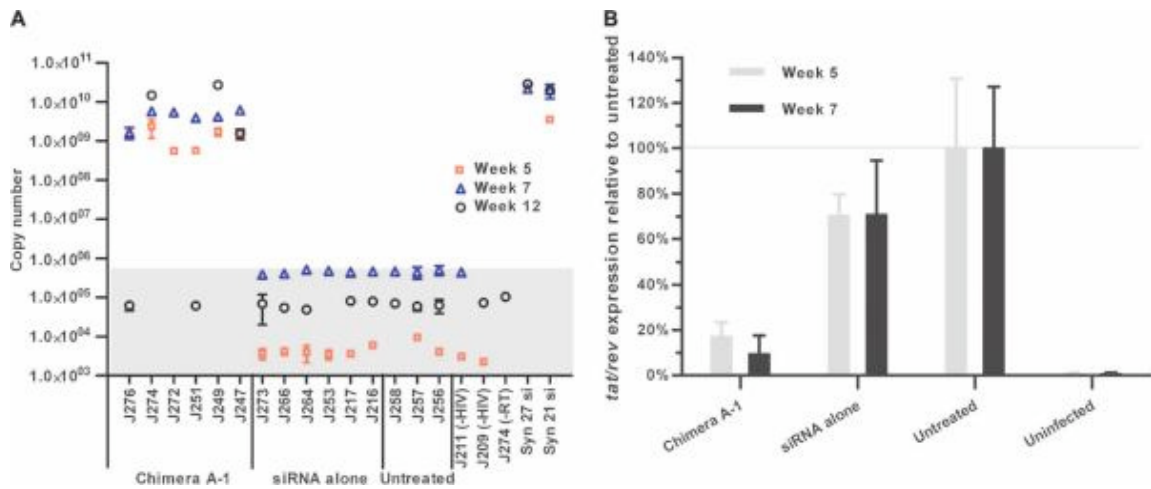


Fig. 5.3 The detection and function of *tat/rev* siRNA in PBMCs from treated RAG-hu mice. (A) Detection of the siRNA sequences in PBMCs during (weeks 5 and 7 after infection) and after (week 12) treatment with Ch A-1 and siRNA only, and in untreated mice and uninfected mice (animals from Fig. 6.2A). One minus RT control, J274 (-RT), also was set up. The synthetic 27- and 21-mer *tat/rev* siRNAs were used as positive controls. The background copy number of siRNA is $<10^6$ (gray area). Error bars indicate SD ($n = 4$ measurements per sample). Some of the error bars are not discernible in the graph because their relative percentage was less than 5%. (B) Expression of *tat/rev* gene transcripts at the first and third weeks of treatment (weeks 5 and 7 after infection) with Ch A-1 and siRNA only and in untreated and uninfected animals (animals from Fig. 6.2A). Gene expression was normalized to that of a representative HIV-1-infected untreated mouse.

To confirm that the *tat/rev* siRNA was indeed functioning through the RNAi mechanism *in vivo*, a modified 5'-RACE (Rapid amplification of cDNA ends) PCR was performed on RNAs isolated from PBMCs of the second group of treated animals represented in Figure 2B. It has been established that Ago2 mediates cleavage between bases 10 and 11 relative to the 5' end of the siRNA guide strand (236,237). Thus the RACE PCR product sequence analyses should reveal a linker addition at the base 10 nucleotides downstream from the 5' end of the siRNA guide strand. PCR bands of the predicted lengths were detected in the PBMC samples from mice treated with the chimera Ch A-1 following three nested PCR reactions (Figure 5.4A). No appropriately sized products were generated from total RNAs isolated from PBMCs of non-treated animals

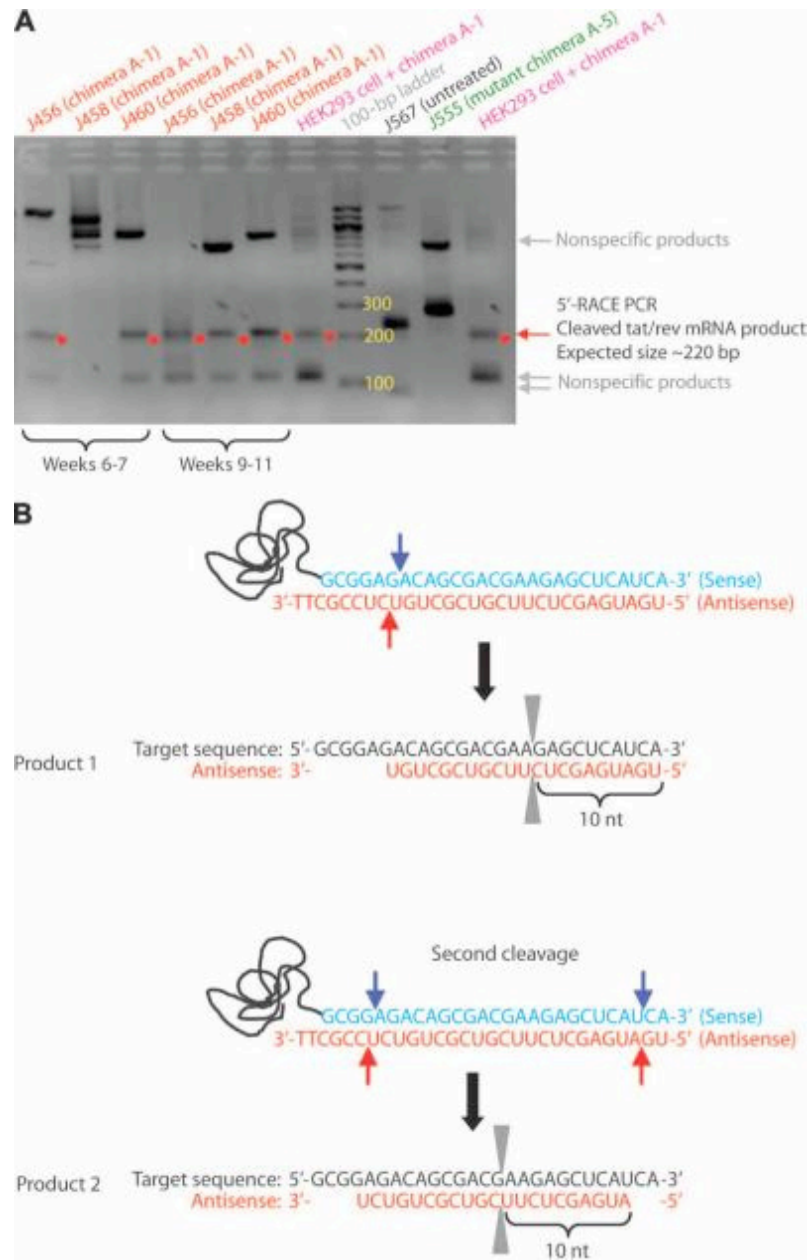


Fig. 5.4 5'-RACE PCR analysis of in vivo *tat/rev* siRNA delivered by Ch A-1. (A) Nested PCR products were resolved in an agarose gel; specific siRNA-mediated RACE PCR cleavage mRNA products are marked by a red arrow. (B) DNA sequence analyses of cloned RACE PCR products. The positions of the two different siRNA-directed cleavage sites in the *tat/rev* target RNA are indicated. nt, nucleotides.

or from those treated with the mutant aptamer-siRNA chimera Ch A-5. The gel-purified bands of the predicted lengths were cloned and individual clones were characterized by DNA sequencing to verify the expected PCR products. Two different cleavage sites were found in the samples from the Ch A-1 treatment (Figure 5.4B). One cleavage takes place between positions 10 and 11 from the 5' end of the siRNA antisense strand (Figure 5.4B). The second RACE product was displaced by two nucleotides along the mRNA suggesting a different Dicer product of the *tat/rev* siRNA, generating a guide strand shifted by two bases relative to the other cleavage product. In total, these data provide strong evidence that the chimera delivered siRNAs are processed intracellularly and are functionally incorporated into RISC, thus triggering sequence specific degradation of the HIV *tat/rev* target RNA.

5.3d The anti-gp120 aptamer and chimeric aptamer-siRNA provide protection against HIV-1 mediated T-cell depletion

A major characteristic of HIV-1 infection is helper CD4+ T-cell loss during the acute stage of infection followed by a return to a set point for several months/years with an eventual depletion leading to AIDS (238, 239). Therefore, prevention of CD4+ helper T-cell loss would contribute to immune reconstitution and restoration of immune function. To determine whether treatment of HIV-1 infected RAG-hu mice with the Ch A-1 chimera could protect against depletion of CD4+ T-cells, CD4+ T-cell levels were evaluated in peripheral blood collected at weekly intervals during and post treatment (Figures 5.5, 5.6 and Tables S5.2A). In the first set of animals tested the protection against T-cell depletion was significant when we compared the non-treated group with

the chimera A-1 group ($P = 0.0476$) (Figure 5.5A and Table S5.2A). In control, non-infected mice (HIV negative) the levels of CD4⁺ T-cells remained relatively stable within a 5% variation range, whereas in untreated HIV-1 infected mice the CD4⁺ T-cell levels began to decline beginning at 4 weeks post infection to below 50% of the starting levels at 18 weeks post-infection. In contrast, the levels of CD4⁺ T-cells in Ch A-1 treated mice remained at or near the levels of uninfected mice and this level remained stable well beyond the last treatment, indicating that the chimeric construct provides protection against CD4⁺ cell depletion. While the protection against T-cell depletion in the second group of animals is clearly discernable, due to the shorter time frame of A-1 and Ch A-1 injections (3 weeks vs 5 weeks for the first group of animals) it approached, but did not reach statistical significance ($P = 0.0920$) (Figure 5.5B and Table S5.2B).

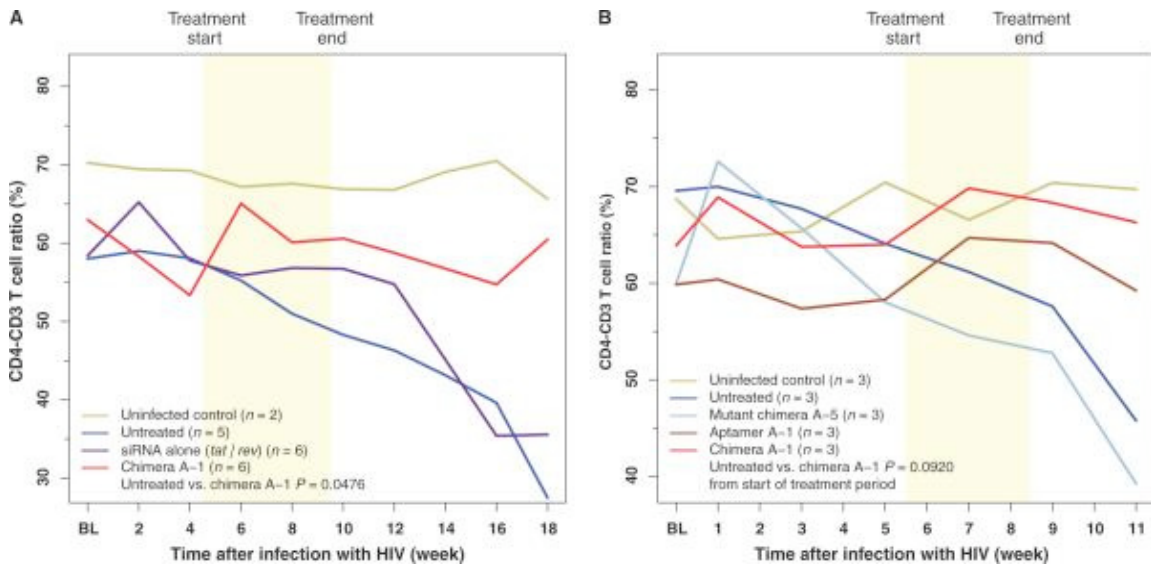


Fig. 5.5 Protection of RAG-hu mice from CD4⁺ T cell loss by the Ch A-1 chimera. CD4⁺ T cell levels were assessed by FACS at each indicated week before and after siRNA treatment. BL, baseline measurement. Treatment duration is indicated by the yellow region. (A) Mice from the first experiment (shown in Fig. 6.2A) group. Uninfected mice ($n = 2$), untreated mice ($n = 5$), *tat/rev* siRNA–treated mice ($n = 6$), and chimera Ch A-1–treated mice ($n = 6$). (B) Mice from second experiment (shown in Fig. 6.2B). CD4-CD3 T cell ratios were assessed by FACS at each indicated week before and after treatment. P values for both experiments were determined as described in Materials and Methods. For baseline measurements, each individual mouse was bled twice before HIV-1 infection and the CD4-CD3 values were averaged within treatment groups to establish a baseline CD4-CD3 level. The data for individual mice are presented in fig. S6.4 and table S6.2.

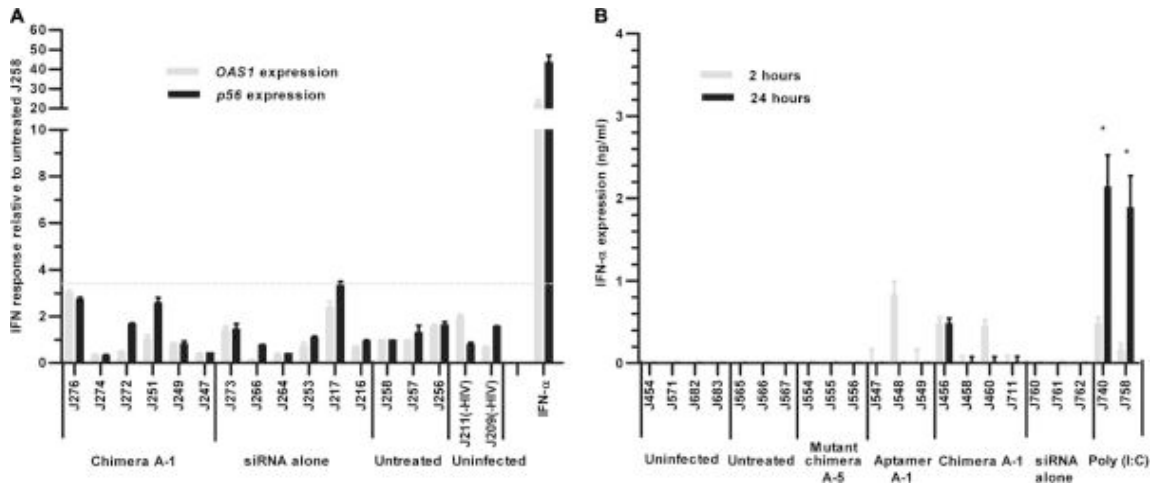


Fig. 5.6 Effect of in vivo administration of Ch A-1 on type I IFN. (A) The effect of aptamer A-1 and chimera A-1 on expression of type I IFN response genes (*p56* and *OAS1*) at week 7 after infection. IFN- α -treated, infected human PBMCs were used as a positive control. Gene expression was normalized to the *gapdh* mRNA. Error bars indicate SD ($n = 4$). (B) Expression of IFN- α 2 or 24 hours after RNA injection as measured by an ELISA. Poly I:C-treated, HIV-infected RAG-hu mice were used as a positive control. Error bars indicate SD ($n = 3$).

5.3e Anti-gp120 aptamer-siRNA chimera does not trigger type I interferon response

in vivo

It has been demonstrated that systemic administration of synthetic siRNA duplexes can activate innate immune responses, inducing cytokines such as tumor necrosis factor- α (TNF- α), interleukin-6 (IL-6), and interferons (IFNs), particularly IFN- α (IFN- α) (215). Such non-specific immune activation by siRNA-based drugs could contribute to the anti-viral effects but can also create undesirable toxicities. We therefore assessed the potential induction of type I IFN-regulated gene expression using quantitative RT-PCR expression assays on PBMC derived RNAs isolated from chimera treated and control mice (Figure 5.6A). We used IFN- α treated PBMCs as a positive control to compare up-regulation of *p56* and *OAS1* gene expression. We did not observe type I IFN responses in PBMCs from any of the animals at different times post-treatment (Figure 5.6A). Using an ELISA assay we also directly monitored IFN- α levels in treated

mice at 2 hours and 24 hours post-injection of the experimental RNAs (Figure 5.6B). Less than 1 ng/mL of IFN- α was detected in one of the aptamer and two of the Ch A-1 treated animals, but these levels are several folds lower than those induced by Poly I:C (Figure 5.6B).

5.3f Deep sequence analyses of viral RNAs for envelope and *tat/rev* target mutations

Development of viral resistance is a common setback with HIV-1 therapies due to generation of viral escape mutants. To assess the possible emergence of viral mutants in the HIV envelope and *tat/rev* sequences we carried out deep sequencing analyses of these two regions of the virus. Our goal was to determine whether or not a specific class of mutations predominated in the samples from treated versus non-treated, HIV infected animals. In order to have enough material to carry out these analyses we used pooled virus from serum collected from Ch A-1 treated animals at weeks 7 through 9 of the first set of experiments and compared this sample with virus collected from animals not receiving anti-viral treatment. Solexa deep sequence analyses of viral RNAs showed a small increase in the percentage of point mutations in the envelope sequences of Ch A-1 chimera treated animals relative to non-treated controls, but no dominant mutant(s). Figure S6.3 lists all the point mutations in the HIV-1 envelop domain with a frequency above 1%. More changes were detected in the gp120 domain (31 mutations) compared to the gp41 domain (5 mutations). There were only 7 mutations (less than 1%) in the *tat/rev* target sequence (Figure S5.3). These results suggest some selective pressure on the HIV-1 gp120 envelope exerted by the aptamer. Nevertheless, even for this gene, the mutation

frequency is less than 5% above the frequency observed in non-treated animals and most importantly, no dominant mutations were found.

5.4 Discussion

In the present study we have tested RNA based combinatorial approach for treatment of HIV-1 infection in a humanized mouse model that supports HIV-1 replication and T-cell decline as a consequence of HIV-1 infection. Prior to our studies, single chain antibody-siRNA chimeras targeting either gp120 expressing cells or the T-cell specific CD7 receptor have been shown to functionally deliver anti-HIV-1 siRNAs *in vivo* (122). However, in these studies only the siRNA component has been shown to have antiviral activity. In contrast, we observe potent anti-viral activity by the aptamer itself, and this is enhanced by aptamer mediated delivery of an anti-HIV-1 delivered siRNA.

The animal model we used for delivering the aptamer-siRNA chimera provides a very stringent and relevant test for anti-HIV-1 activity in human cells. An advantage of this animal model versus non-human primates is that the humanized mice can be infected with any strain of HIV-1 that is capable of infecting humans whereas the non-human primate models require the use of SIV or SIV-HIV hybrid SHIVs. Thus efficacious therapeutic approaches in the humanized mouse model do not have to be redesigned for human applications. In this system HIV-1 infection results in high levels of viral replication prior to the injection of the aptamer and Ch A-1 chimeric construct. The aptamer and aptamer-siRNA chimera decreased viral loads by several logs in all the treated animals within a week following intravenous administration. The suppression of

viral load averaged three orders of magnitude or greater relative to controls and persisted throughout and beyond the treatment period in seven of nine animals tested in this study.

The results presented in this study provide an *in vivo* validation of the anti-HIV-1 efficacy of the anti-gp120 aptamer siRNA chimera. We have used the aptamer both as an HIV neutralizing agent and as a vehicle for delivering a siRNA for triggering RNAi mediated down regulation of the HIV-1 *tat/rev* transcripts. Using real time RT-PCR and RACE PCR assays we demonstrated that the aptamer delivered siRNA is functionally active *in vivo*. The combinatorial inhibitory functions of the aptamer and siRNA make this approach potentially superior to the other anti-siRNA delivery approaches reported prior to this work (122). In these other studies, only the siRNA was demonstrated to be functional as an anti-HIV agent. The high potency and enhanced duration of viral suppression of the current approach is largely attributable to the dual anti-HIV activities of both the aptamer and aptamer delivered siRNA. In contrast to the antibody mediated siRNA delivery, which requires biological production of the antibodies and creation of chimeric antibody-cationic peptide conjugates, the chimeric aptamer-siRNAs can be synthesized as a single unit or as two separate but combinable units using either biochemical or chemical methods. Since these RNA based molecules are not antigenic, they can be administered repeatedly without concerns about generating undue immunological responses expected with antibody-peptide conjugates.

The aptamer-siRNA technology can be developed to avert viral resistance by the use of a cocktail of gp120 aptamers of different specificities that are combined with siRNAs directed against different mRNA targets (both viral and cellular). We envision

that the first dual-function aptamer-siRNA chimeras can be applied to patients who harbor virus resistant to antiretroviral drugs.

5.5 Acknowledgements

We thank NIH AIDS Research and Reference Reagents Program for HIV-1 related reagents used in this work.

CHAPTER 6
INHIBITION OF HIV-1 T CELL DEPLETION IN RAG-HU MICE BY LENTIVIRAL
VECTOR DELIVERY OF THREE ANTI-HIV GENES INTO HUMAN HSCs

Work presented in this chapter is in prepration for journal submission.

6.1 Overview

The development of efficacious anti-HIV gene constructs has provided a promising approach for gene therapeutic strategies that restrict human immunodeficiency virus (HIV) infections and AIDS progression. CD34+ hematopoietic stem cells are an optimal choice to deliver such anti-HIV constructs into CD4+ HIV-1 susceptible cells, since they can be transduced with constructs prior to host engraftment. Additionally, following implantation these cells will differentiate into the HIV-1 susceptible cells namely, macrophages, CD4 T cells and dendritic cells, which also possess an integrated anti-HIV defense. Lentiviral vectors provide the means of transduction, able to transduce non-dividing cells with the constructs of choice.

For our studies we selected three previously developed and described anti-HIV gene constructs with different modes of action namely, small interfering RNAs (siRNAs), RNA decoys, and ribozymes. This triple combinatorial approach limits HIV mutant escape by targeting different steps of the viral infection cycle, much like current combinatorial anti-retroviral therapies. All three constructs were utilized in a lentiviral backbone to form a Triple-R construct, and our previous work has demonstrated the safety and efficacy of Triple-R vector-transduced CD34 cells in SCID-hu mice. Here we have expanded our previous work by hepatically injecting CD34 Triple-R vector-transduced cells into RAG-hu mice, showing high levels of hematopoietic engraftment. This resulted in Triple-R transduced T cells and macrophage that resist HIV infection, effectively preventing CD4 T cell decline and efficiently developing an HIV resistant humanized mouse. These results illustrate the potential for gene therapy approaches in combating HIV and AIDS in an animal model.

6.2 Materials and Methods:

6.2a Combinatorial lentiviral vector design and production

A third-generation HIV-derived lentiviral vector containing an EGFP reporter gene, HIV7-GFP, was used in this study as previously described (189). The construction of the combination Triple-R lentiviral vector along with the production of high-titer vectors was described previously (189). In brief, the shRNA component targeting *rev/tat* is placed under the control of a U6 promoter, whereas the TAR decoy is embedded in the U16 small nucleolar RNA backbone for nucleolar localization and is also driven by a U6 promoter. The CCR5 ribozyme is under the control of an adenoviral VA1 promoter. Lentiviral vectors were generated in 293T cells. In all, 15 µg of the packaging construct, pCHGP-2, 15 µg of HIV7-GFP (control empty vector) or Triple-R (combination) transfer vector, 5 µg of vesicular stomatitis virus glycoprotein (pseudotyping envelope), and 5 µg of cytomegalovirus-Rev were transfected into cells cultured on 100-mm plates by calcium phosphate transfection. Vector supernatants were collected at 24, 36, 48, and 60 hours after transfection and concentrated by ultracentrifugation. Vector titers were obtained by transduction of 293T cells and measured for EGFP expression by FACS. The titers were 3.8×10^8 and 7.2×10^8 transduction units for the HIV7-GFP control and Triple-R vectors, respectively.

6.2b Isolation and transduction of CD34 HSCs

CD34 HSCs were purified from human fetal liver using monoclonal antibody–conjugated immunomagnetic beads (Miltenyi Biotech, Auburn, CA). The purity of CD34

cells obtained was routinely >97% (data not shown). Cells were cultured in Iscove's medium containing 10% fetal bovine serum and 10 ng/ml of each of the cytokines IL-3, IL-6, and stem cell factor (SCF). For transductions, CD34 cells were incubated with the respective vectors (MOI 15), HIV7-GFP and Triple-R, overnight in the presence of 8 µg/ml polybrene. Two rounds of transductions were performed on two consecutive days. Transduction efficiencies ranged from 74.9 to 92.4% for HIV7-GFP and Triple-R, respectively.

6.2c Reconstitution of Rag-hu mice with transduced CD34+ cells

To evaluate the capabilities of shRNA/TAR decoy/CCR5 ribozyme transduced CD34+ to develop hematopoietic cells, a Rag2^{-/-}γ^{-/-} mouse model, that supports multilineage hematopoiesis was used. Transduced CD34+ cells, 2 x 10⁶ cells per mouse, were injected intrahepatically. Eight weeks post-injection, peripheral blood was collected and analyzed for huCD45 and EGFP expression by FACS to evaluate reconstitution levels.

6.2d Measurement of viral load in plasma

To quantify cell-free HIV-1 by qRT-PCR, we extracted RNA from 25 to 50 ml of EDTA-treated plasma with the QIAamp Viral RNA kit (Qiagen). cDNAs were produced with SuperScript III reverse transcriptase (Invitrogen) with a primer set specific for the HIV-1 long terminal repeat (LTR) sequence, and qPCR was performed with the same primer set and an LTR-specific probe with Supermix UDG (Invitrogen) as previously described (55).

6.2e Flow cytometry

Whole blood was collected and red blood cells were lysed as reported (54). Peripheral blood cells were stained by hCD3-PE and hCD4- PE-Cy5 (Caltag) antibodies and analyzed with a Coulter EPICS XL-MCL FACS analyzer (Beckman Coulter). For transgenic mice, CD4⁺ T cell levels were calculated as a ratio of the entire CD3 population (CD4⁺CD3⁺-CD4⁻CD3⁺). Percent of transgene expression was determined on the EGFP⁺ of the CD3⁺-CD4⁺ population of cells.

6.2f Multi-parametric FACS analysis of transgenic hematopoietic lineage

To determine whether transgenic CD34⁺ cells differentiated in the Rag-hu mice, various cell surface markers were analyzed. Cells were stained with respective antibodies to CD3, a pan-T cell marker, CD4, and CD8 to detect sub-populations of T-helper, T-cytotoxic, and immature double-positive cells, CD19 for B cell populations and CD14 for macrophages. The following antibodies were used for analysis: PE-Texas Red-CD3, Alexa Fluor 405-CD8 (Caltag, Burlingame, CA), PE-CY7-CD14, APC-CD45, PE-CD20, and PE-CY5-CD4 (BD Biosciences, San Jose, CA). Stained cells were analyzed on a Beckman Coulter ARIA flow cytometer. For evaluation of transgenic mice, cells expressing EGFP were analyzed. CD45-positive and EGFP-negative cells present in the mice were used as non-transduced internal cell controls for these analyses.

6.2g Detection of transgene tat/rev siRNA expression

The Rag-hu mice were engrafted with transgenic CD34 HECs as described. Thirty-two weeks later blood samples were collected, PBMCs extracted and small RNAs were isolated with MirVana miRNA isolation Kit (Applied Biosystems) according to the manufacturer's instruction. The transgene siRNA quantification was performed using TaqMan MicroRNA Assay according to manufacturer's recommended protocols (Applied Biosystems), as previously described (201). Briefly, ten nanograms of small RNA, 0.2 M stem-loop RT primer, RT buffer, 0.25 mM each dNTP, 3.33 units/mL MultiScribe reverse transcriptase (RT) and 0.25 units/mL RNase inhibitor were used in 15 L RT reactions for 30 min at 16°C, 30 min at 42°C, and 5 min at 85°C, using the TaqMan MicroRNA reverse transcription Kit (Applied Biosystems). For real-time PCR, 1.33 L of cDNA, 0.2 mM TaqMan Probe, 1.5 mM forward primer, 0.7 mM reverse primer, and TaqMan Universal PCR Master Mix were added in 20 L reactions for 10 min at 95°C and 40 cycles of 15 sec at 95°C and 1 min at 60°C.

6.3 Results

6.3a Triple-R and HIV7-GFP vector-transduced CD34 cells can reconstitute Rag2/- γ c-/- mice

CD34+ hematopoietic cells were isolated from fetal liver and transduced with either HIV7-green fluorescent protein (HIV7-GFP) or Triple-R vector. Levels of transduction efficiency were evaluated for EGFP expression by fluorescence-activated cell sorting (FACS) and were 74.9% and 92.4% for HIV7-GFP and Triple-R, respectively

(Figure 6.1). A variation in transduction efficiency was observed but is consistent with what we have previously reported (193).

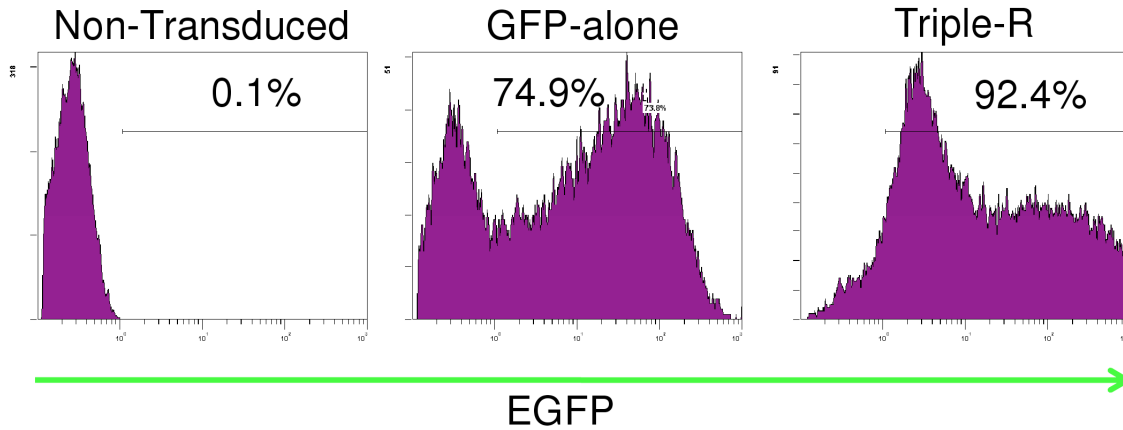


Figure 6.1. Lentiviral vector transduction efficiency in CD34 cells. Purified CD34 cells were transduced with either control human immunodeficiency virus-7 green fluorescent protein (HIV7-GFP) or Triple-R vector and analyzed by fluorescence-activated cell sorting (FACS) for EGFP expression to determine transduction efficiency. The percentage of EGFP-positive cells is indicated for each vector.

Transgenic CD34⁺ cells were intra-hepatically injected into the Rag^{-/-}γg^{-/-} (RAG-hu) mice which offer an ideal environment for hematopoiesis (55). Eight weeks post engraftment levels of reconstitution were determined by staining peripheral blood for the human pan leukocyte marker CD45 and for EGFP expression by FACS. Levels of total human engraftment (huCD45⁺) ranged from 10-66.4% for HIV7-GFP and 6.9-72.5% for Triple-R transgenic mice (Table 6.1). Transgene expression (EGFP) averaged 52% and 49.25% for HIV7-GFP and Triple-R, respectively. Representative FACS plots for huCD45⁺ EGFP⁺ cells obtained from HIV7-GFP and Triple-R mice are shown (Figure 6.2).

6.3b Transgenic cell engraftment persists and results in normal hematopoietic differentiation

To verify long term persisting cell engraftment and retained expression of transgenes, RAG-hu transgenic mice were monitored weekly for human leukocyte engraftment and EGFP expression (Figure 6.3a and 6.3b). A marked decrease in engraftment as compared to the non-manipulated mice is seen but is consistent with published data (216) (Figure 3a). Additionally, although engraftment mildly decreases over the 34 week study period, average engraftment persists over 30% and transgene expression remains stable for both treatment groups (Figure 6.3a and 6.3b).

GFP-alone					Triple-R				
Mouse #	CD45+	CD45+GFP+	Total Engraftment	%GFP Expression	Mouse #	CD45+	CD45+GFP+	Total Engraftment	%GFP Expression
GFP 1	17.90%	18.90%	36.80%	51.36%	TX 1	2.40%	4.50%	6.90%	65.22%
GFP 2	11.40%	13.20%	24.60%	53.66%	TX 2	3.70%	2.10%	5.80%	36.21%
GFP 3	32.10%	28.60%	60.70%	47.12%	TX 3	23.60%	22.20%	45.80%	48.47%
GFP 4	9.30%	11.20%	20.50%	54.63%	TX 4	22.00%	28.10%	50.10%	56.09%
GFP 5	24.10%	24.40%	48.50%	53.63%	TX 5	33.00%	39.50%	72.50%	54.48%
GFP 6	19.20%	12.70%	31.90%	39.81%	TX 6	26.40%	12.70%	39.10%	32.48%
GFP 7	14.60%	14.30%	28.90%	49.48%	TX 7	34.50%	36.20%	70.70%	51.20%
GFP 8	3.40%	6.60%	10.00%	66.00%	TX 8	23.90%	12.00%	35.90%	33.43%
GFP 9	13.90%	12.00%	25.90%	46.33%	TX 9	30.50%	32.20%	62.70%	51.36%
GFP 10	21.50%	35.40%	56.90%	62.21%	TX 10	29.50%	31.80%	61.30%	51.88%
GFP 11	28.40%	32.20%	60.60%	53.14%	TX 11	13.60%	21.20%	34.80%	60.92%
GFP 12	33.20%	33.20%	66.40%	50.00%	Average	22.10%	22.05%	44.15%	49.25%
Average	19.08%	20.23%	39.31%	52.00%					

Table 6.1. Enhanced green fluorescent protein (EGFP) expression by leukocytes derived in RAG-hu mice. Vector-transduced CD34 cells were injected intra-hepatically into the RAG-hu mice and allowed to differentiate into leukocytes. At 8 weeks post engraftment peripheral blood was collected and analyzed by FACS for the pan leukocyte marker huCD45 and EGFP expression.

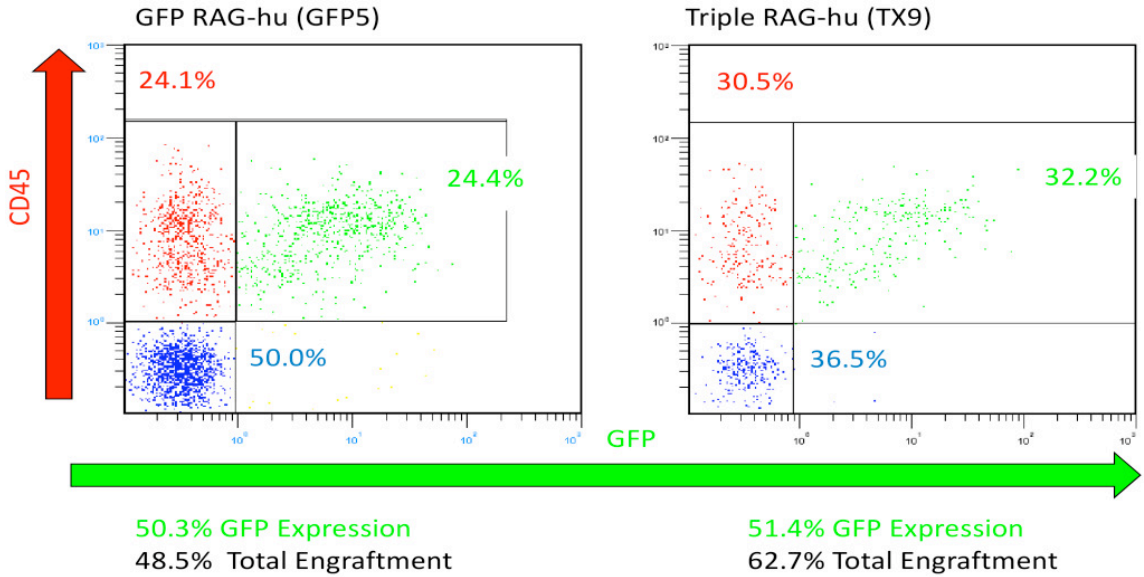


Figure 6.2. Enhanced green fluorescent protein (EGFP) expression by leukocytes derived in RAG-hu mice. Vector-transduced CD34 cells were injected intra-hepatically into the RAG-hu mice and allowed to differentiate into leukocytes. At 8 weeks post engraftment peripheral blood was collected and analyzed by FACS for the pan leukocyte marker huCD45 and EGFP expression. Representative examples of a GFP and Triple-R mice are shown. The percentages of huCD45-positive and EGFP-positive cells are indicated.

Foreign transgenes can cause undesirable effects thus it is essential to evaluate transgenic cells to determine if they are physiologically normal. Phenotypic analyses were performed to detect the normal differentiation of various hematopoietic cells. The data shown are representative figures from all replicates analyzed. As shown in Figure 6.4, within a mouse, comparable levels of GFP⁺ and GFP⁻ immune cells including T cells, B cells and macrophages were found in peripheral blood. This illustrates normal development of hematopoiesis from transgenic CD34⁺ stem cells.

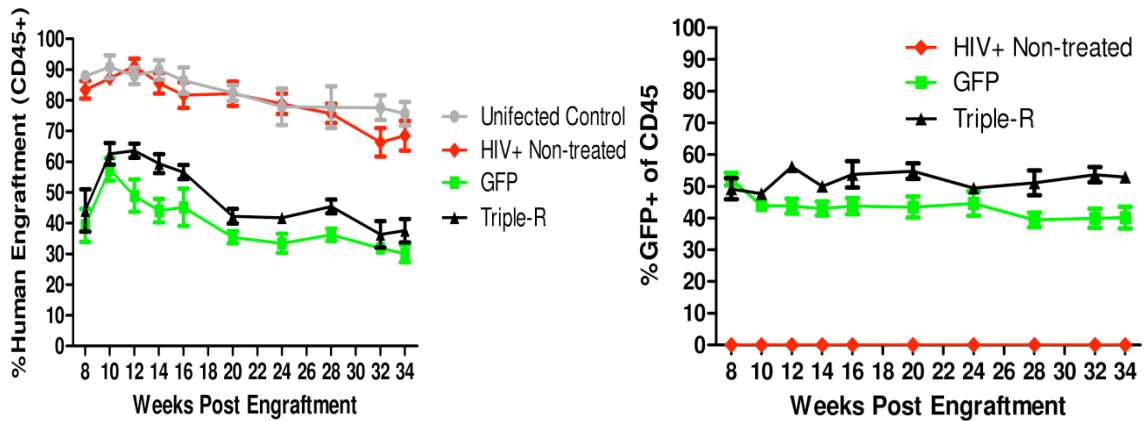


Figure 6.3. Transgenic huCD45 engraftment in Rag-hu mice. A) Peripheral blood was collected and stained for huCD45 weekly to determine transgenic engraftment levels during the study period. B) EGFP was analyzed using FACS analysis to determine transgenic percentage weekly.

6.3c Triple-R vector-transduced CD34 reconstituted RAG-hu mice are resistant to HIV challenge and are completely protected against CD4 T cell depletion

To determine the levels of viral inhibition conferred by Triple-R transduced CD34+ derived hematopoietic cells in Rag-hu mice, mice were challenged with R5-tropic BaL HIV-1 (3.4×10^6 i.u.) in a 100 μ L volume injected intraperitoneally. Resistance to productive infection was observed with Triple-R transgenic mice compared to nontransduced and GFP-alone transgenic mice (Figure 6.5). The lower viral loads in HIV7-GFP compared to the non-manipulated group reflects the lower engraftment levels and subsequent targets of HIV for high infection levels, however; a greater than a 1.2 log inhibition in Triple-R compared to control HIV7-GFP mice, which have similar levels of engraftment, was observed at all time points. These data suggest the resistance of Triple-R transgenic mice to HIV-1 infection.

The primary target of HIV-1 is CD4+ T cells, causing depletion of these cells to be a distinct characteristic of infection. Loss of CD4+ T cells leads to AIDS, thus protection of these cells against HIV mediated depletion is a primary focus. To determine

whether Triple-R transgenic mice were protected against CD4⁺ T cell depletion we measured cell levels of CD4 and CD3 in peripheral blood collected bi-weekly and expressed them as a T cell ratio (Figure 6.6a). HIV⁺ non-treated as well as HIV7-GFP animals had marked reduction in T cell levels (>20%) in contrast to the Triple-R mice which were completely protected against HIV mediated CD4⁺ depletion (Figure 6.6a). In control uninfected mice stable levels, with in a 5% variation range, were seen whereas in untreated HIV-1 and HIV7-GFP mice, the CD4⁺ T cell levels began to decline within 2 weeks after HIV infection to below 50% and 60% of initial levels for HIV7-GFP and HIV⁺ non-treated control mice, respectively.

To further verify the efficacy of protection by the Triple-R transgenes against CD4⁺ T cell depletion we analyzed EGFP expression in the CD4⁺ T cell population. Although lower transgene expression in CD4⁺ T cells by FACS analysis for EGFP was seen compared to transgene expression in CD45⁺ cells in the same animals a stable expression rate remained even after HIV challenge in the Triple-R transgenic mice (Figure 6.6b). This is in contrast to the HIV7-GFP mice which have a mild decrease.

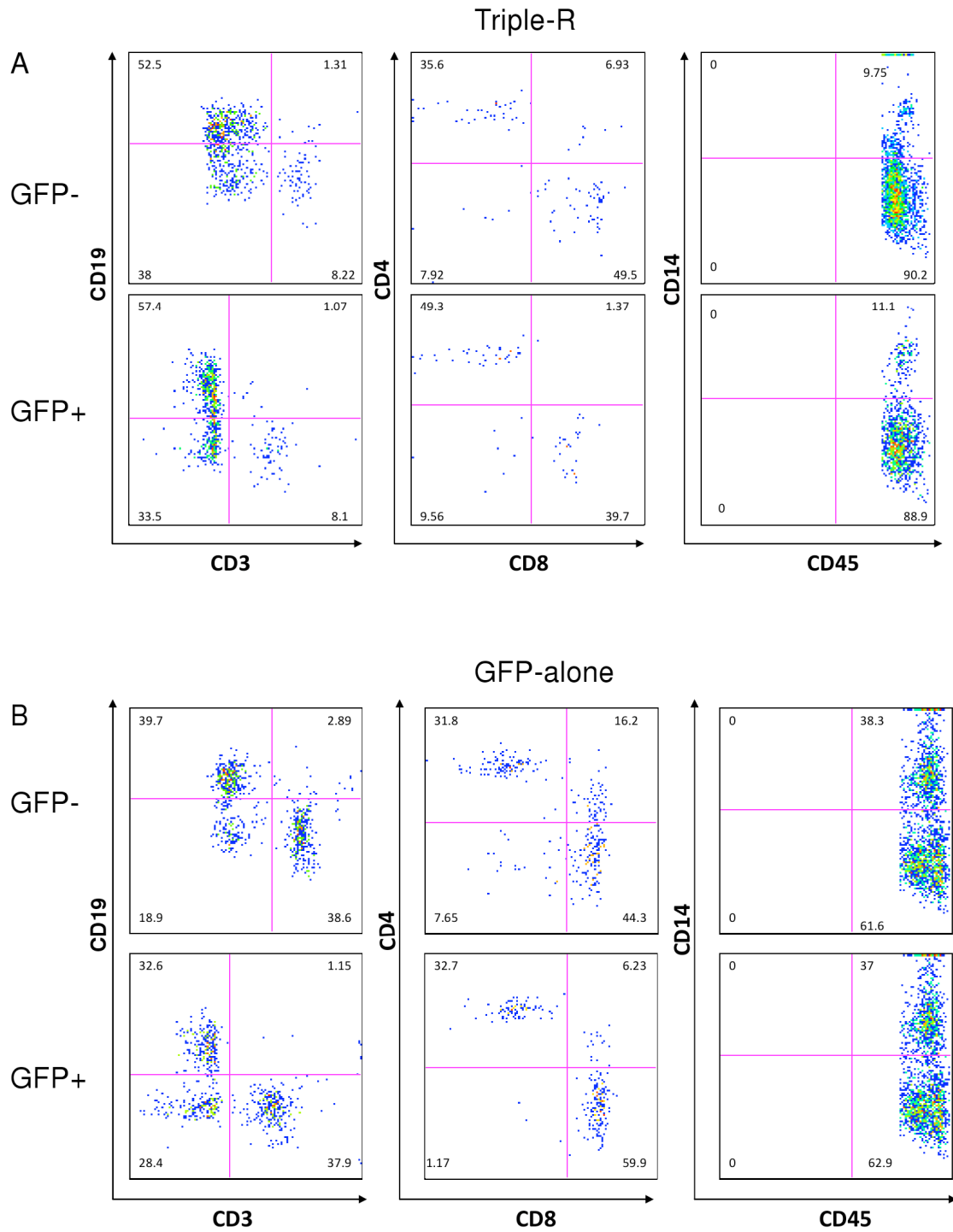


Figure 6.4. Multicolor FACS analysis of RAG-hu derived hematopoiesis. Whole blood was collected and stained with antibodies against CD3, CD4, CD14, CD 19, and CD45 and subjected to fluorescence-activated cell sorting (FACS) analysis. Representative examples from each treatment group are shown.

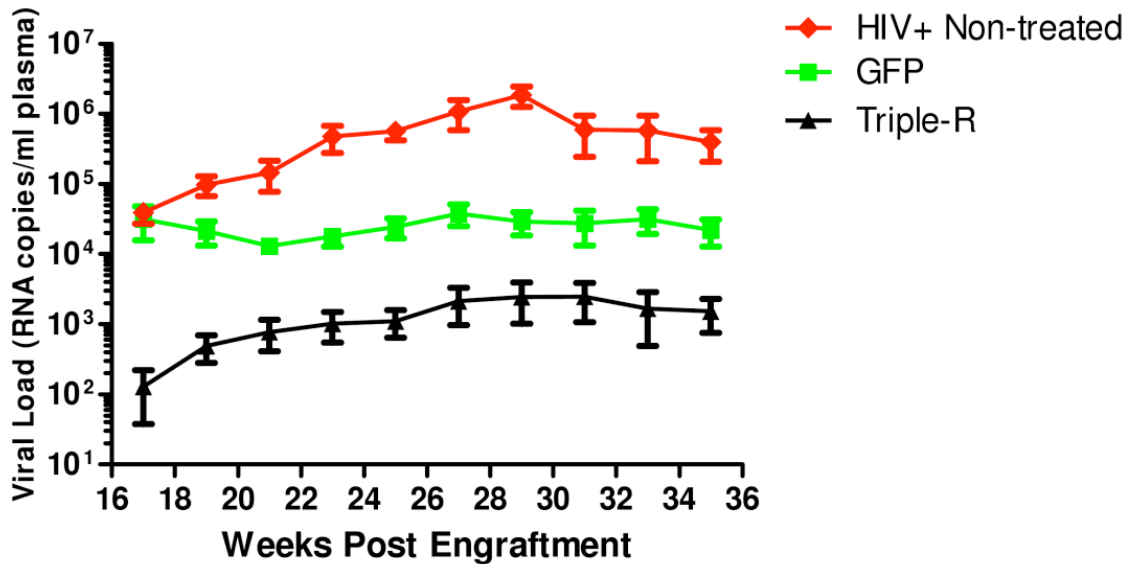


Figure 6.5. Human immunodeficiency virus-1 (HIV-1) resistance by Triple-R transduced engrafted RAG-hu mice. Vector-transduced CD34 cells were injected into the liver of irradiated RAG-hu pups and allowed to recapitulate hematopoiesis. Mice were challenged with HIV-1 BaL at 14 weeks post engraftment. Plasma collected from each mouse was subjected to q-RT-PCR for viral RNA levels.

When the total CD4⁺ decline and the EGFP expression are taken together it is inferred that the transgenic T cells in the HIV7-GFP mice decline at a similar or slightly faster rate than the non-transduced T cells in the same animals (Figure 6.6a and 6.6b). The Triple-R transgenic cells and the non-transduced cells do not decline at all, illustrating a bystander protection by the transgenic cells to the susceptible non-transduced cells.

6.4 Discussion

HIV-1 uses diverse mechanisms of pathogenesis to cause disease progression. Some of these include viral integration, a high mutation rate, viral latency, and the ability to evade the immune system in immunologically privileged sites. In this regard, the use of combinatorial constructs targeting both pre-entry and post-integrations steps are more attractive than monotherapies that only target one step of the viral life cycle. Indeed,

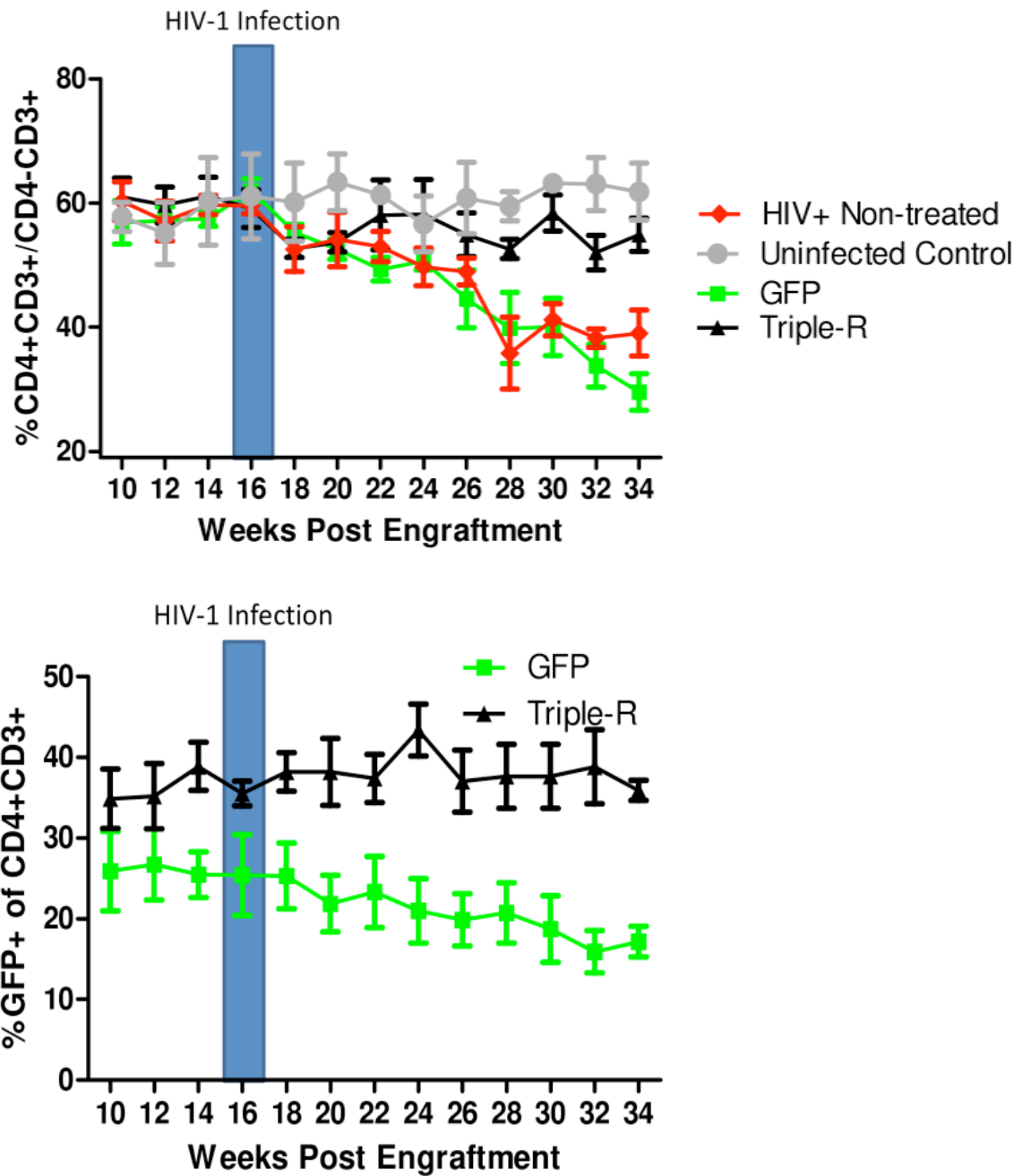


Figure 6.6. Triple-R protection against HIV-1 mediated CD4 depletion. Mice engrafted with transduced CD34 cells were challenged with HIV-1 BaL at 16 weeks post engraftment and CD4 T cell levels were monitored. Triple-R transduced CD4+ T cells are resistant to HIV-1 infection as can be seen by maintained CD4 levels compared to the non-transduced and GFP-alone groups.

previous work has demonstrated the synergistic benefit of combined anti-HIV strategies into a single lentiviral vector in reducing the chances of generating viral escape mutants when compared to individual constructs.

A number of recent studies have demonstrated the ability of RNAi and other HIV-1 RNA inhibitory molecules to resist viral replication *in vitro* and *in vivo*. Ribozymes, decoys, and shRNAs, to name a few, are potential effective antiviral RNA molecules. Utilizing different modes of action also limits potential competition with host machinery which could be detrimental to the cell. Lentiviral vectors are ideal to deliver these anti-HIV constructs into target cells as they are able to transduce nondividing cells, including hematopoietic stem cells which can derive into HIV-1 susceptible cells.

Based on this concept, a Triple-R lentiviral vector construct was designed to target multiple stages of HIV's life cycle. For entry into target cells during early infection HIV utilizes a chemokine coreceptor, CCR5, in conjunction with CD4. This derives a critical target for early HIV life cycle; as such a ribozyme under the control of an adenoviral VA1 promoter is utilized to down-regulate CCR5 expression. After infection two essential regulatory proteins are produced by HIV-1. These two proteins, rev and tat, were also targeted by a shRNA under the control of a U6 Poly-III promoter that targets an overlapping ORF of both rev and tat transcripts. Tat is further targeted by a TAR decoy that acts to sequester tat and decrease transactivation of viral transcripts. Each of these expression cassettes were expressed under separate promoters and were previously shown to accumulate in high quantities. As addressed above, using a combination of these anti-HIV-1 transgenes in a single lentiviral vector offers a reduced chance of viral escape mutants.

In the present study, the ability of this Triple-R lentiviral vector in transducing hematopoietic CD34+ stem cells was tested. High efficient transduction of these cells was seen with transduction efficiencies at >70% with only two rounds of transductions. However, normal physiological development may be disrupted by off-target effects of transgene RNA inhibitory molecules. To evaluate if phenotypically normal cells of the immune system develop from genetically modified HSCs we engrafted Rag-hu mice, which give an ideal environment for hematopoiesis. We show that cells of the hematopoietic lineage, including T cells, B cells and macrophages, dedifferentiate normally.

To determine whether transduction of these three anti-HIV-1 transgenes conferred HIV-1 resistance, reconstituted mice were challenged with the macrophage tropic BaL HIV-1. Both the non-treated and the GFP-alone transgenic mice showed high levels of infection based on qRT-PCR analysis of HIV viral loads in contrast to the Triple-R mice which had a several log fold reduction. Additionally, protection of the primary target of HIV, CD4+ T cells, was seen in only the Triple-R transgenic mice. Surprisingly, in these HIV-1 resistant mice, the non-transduced cells were also protected. This unexpected effect of bystander protection, which may be a result from the reduced viral load, should be further evaluated in future studies. These data taken together suggest the efficacy of the Triple-R construct to protect against HIV infection *in vivo*. With efficacy reported here and previously this vector is an attractive candidate for clinical trials.

CHAPTER 7
SUMMARY AND FUTURE CONSIDERATIONS

7.1 Summary

Without the advent of a vaccine the spread of HIV/AIDS continues to rise. With HAART therapy, slowed disease progression and extend patient's lifespan occurs. However, with the relatively high cost of this treatment, toxic side effects, and drug resistance, new and innovative alternative therapies need to be developed. In this regard here we present several novel strategies for alternative or adjunct HAART therapy.

In preventative therapeutic studies, we have shown that oral administration of clinically approved drugs namely, raltegravir or maraviroc, mediate complete protection against HIV-1 vaginal viral challenge in humanized mice, elaborating their potential utility as PrEPs. These two compounds have different modes of action. Maraviroc is a low molecular weight CCR5 antagonist which inhibits the binding of the natural ligands of CCR5, namely chemokine ligand 3 (CCL3 also known as MIP-1 α), CCL4 (MIP1- β) and CCL5 (RANTES) (195). It is a functional CCR5 antagonist devoid of agonist activity and shown to have a long lasting physical and functional occupancy of CCR5 leading to sustained antiviral activity. Topical vaginal application of maraviroc, as shown in chapter 3, also is able to fully protect humanized mice from HIV-1 vaginal viral challenge. Raltegravir is an integrase strand transfer inhibitor that interferes with the viral DNA integration which is an essential step in viral replication. It is active against multidrug-resistant and both CCR5-tropic and CXCR4-tropic HIV-1 strains. Topically applied formulations of Raltegravir are currently being evaluated for their protective applications and our preliminary data indicates successful application. However, being an intercellular acting compound, it appears that full protection is unattainable.

The complexity of HIV illustrates the difficulties that have hindered the development of an effective vaccine. In this regard alternative approaches have become crucial in the attempts to curb the pandemic scale of HIV/AIDS. We have established that the RAG-hu mouse is suitable for studying HIV-1 pathogenesis, novel therapeutics and preventative methods. Our present results have provided the proof-of-concept data for further investigating the potential of raltegravir and maraviroc as PrEPs thus identifying additional novel classes of molecules with different modes of action (194). Based on their proven broad spectrum of activity against divergent HIV strains in clinical situations, both these drugs make excellent candidates for PrEP. In this proof-of-concept study only one dose given sequentially for 7 days was tested and found to be efficacious in the prevention of HIV-1 infection.

Synthetic vehicles such as dendrimers which can be synthesized with controlled and defined structures are amenable to chemical modification, stable in biological fluids and are not immunogenic. Importantly, an ideal siRNA delivery system for treatment of HIV-1 infection should have the capacity for combining siRNAs with different targets, both viral and cellular, to avert viral escape mutants. We have tested a PAMAM generation 5 dendrimer-dsiRNA delivery system for the treatment of HIV-1 infection both in cell culture and in a humanized mouse model.

In work presented here we provided data demonstrating that a cocktail of three dsiRNAs targeting HIV-1 *tat/rev* and two cellular targets, CD4 and TNPO3 resulted in down-regulation of all three targeted transcripts *in vivo*. The inhibition of these targets resulted in a reduction of the viral RNA load and protection of CD4+ T cells from HIV-1 mediated depletion. Furthermore the results of this study demonstrate that a combination

of dsRNAs can be functionally delivered to T-lymphocytes *in vivo* in the absence of any apparent toxicity. Importantly, we also showed that three months after we stopped the first treatments-allowing viral loads to become elevated again, animals could be re-treated with the dendimer- cocktail dsRNA, resulting once again in strong inhibition of HIV-1. Collectively, our results demonstrate the capacity of the G₅ dendrimer delivered dsRNAs to achieve marked viral suppression *in vivo*, resulting in protection of CD4 T cells from HIV-1 mediated depletion. Given the importance and challenge of siRNA delivery, it is of significance that our results provided the first demonstration of nanoparticle mediated delivery of siRNAs to hematopoietic cells *in vivo*, thus providing the impetus for further clinical development of this strategy.

Single chain antibody-siRNA chimeras targeting either gp120 expressing cells or the T-cell specific CD7 receptor have been shown to functionally deliver anti-HIV-1 siRNAs *in vivo* (116). However, in these studies only the siRNA component has been shown to have antiviral activity. As presented in chapter five we observed potent antiviral activity by the aptamer itself, and this is further enhanced by aptamer mediated delivery of an anti-HIV-1 delivered siRNA. The aptamer and aptamer-siRNA chimera decreased viral loads in HIV-1 infected humanized mice, by several logs in all the treated animals within a week following intravenous administration. The suppression of viral load averaged three orders of magnitude or greater relative to controls and persisted throughout and beyond the treatment period in seven of nine animals tested in this study.

The results presented in this study provide an *in vivo* validation of the anti-HIV-1 efficacy of the anti-gp120 aptamer siRNA chimera. We have used the aptamer both as an HIV neutralizing agent and as a vehicle for delivering a siRNA for triggering RNAi

mediated down regulation of the HIV-1 *tat/rev* transcripts. The combinatorial inhibitory functions of the aptamer and siRNA make this approach potentially superior to the other anti-siRNA delivery approaches reported prior to this work (122). The high potency and enhanced duration of viral suppression of the current approach is largely attributable to the dual anti-HIV activities of both the aptamer and aptamer delivered siRNA. Since these RNA based molecules are not antigenic, they can be administered repeatedly without concerns about generating undue immunological responses.

A Triple-R lentiviral vector construct was designed to target multiple stages of HIV's life cycle. Included in this construct are a ribozyme utilized to down-regulate CCR5 expression, a *tat/rev* shRNA and a TAR decoy. Using a combination of these anti-HIV transgenes in a single lentiviral vector offers a reduced chance of viral escape mutants.

In the present study, the ability of this Triple-R lentiviral vector in transducing hematopoietic CD34+ stem cells was tested. Highly efficient transduction of these cells was seen with transduction efficiencies at >70% with only two rounds of transductions. We show that cells of the hematopoietic lineage, including T cells, B cells and macrophages, differentiate normally.

To determine whether transduction of these three anti-HIV-1 transgenes conferred HIV-1 resistance, reconstituted mice were challenged with the macrophage tropic BaL HIV-1. Both the non-treated and the GFP-alone transgenic mice showed high levels of infection based on qRT-PCR analysis of HIV viral loads in contrast to the Triple-R mice which had a several fold reduction. Additionally, protection of the primary target of HIV, CD4+ T cells, was seen in only the Triple-R transgenic mice. Surprisingly, in these

HIV-1 resistant mice, the non-transduced cells were also protected. This unexpected effect of bystander protection should be further evaluated in future studies. These data taken together suggest the efficacy of the Triple-R construct to protect against HIV infection *in vivo*.

All of the studies reported here were conducted in the RAG-hu mouse model, illustrating the utility of this model for HIV-1 preventative and therapeutic research. In this regard, humanized mice are likely to fill the gap for deriving preliminary data and in laying the ground work for subsequent macaque studies. Since HIV-1 itself can be used as a challenge virus, various drug resistant mutants that exist in the field can also be evaluated against different combinations of potential promising compounds. Now it is possible to conduct large scale *in vivo* preliminary screenings of a large number of potential microbicides, PrEP compounds, siRNA delivery vehicles, and gene therapy strategies in a cost effective manner.

7.2 Future considerations

Future studies of microbicides and other PrEPs should evaluate variations in the dose, timings of drug administration prior to vaginal challenge and duration of efficacy without further dosing after viral challenge to determine the memory effect. Additionally, drugs with a similar mechanism may be examined in the future for their likely similar protection. It is also necessary that field and drug resistant viruses be tested in this humanized mouse model. Furthermore, use of more than one drug in any PrEP will be more effective in field conditions. This can also be tested in this mouse model using a

combination of raltegravir and maraviroc to derive pre-clinical data. Such evaluations will fine tune the PrEP regimens to be more practically applicable for clinical testing.

With regards to siRNA therapeutics our data here supports future use of combinatorial multi-targeting dsRNAs for treating HIV-1 infection as a stand alone therapy or as an adjunct to HAART therapy. Additionally, the aptamer-siRNA technology can be developed to avert viral resistance by the use of a cocktail of gp120 aptamers of different specificities that are combined with siRNAs directed against different mRNA targets (both viral and cellular). We envision that the first dual-function aptamer-siRNA chimeras can be applied to patients who harbor virus resistant to antiretroviral drugs.

Although we present successful development of an anti-HIV-1 transgenic mouse many questions remain, particularly with assessing normal function of the immune cells after transduction, the prolonged effects of introduced endogenously expressed miRNAs and required transduced engraftment efficiency for viral suppression and T cell protection. Additionally, here we used a combinatorial approach but to limit potential adverse side effects and for their efficacy it would be beneficial to analyze each of the three constructs individually.

The work presented throughout this dissertation was done in a preclinical setting utilizing the humanized mouse. In this regard an ultimate goal for these data presented is for use in a clinical scene. Here the ground work for such evaluations has been laid.

REFERENCES

- 1) CDC, (2006) Twenty-five years of HIV/AIDS—U.S., 1981–2006, *MMWR Morb Mortal Wkly Rep*, 55 pp. 585–589.
- 2) Merson M. (2006) The HIV-AIDS pandemic at 25 - the global response. *N Engl J Med*. 354:2414–2417.
- 3) McGovern SL, Caselli E, Grigorieff N, Shoichet BK (2002) A common mechanism underlying promiscuous inhibitors from virtual and high-throughput screening. *J Med Chem* 45 (8): 1712–22.
- 4) Knipe, DM, Howley PM (2001). *Fields Virology*, 4th ed. Lippincott Williams & Wilkins, Philadelphia, Pa.
- 5) Werner Abfaltrerer, Gayathri Athreya, Will Fischer, Bob Funkhouser, Brian Gaschen, Peter Hrabec, Chien-Chi Lo, Jennifer Macke, James J. Szinger, James Thurmond, Hyejin Yoon, Ming Zhang (2008) HIV Sequence Compendium 2008 Introduction. Retrieved 2009-03-31.
- 6) Chan, DC., Fass, D., Berger, JM., Kim, PS. (1997). Core Structure of gp41 from the HIV Envelope Glycoprotein. *Cell* 89 (2): 263–73.
- 7) Garcia JV, Miller AD (1991). Serine phosphorylation-independent downregulation of cell-surface CD4 by nef. *Nature* 350 (6318): 508–11.
- 8) Schwartz O, Maréchal V, Le Gall S, Lemonnier F, Heard JM (1996). Endocytosis of major histocompatibility complex class I molecules is induced by the HIV-1 Nef protein. *Nat. Med.* 2 (3): 338–42.
- 9) Ouellet DL, Plante I, Landry P, *et al.* (2008). Identification of functional microRNAs released through asymmetrical processing of HIV-1 TAR element. *Nucleic Acids Res.* 36 (7): 2353–65.

- 10) Deng H, Liu R, Ellmeier W, Choe S, Unutmaz D, Burkhart M, Di Marzio P, Marmon S, Sutton RE, Hill CM, Davis CB, Peiper SC, Schall TJ, Littman DR, Landau NR. (1996) Identification of a major co-receptor for primary isolates of HIV-1. *Nature* 381 (6584): 661–6.
- 11) Knight, S. C., Macatonia, S. E. and Patterson, S. (1990) HIV I infection of dendritic cells. *Int. Rev. Immunol.* 6 (2–3): 163–75.
- 12) Chan D, Kim P (1998) HIV entry and its inhibition. *Cell* 93 (5): 681–4.
- 13) Zheng, Y. H., Lovsin, N. and Peterlin, B. M. (2005) Newly identified host factors modulate HIV replication. *Immunol. Lett.* 97 (2): 225–34.
- 14) Pollard, V. W. and Malim, M. H. (1998) The HIV-1 Rev protein. *Annu. Rev. Microbiol.* 52: 491–532.
- 15) Levy, JA (1998) HIV and the Pathogenesis of AIDS, 2nd ed. ASM Press, Washington, D.C.
- 16) Sheehy, AM, Gaddis NC, Choi JD, Malim MH (2002) Isolation of a human gene that inhibits HIV-1 infection and is suppressed by the viral Vif protein. *Nature* 418:646-650
- 17) Martin KL, Johnson M, D'Aquila RT. (2011) APOBEC3G Complexes Decrease Human Immunodeficiency Virus Type 1 (HIV-1) Production. *J Virol.*
- 18) Gelderblom, H. R (1997) Fine structure of HIV and SIV. In Los Alamos National Laboratory (ed.)
- 19) Boily MC, Baggaley RF, Wang L, Masse B, White RG, Hayes RJ, Alary M (2009) Heterosexual risk of HIV-1 infection per sex act: Systematic review

- and meta-analysis of observational studies. *Lancet Infectious Diseases* 9:118-129.
- 20) National Institutes of Health, Department of Health and Human Services (2001)
- 21) Swan T, (2004) Hepatitis C Virus (HCV) and HIV/HCV Coinfection: A Critical Review of Research and Treatment, I. Epidemiology and Transmission of Hepatitis C
- 22) McCune, JM (2001) The dynamics of CD4+ T-cell depletion in HIV disease. *Nature* 410:1002-1007
- 23) Hellerstein, M, Hanley MB, Cesar D, Siler S, Papageorgopoulos C, Wider E, Schmidt D, Hoh R, Neese R, Macallan D, Deeks S, McCune JM (1999) Directly measured kinetics of circulating T lymphocytes in normal and HIV-1 infected humans. *Nat. Med.* 5:83-89
- 24) Holmes CB, Losina E, Walensky RP, Yazdanpanah Y, Freedberg KA (2003) Review of human immunodeficiency virus type 1-related opportunistic infections in sub-Saharan Africa. *Clin. Infect. Dis.* 36 (5): 656–662.
- 25) Boshoff C, Weiss R (2002) AIDS-related malignancies. *Nat. Rev. Cancer* 2 (5): 373–382.
- 26) Morgan D, Mahe C, Mayanja B, Okongo JM, Lubega R, Whitworth JA (2002): HIV-1 infection in rural Africa: is there a difference in median time to AIDS and survival compared with that in industrialized countries? *AIDS*, 16:597-603.

- 27) Haigwood, N. L. (2004), Predictive value of primate models for AIDS. *AIDS Rev.* 6:187–198.
- 28) Polacino, P. Larsen K, Galmin L, Suschak J, Kraft Z, Stamatatos L. et al. (2008), Differential pathogenicity of SHIV infection in pig-tailed and rhesus macaques. *J. Med. Primatol.* 37: 13–23.
- 29) Barouch, D. H., (2008) Challenges in the development of an HIV-1 vaccine. *Nature.* 455:613–619.
- 30) Pedersen NC, Ho EW, Brown ML, Yamamoto JK. (1987) Isolation of a T-lymphotropic virus from domestic cats with an immunodeficiency-like syndrome. *Science* 235:790–3.
- 31) Brown WC, Bissey L, Logan KS, Pedersen NC, Elder JH, Collisson EW. Feline (1991) immunodeficiency virus infects both CD4+ and CD8+ T lymphocytes. *J of Vir* ;65:3359–64.
- 32) Willett BJ, Hosie MJ, Callanan JJ, Neil JC, Jarrett O. (1993) Infection with feline immunodeficiency virus followed by the rapid expansion of a CD8+ lymphocyte subset. *Immunology* 78:1–6.
- 33) de Parseval A, Chatterji U, Sun P, Elder JH. (2004) Feline immunodeficiency virus targets activated CD4 +T cells by using CD134 as a binding receptor. *Proc Natl Acad Sci U S A* 101:13044–9.
- 34) Elder JH, Lin YC, Fink E, Grant CK (2010) Feline immunodeficiency virus (FIV) as a model for study of lentivirus infections: parallels with HIV. *Curr HIV Res* 8: 73–80.

- 35) Peters SO, Kittler EL, Ramshaw HS et al. (1995) Murine marrow cells expanded in culture with IL-3, IL-6, IL-11, and SCF acquire an engraftment defect in normal hosts. *Exp Hematol*;23:461-469.
- 36) Ganick DJ, Sarnwick RD, Shahidi NT et al. (1980) Inability of intravenously injected monocellular suspensions of human bone marrow to establish in the nude mouse. *Int Arch Allergy Appl Immunol*;62:330-333.
- 37) Urist MR, Grant TT, Lindholm TS et al. (1979) Induction of new-bone formation in the host bed by human bone-tumor transplants in a thymic nude mice. *J Bone Joint Surg*;61:1207-1216.
- 38) Watanabe S, Shimosato Y, Kameya T et al. (1978) Leukemic distribution of a human acute lymphocytic leukemia cell line (Ichikawa strain) in nude mice conditioned with whole-body irradiation. *Cancer Res*;38:3494-3498.
- 39) Kirchgessner CU, Patil CK, Evans JW et al. (1995) DNA-dependent kinase (p350) as a candidate gene for the murine SCID defect. *Science*;267:1178-1183.
- 40) Blunt T, Gell D, Fox M et al. (1996) Identification of a nonsense mutation in the carboxyl-terminal region of DNA-dependent protein kinase catalytic subunit in the scid mouse. *Proc Natl Acad Sci USA*;93:10285-10290.30
- 41) Fried LM, Koumenis C, Peterson SR et al. (1996) The DNA damage response in DNA-dependent protein kinase-deficient SCID mouse cells: replication protein A hyperphosphorylation and p53 induction. *Proc Natl Acad Sci USA*;93:13825-13830.

- 42) Araki R, Fujimori A, Hamatani K et al. (1997) Nonsense mutation at Tyr-4046 in the DNA-dependent protein kinase catalytic subunit of severe combined immune deficiency mice. *Proc Natl Acad Sci USA*;94:2438-2443.
- 43) Bosma GC, Custer RP, Bosma MJ (1983) A severe combined immune deficiency mutation in the mouse. *Nature* 301(5900):527-30.
- 44) Lieber MR, Hesse JE, Lewis S et al. (1988) The defect in murine severe combined immune deficiency: joining of signal sequences but not coding segments in V(D)J recombination. *Cell*;55:7-16.
- 45) Nonoyama S, Smith FO, Bernstein ID et al. (1993) Strain-dependent leakiness of mice with severe combined immune deficiency. *J Immunol*;150:3817-3824.
- 46) McCune JM, Namikawa R, Kaneshima H et al. (1988) The SCID-hu mouse: murine model for the analysis of human hematolymphoid differentiation and function. *Science*;241:1632-1639.
- 47) Yurasov S, Kollmann TR, Kim A et al. (1997) Severe combined immunodeficiency mice engrafted with human T cells, B cells, and myeloid cells after transplantation with human fetal bone marrow or liver cells and implanted with human fetal thymus: a model for studying human gene therapy. *Blood*;89:1800-1810.
- 48) Akkina RK, Rosenblatt JD, Campbell AG et al. (1994) Modeling human lymphoid precursor cell gene therapy in the SCID-hu mouse. *Blood*;84:1393-1398.
- 49) Murray L, DiGiusto D, Chen B et al. (1994) Analysis of human hematopoietic stem cell populations. *Blood Cells*;20:364-369; discussion 369.

- 50) Lapidot T, Pflumio F, Doedens M et al. (1992) Cytokine stimulation of multilineage hematopoiesis from immature human cells engrafted in SCID mice. *Science*;255:1137-1141.
- 51) Kataoka S, Satoh J, Fujiya H et al. (1983) Immunologic aspects of the nonobese diabetic (NOD) mouse. *Diabetes*;32:247-253.
- 52) Serreze DV, Leiter EH. (1988) Defective activation of T suppressor cell function in nonobese diabetic mice. Potential relation to cytokine deficiencies. *J Immunol*;140:3801-3807.
- 53) Archer DR, Turner CW, Yeager AM et al. (1997) Sustained multilineage engraftment of allogeneic hematopoietic stem cells in NOD/SCID mice after in utero transplantation. *Blood*;90:3222-3229.
- 54) Soderstrom I, Bergman ML, Colucci F et al. (1996) Establishment and characterization of RAG-2 deficient non-obese diabetic mice. *Scand J Immunol*;43:525-530.
- 55) Berges BK, Akkina SR, Remling L, Akkina R (2010) Humanized Rag2(-/-) gammac(-/-) (RAG-hu) mice can sustain long-term chronic HIV-1 infection lasting more than a year. *Virology* 397: 100-103.
- 56) Berges BK, Wheat WH, Palmer BE, Connick E, Akkina R (2006) HIV-1 infection and CD4 T cell depletion in the humanized Rag2-/-gc-/- (RAG-hu) mouse model. *Retrovirology* 3: 76.
- 57) Berges BK, Akkina SR, Folkvord JM, Connick E, Akkina R (2008) Mucosal transmission of R5 and X4 tropic HIV-1 via vaginal and rectal routes in humanized Rag2-/-gc-/- (RAG-hu) mice. *Virology* 373: 342-351.

- 58) Aldrovandi GM, Feuer G, Gao L, Jamieson B, Kristeva M, et al. (1993) The SCID-hu mouse as a model for HIV-1 infection. *Nature* 363: 732–736.
- 59) Denton PW, Garcia JV (2009) Novel humanized murine models for HIV research. *Curr HIV/AIDS Rep* 6: 13–19.
- 60) Stoddart CA, Bales CA, Bare JC, Chkhenkeli G, Galkina SA, et al. (2007) Validation of the SCID-hu Thy/Liv mouse model with four classes of licensed antiretrovirals. *PLoS ONE* 2: e655.
- 61) Munier CM, Andersen CR, Kelleher AD. (2011) HIV vaccines: progress to date. *Drugs*;71(4):387-414.
- 62) Pantaleo G, Esteban M, Jacobs B, Tartaglia J (2010) Poxvirus vector-based HIV vaccines. *Current Opinion in HIV and AIDS* 5: 391–396.
- 63) Nagelkerke NJ, Hontelez JA, de Vlas SJ. (2011) The potential impact of an HIV vaccine with limited protection on HIV incidence in Thailand: A modeling study. *Vaccine*.
- 64) Blankson JN, (2010) Control of HIV-1 replication in elite suppressors. *Discov Med*. Mar;9(46):261-6.
- 65) Kulpa DA, Collins KL. (2011) The emerging role of HLA-C in HIV-1 infection. *Immunology*. 134(2):116-22.
- 66) Stadnisky MD, Xie X, Coats ER, Bullock TN, Brown MG (2011) Self MHC class I-licensed NK cells enhance adaptive CD8 T-cell viral immunity. *Blood*. 117(19):5133-41.

- 67) Hartigan-O'Connor DJ, Hirao LA, McCune JM, Dandekar S. (2010) Control of HIV-1 replication in elite suppressors. Blankson JN; Th17 cells and regulatory T cells in elite control over HIV and SIV. *Discov Med.* (3):221-7.
- 68) Fauci AS, (2003) HIV and AIDS: 20 years of science. *Nat Med.*;9(7):839-43.
- 69) Gottlieb MS. (2001) AIDS--past and future. *N Engl J Med.* Jun 7;344(23):1788-91.
- 70) Sabin CA. (2002) The changing clinical epidemiology of AIDS in the highly active antiretroviral therapy era. *AIDS.*;16 Suppl 4:S61-8.
- 71) Palmisano L, Vella S. (2011) A brief history of antiretroviral therapy of HIV infection: success and challenges." *Ann Ist Super Sanita.*;47(1):44-8.
- 72) Imaz A, Llibre JM, Mora M, Mateo G, et al. (2011) Efficacy and safety of nucleoside reverse transcriptase inhibitor-sparing salvage therapy for multidrug-resistant HIV-1 infection based on new-class and new-generation antiretrovirals. *J Antimicrob Chemother.*;66(2):358-62.
- 73) Grinsztejn B, Nguyen BY, Katlama C, Gatell JM, Lazzarin A, et al. (2007) Safety and efficacy of the HIV-1 integrase inhibitor raltegravir (MK-0518) in treatment-experienced patients with multidrug-resistant virus: a phase II randomised controlled trial. *Lancet* 369: 1261–1269.
- 74) Reina JJ, Bernardi A, Clerici M, Rojo J. (2010) HIV microbicides: state-of-the-art and new perspectives on the development of entry inhibitors. *Future Med Chem.* Jul;2(7):1141-59.
- 75) Friend DR. (2009) Pharmaceutical development of microbicide drug products. *Pharm Dev Technol.*

- 76) Di Fabio S, Giannini G, Lapenta C, Spada M, Binelli A, et al. (2001) Vaginal transmission of HIV-1 in hu-SCID mice: a new model for the evaluation of vaginal microbicides. *Aids* 15: 2231-2238.
- 77) D'Cruz OJ, Uckun FM. (2007) Limitations of the human-PBL-SCID mouse model for vaginal transmission of HIV-1. *Am J Reprod Immunol* 57: 353-360.
- 78) Di Fabio S, Van Roey J, Giannini G, van den Mooter G, Spada M, et al. (2003) Inhibition of vaginal transmission of HIV-1 in hu-SCID mice by the non-nucleoside reverse transcriptase inhibitor TMC120 in a gel formulation. *Aids* 17: 1597-1604.
- 79) Karim QA, Karim SS, Frohlich JA, Grobler AC, Baxter C, et al. (2010) Effectiveness and Safety of Tenofovir Gel, an Antiretroviral Microbicide, for the Prevention of HIV Infection in Women. *Science*.
- 80) Garcia-Lerma JG, Paxton L, Kilmarx PH, Heneine W (2010) Oral pre-exposure prophylaxis for HIV prevention. *Trends Pharmacol Sci* 31: 74–81.
- 81) Kumwenda NI, Hoover DR, Mofenson LM, Thigpen MC, Kafulafula G, et al. (2008) Extended antiretroviral prophylaxis to reduce breast-milk HIV-1 transmission. *N Engl J Med* 359: 119–129.
- 82) Volmink J, Siegfried NL, van der Merwe L, Brocklehurst P (2007) Antiretrovirals for reducing the risk of mother-to-child transmission of HIV infection. *Cochrane Database Syst Rev* CD003510.
- 83) Polhemus ME, Remich S, Ogutu B, Waitumbi J, Lievens M, et al. (2008) Malaria treatment with atovaquone-proguanil in malaria-immune adults: implications

for malaria intervention trials and for pre-exposure prophylaxis of malaria. *Antimicrob Agents Chemother* 52: 1493–1495.

- 84) Abbas UL, Anderson RM, Mellors JW (2007) Potential impact of antiretroviral chemoprophylaxis on HIV-1 transmission in resource-limited settings. *PLoS One* 2: e875.
- 85) US Food and Drug Administration (2009) Antiretroviral drugs used in the treatment of HIV infection. <http://www.fda.gov/ForConsumers/ByAudience/ForPatientAdvocates/HIVandAIDSActivities/ucm118915.htm>.
- 86) Broder S (2010) The development of antiretroviral therapy and its impact on the HIV-1/AIDS pandemic. *Antiviral Res* 85: 1–18.
- 87) Subbarao S, Otten RA, Ramos A, Kim C, Jackson E, et al. (2006) Chemoprophylaxis with tenofovir disoproxil fumarate provided partial protection against infection with simian human immunodeficiency virus in macaques given multiple virus challenges. *J Infect Dis* 194: 904–911.
- 88) Van Rompay KK, Kearney BP, Sexton JJ, Colon R, Lawson JR, et al. (2006) Evaluation of oral tenofovir disoproxil fumarate and topical tenofovir GS-7340 to protect infant macaques against repeated oral challenges with virulent simian immunodeficiency virus. *J Acquir Immune Defic Syndr* 43: 6–14.
- 89) Garcia-Lerma JG, Otten RA, Qari SH, Jackson E, Cong ME, et al. (2008) Prevention of rectal SHIV transmission in macaques by daily or intermittent prophylaxis with emtricitabine and tenofovir. *PLoS Med* 5: e28.

- 90) Denton PW, Estes JD, Sun Z, Othieno FA, Wei BL, et al. (2008) Antiretroviral pre-exposure prophylaxis prevents vaginal transmission of HIV-1 in humanized BLT mice. *PLoS Med* 5: e16.
- 91) Denton PW, Krisko JF, Powell DA, Mathias M, Kwak YT, et al. (2010) Systemic administration of antiretrovirals prior to exposure prevents rectal and intravenous HIV-1 transmission in humanized BLT mice. *PLoS One* 5: e8829.
- 92) Zamore, P.D., Tuschl, T., Sharp, P.A. & Bartel, D.P. (2000) RNAi: double-stranded RNA directs the ATP-dependent cleavage of mRNA at 21 to 23 nucleotide intervals. *Cell* 101, 25-33
- 93) Jorgensen RA, Cluster PD, English J, Que Q, and Napoli CA. (1996) Chalcone synthase cosuppression phenotypes in petunia flowers: comparison of sense vs. antisense constructs and single-copy vs. complex T-DNA sequences. *Plant Mol Biol.* 31:957-973
- 94) Napoli C, Lemieux C, and Jorgensen R. (1990) Introduction of a chalcone synthase gene into *Petunia* results in reversible co-suppression of homologous genes in trans. *Plant Cell.* 2:279-289
- 95) Fire, A. et al. (1998) Potent and specific genetic interference by double-stranded RNA in *Caenorhabditis elegans*. *Nature* **391**, 806-811
- 96) Guo S, And Kempheus KJ. (1995) Par-1 a gene required for establishing polarity in *C. elegans* embryos, encodes a putative Ser/Thr kinase that is asymmetrically distributed. *Cell.* 81:611-620
- 97) Guru T. (2000) A silence that speaks volumes. *Nature.* 404:804-808

- 98) Kim, D.H. & Rossi, J.J. (2007) Strategies for silencing human disease using RNA interference. *Nat Rev Genet* 8, 173-184
- 99) de Fougères, A., Vornlocher, H.P., Maraganore, J. & Lieberman, J. (2007) Interfering with disease: a progress report on siRNA-based therapeutics. *Nat Rev Drug Discov* 6, 443-453
- 100) Rossi, J.J. (2006) RNAi as a treatment for HIV-1 infection. *Biotechniques Suppl*, 25-29
- 101) Rossi, J.J., June, C.H. & Kohn, D.B. (2007). Genetic therapies against HIV. *Nat Biotechnol* 25, 1444-1454
- 102) Hannon GJ. (2002) RNA interference. *Nature*. 418:244-251.
- 103) Sharp PA. (2001) RNA interference-2001. *Genes and Development*. 15:485-490
- 104) Manche L, Green SR, Schmedt C, and Mathews MB. (1992) Interactions between double-stranded RNA regulators and the protein kinase DAI. *Mol Cell Biol*. 12:5238-5248
- 105) Minks MA, West DK, Benveniste S, and Baglioni C. (1979) Structural requirements of double stranded RNA for the activation of 2'-5' oligo(A) polymerase and protein kinase of interferon-treated HeLa cells. *J Biol Chem*. 254:10180-10183
- 106) Elbashir SM, Harborth J, Lendeckel W, Yalcin A, Weber K, and Tuschke T. (2001) Duplexes of 21-nucleotide RNAs mediate RNA interference in cultured mammalian cells. *Nature*. 411:494-498.

- 107) Caplen NJ, Parrish S, Imani F, Fire A, Morgan RA. (2001) Specific inhibition of gene expression by small double-stranded RNAs in invertebrate and vertebrate systems. *Proc Natl Acad Sci USA*. 98:9742-9747
- 108) Pomerantz RJ. (2003) RNA interference: on the road to an alternate therapeutic strategy. *Rev Med Virol*. 13:373-385.
- 109) Lee, N.S. & Rossi, J.J. (2004) Control of HIV-1 replication by RNA interference. *Virus Res* 102, 53-58
- 110) Scherer, L., Rossi, J.J. & Weinberg, M.S. (2007) Progress and prospects: RNA-based therapies for treatment of HIV infection. *Gene Ther* 14, 1057-1064.
- 111) Martinez, M.A. (2009) Progress in the therapeutic applications of siRNAs against HIV-1. *Methods Mol Biol* 487, 343-368
- 112) Anderson, J., Banerjee, A. & Akkina, R. (2003) Bispecific short hairpin siRNA constructs targeted to CD4, CXCR4, and CCR5 confer HIV-1 resistance. *Oligonucleotides* 13, 303-312
- 113) Das, A.T. et al. (2004) Human immunodeficiency virus type 1 escapes from RNA interference-mediated inhibition. *J Virol* 78, 2601-2605
- 114) Castanotto, D. & Rossi, J.J. (2009) The promises and pitfalls of RNA-interference-based therapeutics. *Nature* 457, 426-433
- 115) Whitehead, K.A., Langer, R. & Anderson, D.G. (2009) Knocking down barriers: advances in siRNA delivery. *Nat Rev Drug Discov* 8, 129-138

- 116) Liu, Z., Winters, M., Holodniy, M. & Dai, H. (2007) siRNA delivery into human T cells and primary cells with carbon-nanotube transporters. *Angew Chem Int Ed Engl* 46, 2023-2027
- 117) Weber, N. et al. (2008) Characterization of carbosilane dendrimers as effective carriers of siRNA to HIV-infected lymphocytes. *J Control Release* 132, 55-64
- 118) Eguchi, A. et al. (2009) Efficient siRNA delivery into primary cells by a peptide transduction domain-dsRNA binding domain fusion protein. *Nat Biotechnol* 27, 567-571
- 119) Song, E. et al. (2005) Antibody mediated in vivo delivery of small interfering RNAs via cell-surface receptors. *Nat Biotechnol* 23, 709-717
- 120) Kumar, P. et al. (2008) T cell-specific siRNA delivery suppresses HIV-1 infection in humanized mice. *Cell* 134, 577-586
- 121) Boas, U. & Heegaard, P.M. (2004) Dendrimers in drug research. *Chem Soc Rev* 33, 43-63
- 122) Perez, A.P., Romero, E.L. & Morilla, M.J. (2009) Ethylenediamine core PAMAM dendrimers/siRNA complexes as in vitro silencing agents. *Int J Pharm* 380, 189-200
- 123) Wu, J. et al. (2005) Polycationic dendrimers interact with RNA molecules: polyamine dendrimers inhibit the catalytic activity of *Candida* ribozymes. *Chem Commun (Camb)*, 313-315
- 124) Zhou, J. et al. (2006) PAMAM dendrimers for efficient siRNA delivery and potent gene silencing. *Chem Commun (Camb)*, 2362-2364

- 125) Liu, X.X. et al. (2009) PAMAM dendrimers mediate siRNA delivery to target Hsp27 and produce potent antiproliferative effects on prostate cancer cells. *ChemMedChem* **4**, 1302-1310
- 126) Dagleish AG, Beverley PC, Clapham PR, Crawford DH, Greaves MF, Weiss RA. (1984) The CD4 (T4) antigen is an essential component of the receptor for the AIDS retrovirus. *Nature*. 312:763–767.
- 127) Klatzmann D, Champagne E, Chamaret S, Gruest J, Guetard D, Hercend T, Gluckman JC, Montagnier L. (1984) T-lymphocyte T4 molecule behaves as the receptor for human retrovirus LAV. *Nature*. 312:767–768.
- 128) Sattentau QJ, Moore JP. (1993) The role of CD4 in HIV binding and entry. *Philos. Trans. R Soc Lond. B Biol. Sci.* 342:59–66.
- 129) Kwong PD, Wyatt R, Robinson J, Sweet RW, Sodroski J, Hendrickson WA. (1998) Structure of an HIV gp120 envelope glycoprotein in complex with the CD4 receptor and a neutralizing human antibody. *Nature*. 393:648–659.
- 130) Ugolini S, Mondor I, Sattentau QJ. (1999) HIV-1 attachment: another look. *Trends Microbiol.*7:144–149.
- 131) Wyatt R, Sodroski J. (1998) The HIV-1 envelope glycoproteins: fusogens, antigens, and immunogens. *Science*.;280:1884–1888.
- 132) Chan DC, Kim PS. (1998) HIV entry and its inhibition. *Cell*. 93:681–684.
- 133) Blair WS, Lin PF, Meanwell NA, Wallace OB. (2000) HIV-1 entry - an expanding portal for drug discovery. *Drug Discov. Today*.5:183–194.

- 134) Cooley LA, Lewin SR. (2003) HIV-1 cell entry and advances in viral entry inhibitor therapy. *J. Clin. Virol.* 26:121–132.
- 135) Kilby JM, Eron JJ. (2003) Novel therapies based on mechanisms of HIV-1 cell entry. *N. Engl. J. Med.* 348:2228–2238.
- 136) Pomerantz RJ, Horn DL. (2003) Twenty years of therapy for HIV-1 infection. *Nat. Med.* 9:867–873.
- 137) Moore JP, Doms RW. (2003) The entry of entry inhibitors: a fusion of science and medicine. *Proc. Natl Acad. Sci. USA.* 100:10598–10602.
- 138) Jiang S, Zhao Q, Debnath AK. (2002) Peptide and non-peptide HIV fusion inhibitors. *Curr. Pharm. Des.* 8:563–580.
- 139) Pierson TC, Doms RW. (2003) HIV-1 entry inhibitors: new targets, novel therapies. *Immunol. Lett.* 85:113–118.
- 140) Meanwell NA, Kadow JF. (2003) Inhibitors of the entry of HIV into host cells. *Curr. Opin. Drug Discov. Devel.* 6:451–461.
- 141) Lin PF, Blair W, Wang T, Spicer T, Guo Q, Zhou N, Gong YF, Wang HG, Rose R, Yamanaka G, et al. (2003) A small molecule HIV-1 inhibitor that targets the HIV-1 envelope and inhibits CD4 receptor binding. *Proc. Natl Acad. Sci. USA.* 100:11013–11018.
- 142) Ryser HJ, Fluckiger R. (2005) Progress in targeting HIV-1 entry. *Drug Discov. Today.* 10:1085–1094.
- 143) Smith DH, Byrn RA, Marsters SA, Gregory T, Groopman JE, Capon DJ. (1987) Blocking of HIV-1 infectivity by a soluble, secreted form of the CD4 antigen. *Science.* 238:1704–1707.

- 144) Hussey RE, Richardson NE, Kowalski M, Brown NR, Chang HC, Siliciano RF, Dorfman T, Walker B, Sodroski J, Reinherz EL. (1988) A soluble CD4 protein selectively inhibits HIV replication and syncytium formation. *Nature*. 331:78–81
- 145) Daar ES, Li XL, Moudgil T, Ho DD. (1990) High concentrations of recombinant soluble CD4 are required to neutralize primary human immunodeficiency virus type 1 isolates. *Proc. Natl Acad. Sci. USA*. 87:6574–6578.
- 146) Schacker T, Coombs RW, Collier AC, Zeh JE, Fox I, Alam J, Nelson K, Eggert E, Corey L. (1994) The effects of high-dose recombinant soluble CD4 on human immunodeficiency virus type 1 viremia. *J. Infect. Dis*. 169:37–40.
- 147) Trkola A, Pomales AB, Yuan H, Korber B, Maddon PJ, Allaway GP, Katinger H, Barbas CF, III, Burton DR, Ho DD, et al. (1995) Cross-clade neutralization of primary isolates of human immunodeficiency virus type 1 by human monoclonal antibodies and tetrameric CD4-IgG. *J. Virol*. 69:6609–6617.
- 148) Allaway GP, Davis-Bruno KL, Beaudry GA, Garcia EB, Wong EL, Ryder AM, Hasel KW, Gauduin MC, Koup RA, McDougal JS, et al. (1995) Expression and characterization of CD4-IgG2, a novel heterotetramer that neutralizes primary HIV type 1 isolates. *AIDS Res. Hum. Retroviruses*. 11:533–539.
- 149) Shearer WT, Israel RJ, Starr S, Fletcher CV, Wara D, Rathore M, Church J, DeVille J, Fenton T, Graham B, et al. (2000) Recombinant CD4-IgG2 in

- human immunodeficiency virus type 1-infected children: phase 1/2 study. The Pediatric AIDS Clinical Trials Group Protocol 351 Study Team. *J. Infect. Dis.* 182:1774–1779.
- 150) Jacobson JM, Lowy I, Fletcher CV, O'Neill TJ, Tran DN, Ketas TJ, Trkola A, Klotman ME, Maddon PJ, Olson WC, et al. (2000) Single-dose safety, pharmacology, and antiviral activity of the human immunodeficiency virus (HIV) type 1 entry inhibitor PRO 542 in HIV-infected adults. *J. Infect. Dis.* 182:326–329.
- 151) Dey B, Lerner DL, Lusso P, Boyd MR, Elder JH, Berger EA. (2000) Multiple antiviral activities of cyanovirin-N: blocking of human immunodeficiency virus type 1 gp120 interaction with CD4 and coreceptor and inhibition of diverse enveloped viruses. *J. Virol.* 74:4562–4569.
- 152) Martin L, Stricher F, Misse D, Sironi F, Pugniere M, Barthe P, Prado-Gotor R, Freulon I, Magne X, Roumestand C, et al. (2003) Rational design of a CD4 mimic that inhibits HIV-1 entry and exposes cryptic neutralization epitopes. *Nat. Biotechnol.* 21:71–76.
- 153) Khati M, Schuman M, Ibrahim J, Sattentau Q, Gordon S, James W. (2003) Neutralization of infectivity of diverse R5 clinical isolates of human immunodeficiency virus type 1 by gp120-binding 2'F-RNA aptamers. *J. Virol.* 77:12692–12698.
- 154) Dey AK, Khati M, Tang M, Wyatt R, Lea SM, James W. (2005) An aptamer that neutralizes R5 strains of human immunodeficiency virus type 1 blocks gp120-CCR5 interaction. *J. Virol.* 79:13806–13810.

- 155) Dey AK, Griffiths C, Lea SM, James W. (2005) Structural characterization of an anti-gp120 RNA aptamer that neutralizes R5 strains of HIV-1. *RNA*. 11:873–884.
- 156) Nimjee SM, Rusconi CP, Sullenger BA. (2005) Aptamers: an emerging class of therapeutics. *Annu. Rev. Med.* 56:555–583.
- 157) Pestourie C, Tavitian B, Duconge F. (2005) Aptamers against extracellular targets for in vivo applications. *Biochimie*. 87:921–930.
- 158) Hicke BJ, Stephens AW. (2000) Escort aptamers: a delivery service for diagnosis and therapy. *J. Clin. Invest.* 106:923–928.
- 159) Lupold SE, Hicke BJ, Lin Y, Coffey DS. (2002) Identification and characterization of nuclease-stabilized RNA molecules that bind human prostate cancer cells via the prostate-specific membrane antigen. *Cancer Res.* 62:4029–4033.
- 160) McNamara JO, II, Andrechek ER, Wang Y, Viles KD, Rempel RE, Gilboa E, Sullenger BA, Giangrande PH. (2006) Cell type-specific delivery of siRNAs with aptamer-siRNA chimeras. *Nat. Biotechnol.* 24:1005–1015.
- 161) Chu TC, Twu KY, Ellington AD, Levy M. (2006) Aptamer mediated siRNA delivery. *Nucleic Acids Res.* 34:e73.
- 162) Chu TC, Marks JW, III, Lavery LA, Faulkner S, Rosenblum MG, Ellington AD, Levy M. (2006) Aptamer:toxin conjugates that specifically target prostate tumor cells. *Cancer Res.* 66:5989–5992.

- 163) Bagalkot V, Farokhzad OC, Langer R, Jon S. (2006) An aptamer-doxorubicin physical conjugate as a novel targeted drug-delivery platform. *Angew. Chem. Int. Ed. Engl.* 45:8149–8152.
- 164) Farokhzad OC, Jon S, Khademhosseini A, Tran TN, Lavan DA, Langer R. (2004) Nanoparticle-aptamer bioconjugates: a new approach for targeting prostate cancer cells. *Cancer Res.* 64:7668–7672.
- 165) Farokhzad OC, Cheng J, Teply BA, Sherifi I, Jon S, Kantoff PW, Richie JP, Langer R. (2006) Targeted nanoparticle-aptamer bioconjugates for cancer chemotherapy in vivo. *Proc. Natl Acad. Sci. USA.* 103:6315–6320.
- 166) Farokhzad OC, Karp JM, Langer R. (2006) Nanoparticle-aptamer bioconjugates for cancer targeting. *Expert Opin. Drug Deliv.* 3:311–324.
- 167) Engels FK, Mathot RA, Verweij J. (2007) Alternative drug formulations of docetaxel: a review. *Anticancer Drugs.* 18:95–103.
- 168) Zhou J, Li H, Li S, Zaia J, Rossi JJ. (2008) Novel dual inhibitory function aptamer-siRNA delivery system for HIV-1 therapy. *Mol. Ther.* 16:1481–1489
- 169) D. Boden, O. Pusch, B. Ramratnam, (2004). HIV-1-specific RNA interference. *Curr. Opin. Mol. Ther.* 6, 373–380
- 170) Lee NS, Dohjima T, Bauer G, Li H, Li M, Ehsani A, Salvaterra P, and Rossi J. (2002) Expression of small interfering RNAs targeted against HIV-1 rev transcripts in human cells. *Nat Biotechnol.* 20:500-505.
- 171) C. Tuerk, L. Gold, (1990). Systematic evolution of ligands by exponential enrichment: RNA ligandsto bacteriophage T4 DNA polymerase. *Science* 249, 505–510

- 172) J. Zhou, P. Swiderski, H. Li, J. Zhang, C. P. Neff, R. Akkina, J. J. Rossi, (2009). Selection, characterization and application of new RNA HIV gp 120 aptamers for facile delivery of Dicer substrate siRNAs into HIV infected cells. *Nucleic Acids Res.* 37, 3094–3109
- 173) J. O. McNamara II, E. R. Andrechek, Y. Wang, K. D. Viles, R. E. Rempel, E. Gilboa, B. A. Sullenger, P. H. Giangrande, (2006). Cell type-specific delivery of siRNAs with aptamer-siRNA chimeras. *Nat. Biotechnol.* 24, 1005–1015
- 174) Li M, Bauer G, Michienzi A, Yee J, Lee NS, Kim J, Li S, Castanotto D, Zaia J, and Rossi J. (2003) Inhibition of HIV-1 infection by lentiviral vectors expressing Pol III-promoted anti-HIV RNAs. *Mol Ther.* 8:196-206
- 175) Banerjea A, Li M, Bauer G, Remling L, Lee NS, Rossi J, and Akkina R. (2003) Inhibition of HIV-1 by lentiviral vector-transduced siRNAs in lymphocytes differentiated in SCID-hu mice and CD34+ progenitor cell-derived macrophages. *Mol Ther.* 8:62-71.
- 176) Li MJ, Kim J, Li S, Zaia J, Yee JK, Anderson J, Akkina R, and Rossi JJ. (2005) Long-term inhibition of HIV-1 infection in primary hematopoietic cells by lentiviral vector delivery of a triple combination of anti-HIV shRNA, anti-CCR5 ribozyme and a nucleolar-localizing TAR decoy. *Mol Ther.* 13
- 177) Bonyhadi, M.L., et al. (1997) RevM10-expressing T cells derived in vivo from transduced human hematopoietic stem-progenitor cells inhibit HIV replication. *J. Virol.* 71:4707-4716

- 178) Strayer DS, Akkina R, Bunnell BA, Dropulic B, Planelles V, Pomerantz RJ, Rossi JJ, Zaia J. (2005) Current status of gene therapy strategies to treat HIV/AIDS. *Mol Ther.* 11:823-842
- 179) Mitchell RS. (2004) Retroviral RND integration: ASLV, HIV and MLV show distinct target site preferences. *PloS Biol.* 2:1127-1136
- 180) Roe T, Reynolds T, Yu G, and Brown PO. (1993) Integration of murine leukemia virus DNA depends on mitosis. *EMBO J.* 12:2099-2108
- 181) Varma NR, Janic B, Ali MM, Iskander A, Arbab AS. (2011) Lentiviral Based Gene Transduction and Promoter Studies in Human Hematopoietic Stem Cells (hHSCs). *J Stem Cells Regen Med.*;7(1):41-53.
- 182) Akkina RK, Walton RM, Chen ML, Li QX, Planelles V, and Chen IS. (1996) High-efficiency gene transfer into CD34+ cells with a human immunodeficiency virus type 1-based retroviral vector pseudotyped with vesicular stomatitis virus envelope glycoprotein G. *J Virol.* 70:2581-2585
- 183) Zufferey, R, Nagy D, Mandel R, Naldini L, and Trono D.(1997) Multiply attenuated lentiviral vector achieves efficient gene delivery in vivo. *Nat Biotechnol.* 15:871-875
- 184) Miyoshi H, Blomer U, Takahashi M, Gage F, and Verma I.(1998) Development of a self-inactivating lentivirus vector. *J Virol.* 72:8150-8157
- 185) Akkina, R., Banerjea, A., Bai, J., Anderson, J., Li, M.J., Rossi, J. (2003). siRNAs, ribozymes and RNA decoys in modeling stem cell-based gene therapy for HIV/AIDS. *Anticancer Res.* 23

- 186) Unwalla HJ, Rossi JJ. (2010) A dual function TAR Decoy serves as an anti-HIV siRNA delivery vehicle. *Virol J.*;7:33.
- 187) Anderson, J., Akkina, R. (2005). HIV-1 resistance conferred by siRNA cosuppression of CXCR4 and CCR5 coreceptors by a bispecific lentiviral vector. *AIDS Res. And Therapy.* 2: 1-12.
- 188) Anderson, J., Banerjea, A., Akkina, R. (2003). Bispecific short-hairpin siRNA constructs targeted to CD4, CXCR4, and CCR5 confer HIV-1 resistance. *Oligonucleotides.* 13: 303-312.
- 189) Anderson J, Li MJ, Palmer B, Remling L, Li S, Yam P, Yee JK, Rossi J, Zaia J, Akkina R. (2007) Safety and efficacy of a lentiviral vector containing three anti-HIV genes--CCR5 ribozyme, tat-rev siRNA, and TAR decoy--in SCID-hu mouse-derived T cells. *Mol Ther.* (6):1182-8.
- 190) Broder S (2010) The development of antiretroviral therapy and its impact on the HIV-1/AIDS pandemic. *Antiviral Res* 85: 1–18
- 191) MacArthur RD, Novak RM (2008) Reviews of anti-infective agents: maraviroc: the first of a new class of antiretroviral agents. *Clin Infect Dis* 47: 236–241
- 192) Lieberman-Blum SS, Fung HB, Bandres JC (2008) Maraviroc: a CCR5-receptor antagonist for the treatment of HIV-1 infection. *Clin Ther* 30: 1228–1250.
- 193) Kromdijk W, Huitema AD, Mulder JW (2010) Treatment of HIV infection with the CCR5 antagonist maraviroc. *Expert Opin Pharmacother* 11: 1215–1223.

- 194) Veazey RS, Ketas TJ, Dufour J, Moroney-Rasmussen T, Green LC, et al. (2010) Protection of rhesus macaques from vaginal infection by vaginally delivered maraviroc, an inhibitor of HIV-1 entry via the CCR5 co-receptor. *J Infect Dis* 202: 739–744.
- 195) Grinsztejn B, Nguyen BY, Katlama C, Gatell JM, Lazzarin A, et al. (2007) Safety and efficacy of the HIV-1 integrase inhibitor raltegravir (MK-0518) in treatment-experienced patients with multidrug-resistant virus: a phase II randomised controlled trial. *Lancet* 369: 1261–1269.
- 196) Hazuda DJ, Felock P, Witmer M, Wolfe A, Stillmock K, et al. (2000) Inhibitors of strand transfer that prevent integration and inhibit HIV-1 replication in cells. *Science* 287: 646–650.
- 197) Van Rompay KK, Berardi CJ, Aguirre NL, Bischofberger N, Lietman PS, et al. (1998) Two doses of PMPA protect newborn macaques against oral simian immunodeficiency virus infection. *Aids* 12: F79–83.
- 198) Tsai CC, Follis KE, Sabo A, Beck TW, Grant RF, et al. (1995) Prevention of SIV infection in macaques by (R)-9-(2-phosphonylmethoxypropyl)adenine. *Science* 270: 1197–1199.
- 199) Clinicaltrials.gov FEM-PrEP(Truvada): Study to Assess the Role of Truvada in Preventing HIV Acquisition in Women.
- 200) Veazey RS, Klasse PJ, Schader SM, Hu Q, Ketas TJ, et al. (2005) Protection of macaques from vaginal SHIV challenge by vaginally delivered inhibitors of virus-cell fusion. *Nature* 438: 99–102.

- 201) Neff CP, Ndolo T, Tandon A, Habu Y, Akkina R (2010) Oral pre-exposure prophylaxis by anti-retrovirals raltegravir and maraviroc protects against HIV-1 vaginal transmission in a humanized mouse model. *PLoS One* 5: e15257.
- 202) Grant RM, Hamer D, Hope T, Johnston R, Lange J, et al. (2008) Whither or wither microbicides? *Science* 321: 532–534.
- 203) Klasse PJ, Shattock R, Moore JP (2008) Antiretroviral drug-based microbicides to prevent HIV-1 sexual transmission. *Annu Rev Med* 59: 455–471.
- 204) Abdool Karim Q, Abdool Karim SS, Frohlich JA, Grobler AC, Baxter C, et al. (2010) Effectiveness and safety of tenofovir gel, an antiretroviral microbicide, for the prevention of HIV infection in women. *Science* 329: 1168–1174.
- 205) Hladik F, Doncel GF (2010) Preventing mucosal HIV transmission with topical microbicides: challenges and opportunities. *Antiviral Res* 88: Suppl 1S3–9.
- 206) Friend DR (2009) Pharmaceutical development of microbicide drug products. *Pharm Dev Technol* 15: 562–581.
- 207) Neff CP, Zhou J, Remling L, Kuruvilla J, Zhang J, Li H, Smith DD, Swiderski P, Rossi JJ, Akkina R. (2011) An aptamer-siRNA chimera suppresses HIV-1 viral loads and protects from helper CD4(+) T cell decline in humanized mice. *Sci Transl Med.*;3(66):66ra6.
- 208) Berkhout, B. & ter Brake, O. (2009). Towards a durable RNAi gene therapy for HIV-AIDS. *Expert Opin Biol Ther* 9, 161-170

- 209) Brass, A.L. et al. (2008) Identification of host proteins required for HIV infection through a functional genomic screen. *Science* **319**, 921-926
- 210) Anderson, J., Banerjea, A. & Akkina, R. (2003) Bispecific short hairpin siRNA constructs targeted to CD4, CXCR4, and CCR5 confer HIV-1 resistance. *Oligonucleotides* **13**, 303-312
- 211) Novina, C.D. et al. (2002) siRNA-directed inhibition of HIV-1 infection. *Nat Med* **8**, 681-686
- 212) David HA. (1979) Robust estimation in the presence of outliers. In: Launer RL, Wilkinson GN, editors. *Robustness in Statistics*. Academic Press; New York: pp. 61–74.
- 213) Guttman I, Smith DE. (1969) Investigation of rules for dealing with outliers in small samples from the normal distribution. I: Estimation of the mean. *Technometrics*. 11:527–550.
- 214) R Development Core Team R (2010): *A Language and Environment for Statistical Computing*. R Foundation for Statistical Computing; Vienna, Austria
- 215) Hornung V, Guenther-Biller M, Bourquin C, Ablasser A, Schlee M, Uematsu S, Noronha A, Manoharan M, Akira S, de Fougères A, Endres S, Hartmann G. (2005) Sequence-specific potent induction of IFN- α by short interfering RNA in plasmacytoid dendritic cells through TLR7. *Nat. Med.* 11:263–270
- 216) Marquez, R.T. & McCaffrey, A.P. (2008) Advances in microRNAs: implications for gene therapists. *Hum Gene Ther* **19**, 27-38

APPENDIX

Supplemental material for chapters 4 and 5

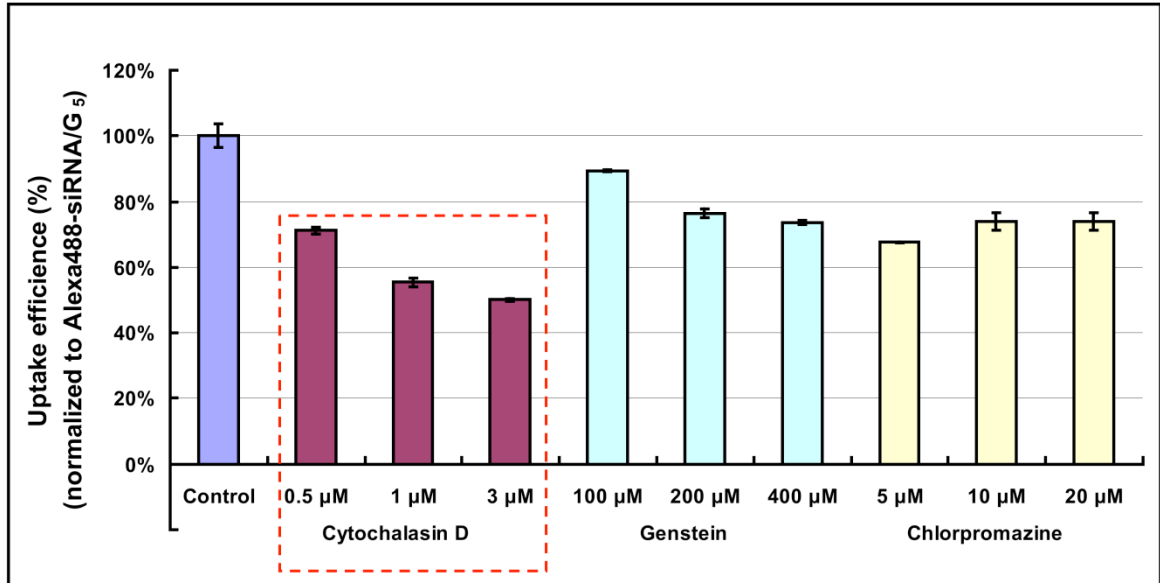


Figure S4.1: Internalization study of dendrimer-siRNA complexes. Different specific endocytic inhibitors were used to investigate the uptake mechanism. An increasing concentration (0.5 to 3 μM) of cytochalasin D (macropinocytosis inhibitor) reduced the cellular uptake of the dendrimer-siRNA complex.

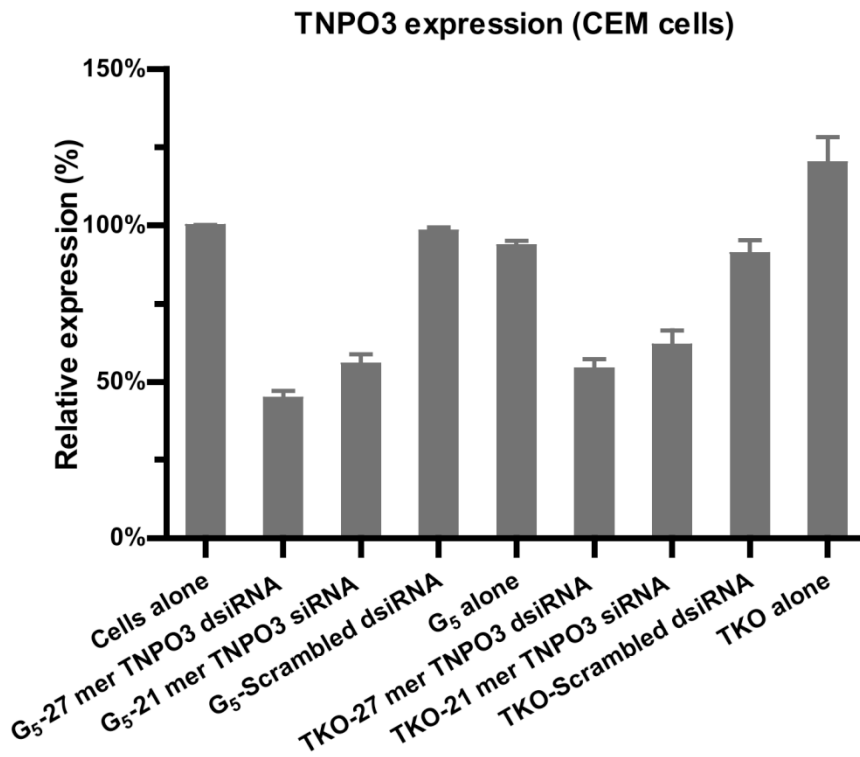


Figure S4.2: Dendrimer-siRNA nanoparticles efficiently release siRNA and mediate specific gene silencing *via* the RNAi pathway *in vitro*. qRT-PCR analysis indicated that G₅-siRNA complexes (at an N/P ratio of 5) efficiently knocked down target TNPO3 gene expression in cultured CEM T-cells. G₅-27 mer anti-TNPO siRNA complexes showed better efficacy than the G₅-21-mer siRNA complexes.

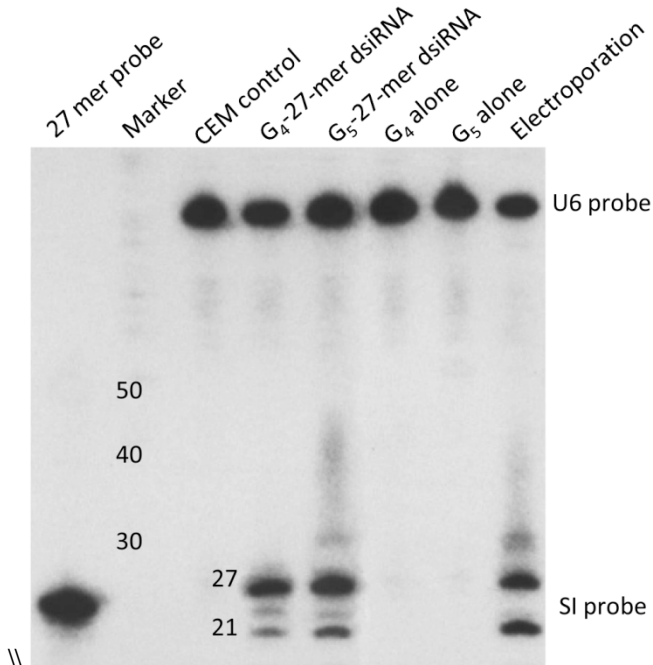


Figure S4.3 Northern blot analyses demonstrate that the 27-mer Dicer substrate siRNA was efficiently delivered to CEM cells and was processed by Dicer into 21-23 mer siRNA.

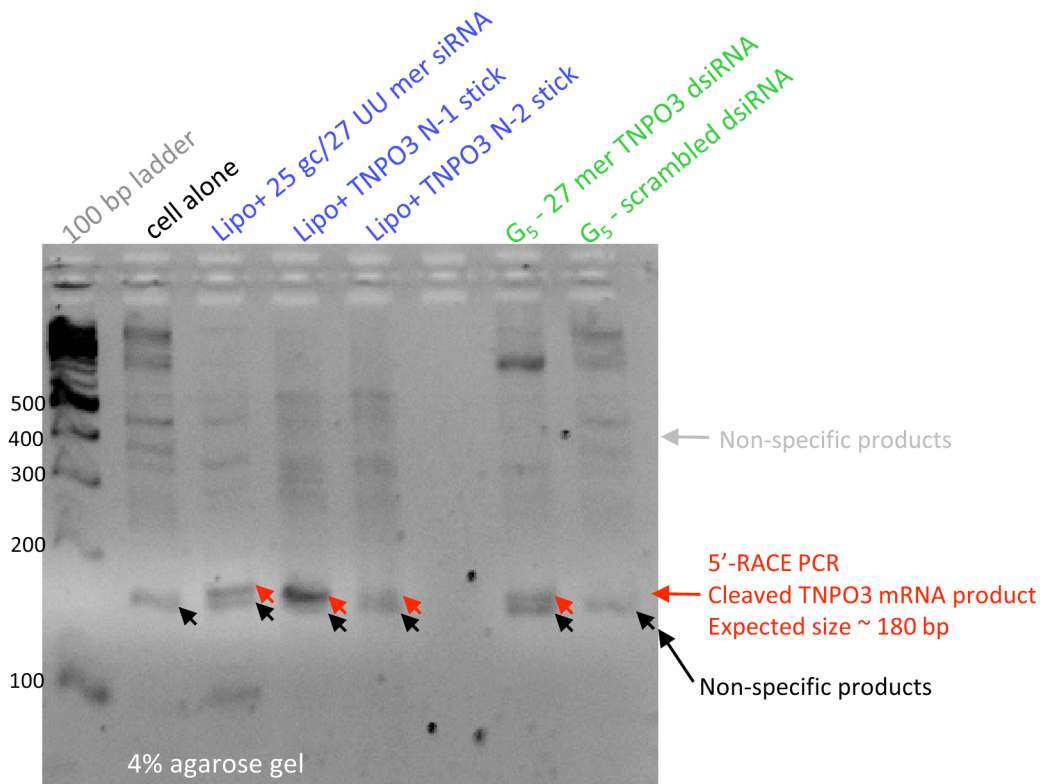


Figure S4.4 5'-RACE PCR analysis. mRNA from CEM cells treated with the G_5 -27-mer TNPO3 siRNA complexes was ligated to an RNA adaptor and reverse transcribed using a gene-specific primer. Depicted is an agarose gel electrophoresis of the 5'-RACE-PCR amplification products using a primer specific to the RNA adaptor and a reverse primer to TNPO3. These results support specific siRNA-mediated cleavage products of TNPO3 mRNA.

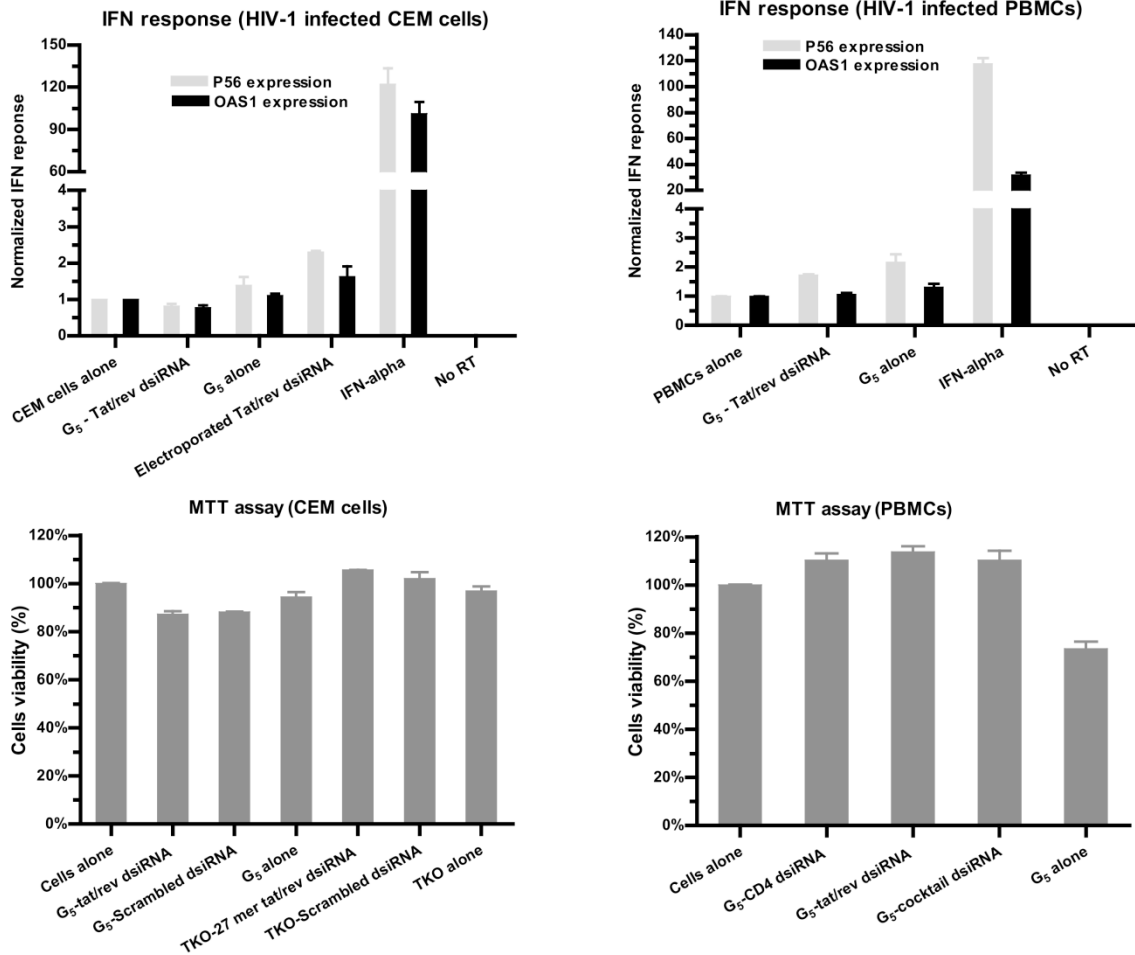


Figure S4.5: Dendrimer-mediated dsRNA delivery system does not trigger type I interferon responses in cultured HIV-1 infected (a) CEM cells and (b) human PBMCs. IFN- α treated HIV-1 infected human PBMCs were used as a positive control. Gene expression was normalized with the GAPDH mRNA. Error bars indicate SD (n = 3). The dendrimer-dsRNA complexes did not induce cellular toxicity in (c) CEM cells and (d) human PBMCs under the experimental conditions used. Cell viability was detected using an MTT assay. Error bars indicate SD (n = 3).

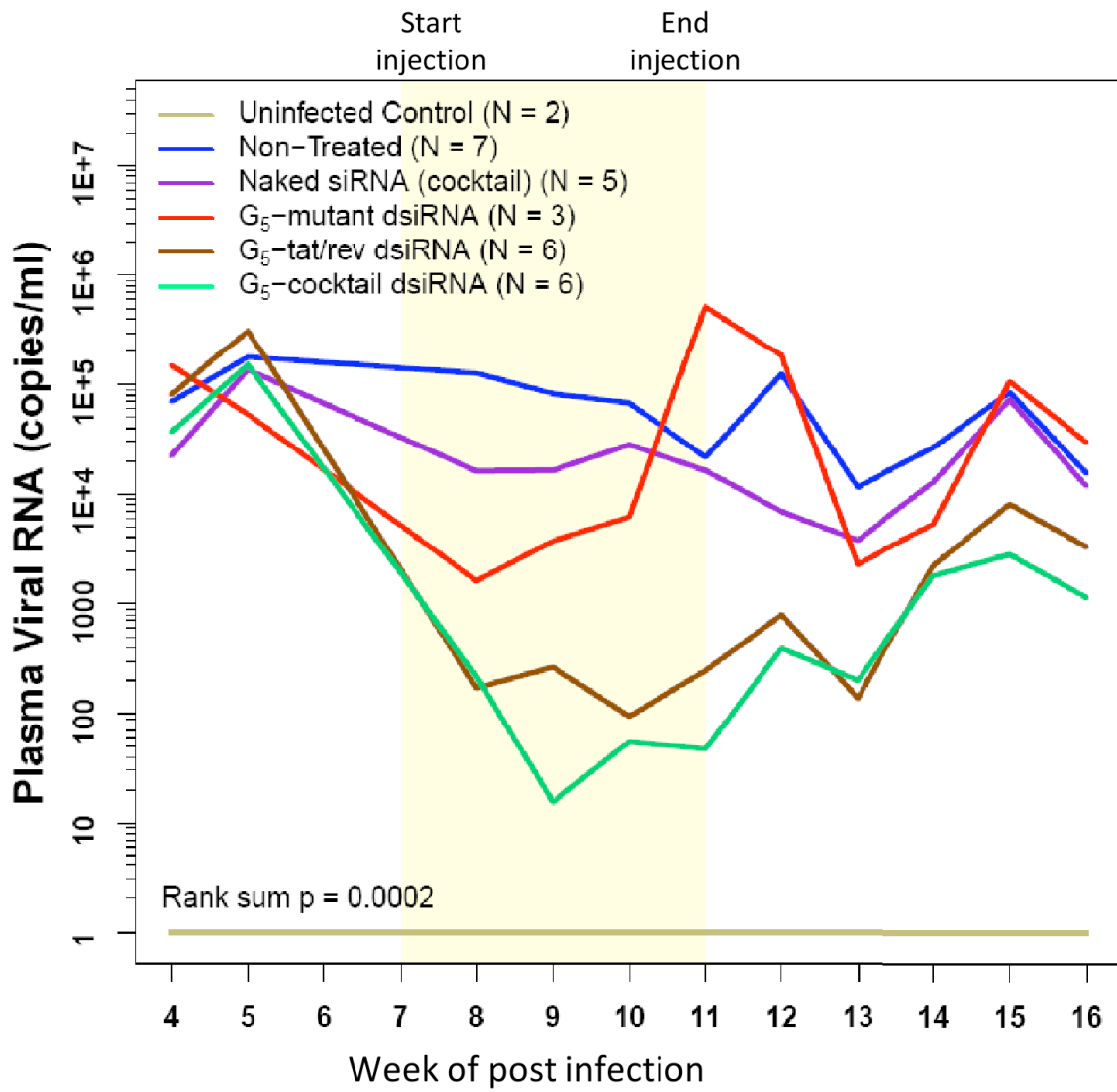


Figure S4.6: Dendrimer-dsiRNA complexes suppress viral loads in HIV-1 infected RAG-hu mice while dendrimer alone has no effect on viral loads. HIV-1 viral loads were monitored at for several weeks post infection as indicated. The beginning and end of the treatment period is indicated by the yellow framed in region. Viral loads at each indicated week pre- and post-treatment and the time point of treatment start and end are indicated. The first-treatment included five weekly injections: The viral loads of uninfected mice (n = 2), non-treated mice (n = 7), naked cocktail dsRNA treated mice (n = 5), **G₅**-mutant-*tat/rev* dsRNA complex treated mice (n = 3), **G₅**-*tat/rev* dsRNA complex treated mice (n = 6) and **G₅**-cocktail siRNA complex treated mice (n = 6) are indicated.

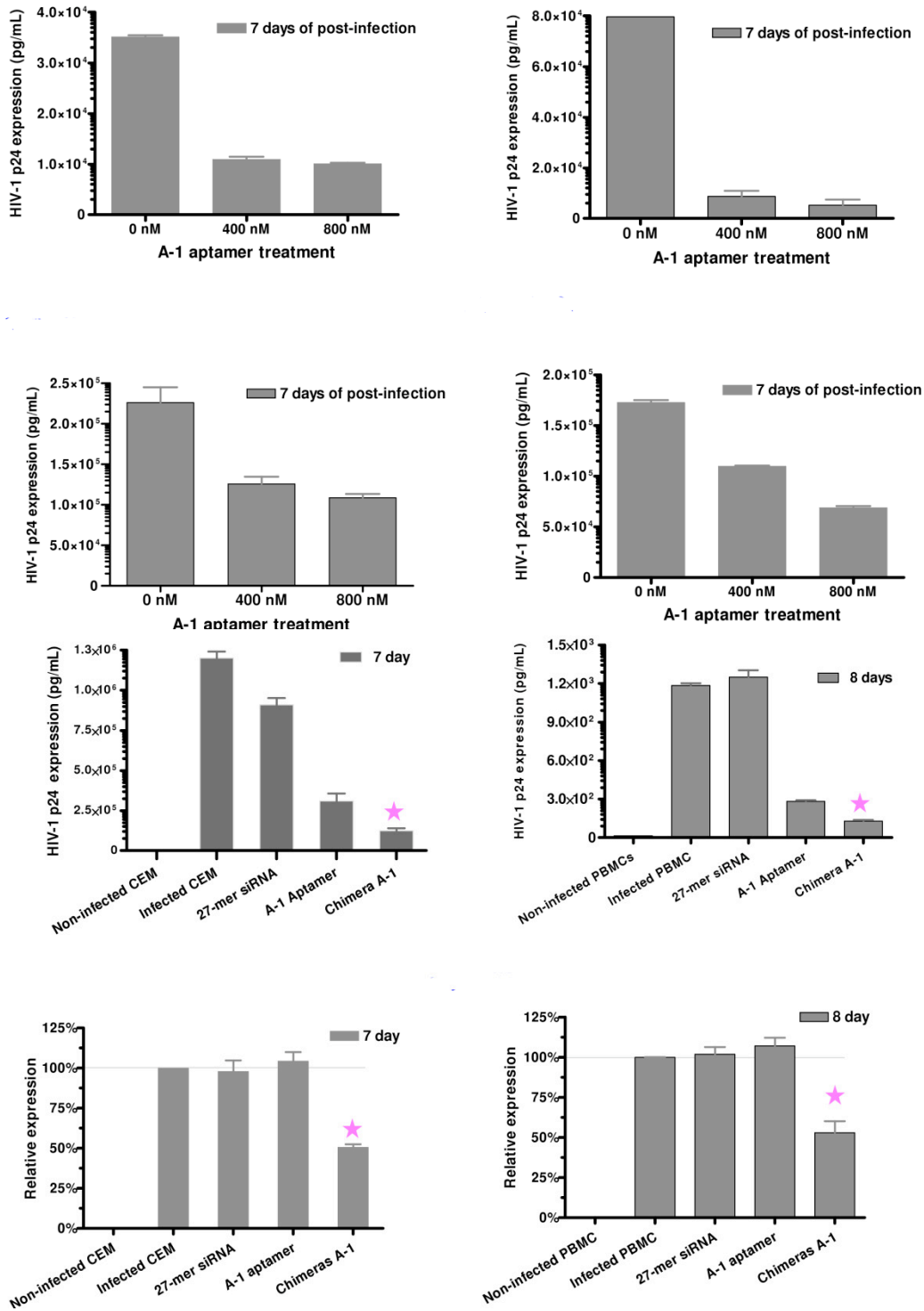


Figure S5.1: HIV-1 suppression by Aptamer A-1 and Aptamer-siRNA Ch A-1 chimera. (A-D) A-1 aptamer inhibition of HIV-1 in PBMCs(A) HIV-1 NL4.3, (B) HIV-1 92UG021, (C) HIV-1 RU570 and (D) HIV-1 98CN009. Inhibition of HIV-1 replication by the Aptamer A-1, Ch A-1 RNA and naked siRNA in (E) CEM cells infected with HIV-IIIIB and in (F) PBMCs infected with BaL. Down regulation of *tat/rev* mRNA mediated by the aptamer delivered siRNA in (G) HIV-1 IIIIB infected CEM cells and in (H) PBMCs cells infected with BaL. Error bars indicate SD (n = 3).

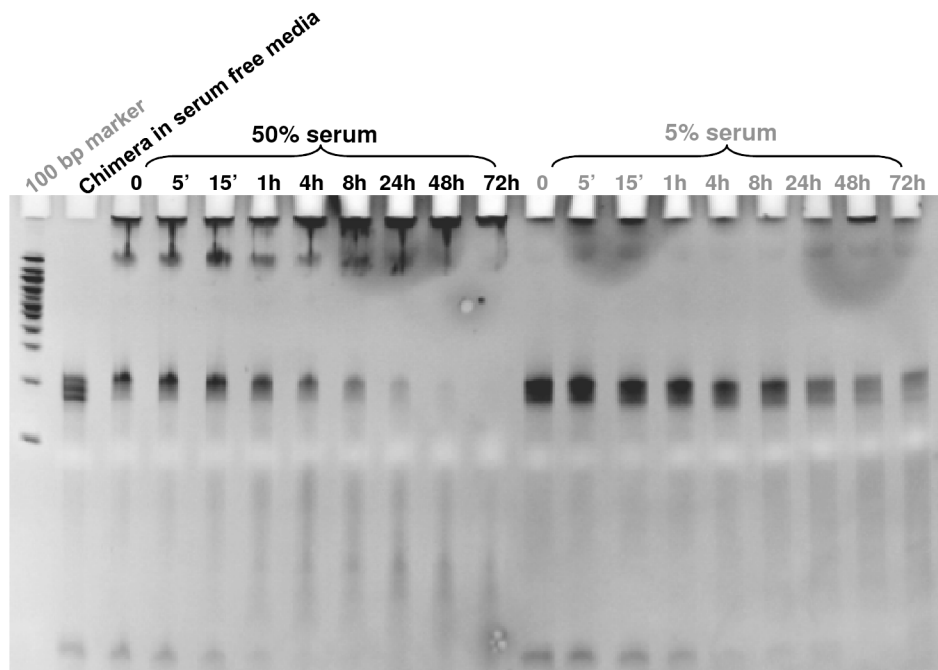


Figure S5.2: Stability of 2'-Fluoro modified chimeric RNA in mouse serum. RNA duplexes were incubated in mouse serum for the lengths of time indicated and were resolved by 8% PAGE. Stability of the **Ch A-1** chimeric construct was evaluated following incubation in 50% or 5% mouse sera.

Table S5.1

		Week1	Week2	Week3	Week4	Week5	Week6	Week7	Week8	Week9	Week10	Week11	Week12
Uninfected Control	J570	1	1	1	1	1	1	1	1	1	1	1	1
	J571	1	1	1	1	1	1	1	1	1	1	1	1
	J572	1	1	1	1	1	1	1	1	1	1	1	1
	Average	1	1	1	1	1	1	1	1	1	1	1	1
Non-treated	J565	15	46	70653	40173	1611916	2655213	978487	60589	13505	107329	81927	13975
	J566	64	16469	526913	167200	3062118	8307855	270938	291214	335899	1731311	988012	46677
	J567	60	2016	491653	3579558	8307830	2302355	593930	5652	42427	8190	33857	6770
	Average	46	6177	363073	1262310	4327288	4421808	614452	119152	130610	615610	367932	22474
Mutant Chimera A-5	J554	1	1146	23277	56175	39446	24263	320608	716431	841330	2035506	49469	24459
	J555	1	849	70653	24425	20593	14871	59073	1257084	39690	6266084	14665	7238
	J556	1	1	526913	166751	1070324	987725	155435	661132	2205710	1733448	93791	13743
	Average	1	665	206948	82450	376788	342286	178372	878216	1028910	3345013	52641	15147
Aptamer A-1	J547	1	3	93229	599425	911450	83	176	1	709	26559	93791	113621
	J548	1	12	302753	494757	494491	188	1	1	2961	4489	29650	38287
	J549	56	79	24952	2296677	36377	429	98	1	3791	1820	599471	106580
	Average	19	31	140312	1130286	480773	233	92	1	2487	10956	240971	86162
Chimera A-1	J456	1	1921	308042	137626	562806	628	104	1	1	1102	2435	3346
	J458	37	1921	125161	40783	479243	429	1	1	1	1304	6800	8774
	J460	510	495	1319090	93745	42772	1	1	1	1	1675	1278	1539
	Average	183	1445	584097	90718	361607	353	35	1	1	1360	3504	4553
		Week1	Week2	Week3	Week4	Week5	Week6	Week7	Week8	Week9	Week10	Week11	Week12
Uninfected Control	J570	1	1	1	1	1	1	1	1	1	1	1	1
	J571	1	1	1	1	1	1	1	1	1	1	1	1
	J572	1	1	1	1	1	1	1	1	1	1	1	1
	Average	1	1	1	1	1	1	1	1	1	1	1	1
Non-treated	J565	15	46	70653	40173	1611916	2655213	978487	60589	13505	107329	81927	13975
	J566	64	16469	526913	167200	3062118	8307855	270938	291214	335899	1731311	988012	46677
	J567	60	2016	491653	3579558	8307830	2302355	593930	5652	42427	8190	33857	6770
	Average	46	6177	363073	1262310	4327288	4421808	614452	119152	130610	615610	367932	22474
Mutant Chimera A-5	J554	1	1146	23277	56175	39446	24263	320608	716431	841330	2035506	49469	24459
	J555	1	849	70653	24425	20593	14871	59073	1257084	39690	6266084	14665	7238
	J556	1	1	526913	166751	1070324	987725	155435	661132	2205710	1733448	93791	13743
	Average	1	665	206948	82450	376788	342286	178372	878216	1028910	3345013	52641	15147
Aptamer A-1	J547	1	3	93229	599425	911450	83	176	1	709	26559	93791	113621
	J548	1	12	302753	494757	494491	188	1	1	2961	4489	29650	38287
	J549	56	79	24952	2296677	36377	429	98	1	3791	1820	599471	106580
	Average	19	31	140312	1130286	480773	233	92	1	2487	10956	240971	86162
Chimera A-1	J456	1	1921	308042	137626	562806	628	104	1	1	1102	2435	3346
	J458	37	1921	125161	40783	479243	429	1	1	1	1304	6800	8774
	J460	510	495	1319090	93745	42772	1	1	1	1	1675	1278	1539
	Average	183	1445	584097	90718	361607	353	35	1	1	1360	3504	4553

Table S5.2a

CD4:CD3 T cell ratio

	Initial	Week2	Week4	Week6	Week8	Week10	Week12	Week14	Week16	Week18
Uninfected Control										
J209	70.2	70.6	70.3	66.9	66.9	65.4	68	69.7	71.4	65.2
J210	70.3	68.3	68.2	67.5	68.3	68.4	65.6	68.5	69.6	66.1
Average	70.25	69.45	69.25	67.2	67.6	66.9	66.8	69.1	70.5	65.65
to baseline	1	0.988612	0.985765	0.956584	0.962278	0.952313	0.95089	0.98363	1.003559	0.93452
Non-Treated										
J258	67.2	57.1	63	72.3	55.4	53.7	44.8	38.1		28.8
J257	54.5	48.5	58	42.2	46	44.3	44.6	45.2	46.6	30.5
J256	52.4	71.4	53	51.2	49.7	48.5	49.7	46.1	33.3	23.1
J246	54.9	46.6	52.4	57	50.4	30.4	40.4	40.2		15
J245	61.1	71.4	64	53.5		64.6	52.1	46.1	39.9	40.1
Average	58.02	59	58.08	55.24	50.375	48.3	46.32	43.14	39.93333	27.5
to baseline	1	1.016891	1.001034	0.952085	0.868235	0.832472	0.798345	0.743537	0.688268	0.473974
Naked siRNA(Tat/Rev)										
J273	57.7	73.2	56	64.3	67.2	64.4	60.9	57.4	54.7	53.8
J266	66.7	71.5	50	71.6	50.9	53.4	50.7	48.4	40	47.9
J264	71.8	67.3	61.3	68.4	50.7	54.3	54.9	29.7	13.3	12.3
J253	50	77.4		37.8	72	65.3	60	42.8	24.9	14.4
J217	54.2	52			65.7	67.4	65			
J216	50			41.2	34.5	35.6	37.1	27.5	14.6	20
Average	58.4	68.28	55.76667	56.66	56.83333	56.73333	54.76667	41.16	29.5	29.68
to baseline	1	1.169178	0.954909	0.970205	0.973174	0.971461	0.937785	0.704795	0.505137	0.508219
Chimera A-1										
J276	46.7	56.7	49.3	64.2	44.7	58.3	44.7	45.4	45.5	47.1
J274	63.2	62.1	45	64.2	44.6	47.5	44.6	53.5	44.4	49.4
J272	68.8	51	54	64.6	51.4					
J251	50	51	45	59.5	63.7	57.4	55.7	60.3	77.8	
J249	60.3	66.7	61.4	65.4	77.2	73.6	79	57.5	46.2	65.4
J247	88.9	62.4	65.4	72.5	79	75.4	77.2	72.4	63.1	71.7
Average	62.98333	58.31667	53.35	65.06667	60.1	62.44	60.24	57.82	55.4	58.4
to baseline	1	0.925906	0.847049	1.033078	0.954221	0.991373	0.956444	0.918021	0.879598	0.927229

Table S5.2b

CD4:CD3 T cell ratio

Uninfected Control		Initial	Week1	Week3	Week5	Week7	Week9	Week11
	J571	72.3	68.2	69.4	74.8	65.9	68.5	71.1
	J572	64.1	59.1	59.4	63.1	64.11	66.9	69.2
	J573	69.8	66.5	67.3	73.4	69.7	75.8	68.9
	Average	68.73333	64.6	65.36667	70.43333	66.57	70.4	69.73333
to baseline	1	0.939864	0.951018	1.024733	0.968526	1.024248	1.014549	
Non-Treated		Initial	Week1	Week3	Week5	Week7	Week9	Week11
	J565	68.3	76.3	69.2	65	62.8	54.5	40
	J566	72.4	71.3	70.1	68		65	47.3
	J567	68	62.4	63.8	59.3	52.7	53.3	50
	Average	69.56667	70	67.7	64.1	57.75	57.6	45.76667
to baseline	1	1.006229	0.973167	0.921418	0.830139	0.827983	0.657882	
Mutant Chimera A-5		Initial	Week1	Week3	Week5	Week7	Week9	Week11
	J554	61.9	78.8	75		42.3	53.3	33.3
	J555	56	63	53.3	47.1	58.7	52.9	32.3
	J556	61.9	76	68.8	52	62.8	52.1	
	Average	59.93333	72.6	65.7	49.55	54.6	52.76667	32.8
to baseline	1	1.211346	1.096218	0.826752	0.911012	0.880423	0.547275	
Aptamer A-1		Initial	Week1	Week3	Week5	Week7	Week9	Week11
	J549	62.5	54.5	55.7	58.9	85.3	83.3	81.8
	J548	57.1	60	52.6		50	50.4	46.9
	J547	60	66.7	63.8	63.4	58.8		49
	Average	59.86667	60.4	57.36667	61.15	64.7	66.85	59.23333
to baseline	1	1.008909	0.958241	1.021437	1.080735	1.116648	0.989421	
Chimera A-1		Initial	Week1	Week3	Week5	Week7	Week9	Week11
	J456	66.7	69	60.5	67.6	66.1	61.5	50
	J458	66.1	71	66	59.1	65.8	68	78.4
	J460	58.9	66.7	64.8	65.3	77.6	75.5	70.5
	Average	63.9	68.9	63.76667	64	69.83333	68.33333	66.3
to baseline	1	1.078247	0.997913	1.001565	1.092853	1.069379	1.037559	